Title 40 CFR Part 191
Compliance Certification
Application
for the
Waste Isolation Pilot Plant

Appendix MASS

United States Department of Energy
Waste Isolation Pilot Plant

Carlsbad Area Office
Carlsbad, New Mexico

Supplemental Information on Modeling Assumptions

CONTENTS

CONTENTS (Continued)

CONTENTS (Continued)

FIGURES

1

TABLES

2

3

4

5

(M)

THIS PAGE INTENTIONALLY LEFT BLANK

ACRONYMS

3	BSEP	Brine Sampling and Evaluation Program
4	CCDF	complementary cumulative distribution function
5	CH	contact-handled
6	CSH	calcium-silicate-hydrate
7	DCCA	Draft Compliance Certification Application
8	DOE	U.S. Department of Energy
9	DRZ	disturbed rock zone
10	DSEIS	Draft Supplement, Environmental Impact Statement
11	EEG	Environmental Evaluation Group
12	EIS	Environmental Impact Statement
13	EPA	U.S. Environmental Protection Agency
14	ERDA	U.S. Energy Research and Development Administration
15	FEIS	Final Environmental Impact Statement
16	FEP	features, events, and processes
17	FSEIS	Final Supplemental Environmental Impact Statement
18	LANL	Los Alamos National Laboratory
19	LEFM	linear elastic fracture mechanics
20	LLNL	Lawrence Livermore National Laboratory
21	MB	marker bed
22	NAS	National Academy of Sciences
23	NIST	National Institute of Standards and Technology
24	ORNL	Oak Ridge National Laboratory
25	PNL	Pacific Northwest Laboratory
26	RH	remote-handled
27	SNL	Sandia National Laboratories
28	SSBI	Small-Scale Brine Inflow
29	SWCF	Sandia National Laboratories WIPP Central Files
30	TDEM	Time Domain ElectroMagnetic
31	TRU	transuranic
32	USGS	United States Geological Survey
33	WIPP	Waste Isolation Pilot Plant
34	WQSP	Water Quality Sampling Program

THIS PAGE INTENTIONALLY LEFT BLANK
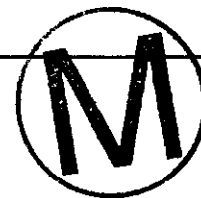
APPENDIX MASS

MASS.1 Introduction

This appendix presents supplementary information regarding the assumptions, simplifications, or approximations used in the models of this performance assessment of the Waste Isolation Pilot Plant (WIPP). In any topic area in this appendix, relevant issues in the formulation or development of the various types of models (for example, conceptual, mathematical, numerical, or computer code) used for the topic may be discussed. Because extensive discussion of computer codes *per se* is presented in stand-alone appendices, there is redundancy between portions of this appendix and other parts of this application. Additionally, where assumptions, simplifications, or approximations are implemented by way of a choice of the value of a parameter, there may be redundancy in this appendix with Appendix PAR.

Several types of information are presented in this appendix, including memoranda prepared during development of the performance assessment by the U.S. Department of Energy (DOE) personnel and documents associated with modeling assumptions tested during development of the performance assessment process. These are included as attachments in this appendix. These attachments are also maintained as project records in the Sandia National Laboratories (SNL) WIPP Central Files (SWCF).

Section MASS.2 contains a historical perspective of the development of the concepts since 1975 about future WIPP performance. The remainder of this appendix is arranged to provide topical information on the major physical processes and systems introduced in Chapter 6.0 (Section 6.4) and modeled in the performance assessment. Section MASS.3 begins this topical piece with a discussion of general modeling assumptions applicable to the disposal system as a whole, including a table of assumptions made in performance assessment models, with cross-references. In some topical discussions, the information relevant to a particular model is more appropriately included in a different appendix. Where this occurs, the reader is referred to the appendix that contains the relevant information.

MASS.2 Historical Development of WIPP Conceptual Models

Concepts about the processes important to the performance of the WIPP have changed since the DOE's inception, as the DOE and its predecessor agencies refined knowledge and understanding of features of the site and the processes and events that might occur there. Although the understanding of the WIPP site has continuously evolved since the early 1970s, the fundamental conceptual models that shaped projections of the WIPP's performance underwent major refinement three times: in the mid-1970s during site selection; in the late 1970s during surface-based site characterization; and again in the mid-to-late 1980s. Since the late 1980s, the fundamental conceptual model has not changed in any major way. Experimental activities since the late 1980s have led to the level of understanding necessary

1 for quantitative, probabilistic performance assessments. This section describes the evolution
2 of the DOE's understanding of the processes and events of importance at the WIPP.
3
4 Techniques used to evaluate the consequences of radionuclide release from the repository
5 have also changed. Changing the methods used to address the consequences of radionuclide
6 exposure pathways has affected both the types of computational modeling used to evaluate
7 performance and the understanding of the relative importance of the many physical properties
8 of the disposal system. Until 1985, when the U.S. Environmental Protection Agency (EPA)
9 promulgated its radiation protection standard for the management and disposal of spent
10 nuclear fuel, high-level and transuranic wastes, 40 CFR Part 191, the consequences of release
11 were primarily evaluated in terms of human exposure to radionuclides that had reached the
12 biosphere by some mechanism, rather than in terms of any specific or quantitative release
13 criterion. Contaminant transport in the geosphere was not regarded as a problem if humans
14 were not exposed. Two principle pathways were of concern. Direct releases to the surface
15 from a borehole could expose drillers and hypothetical future residents of the region who
16 consumed livestock that grazed nearby. Individuals could also be exposed by drinking water
17 from a contaminated source or by eating livestock watered at a contaminated stock pond. For
18 example, the hypothetical exposed person was someone who drank water and ate fish from the
19 Pecos River near Malaga Bend, a discharge point for contaminated groundwater from the
20 Rustler (DOE 1980, 9 – 128, K23 – K24). (The release of contaminated Rustler groundwater
21 at Malaga Bend is no longer considered plausible.) The consequences of release by diverse
22 transport pathways were treated deterministically and individually. The time period
23 considered for evaluating the effectiveness of the WIPP was usually about a quarter of a
24 million years, roughly ten half-lives of ^{239}Pu, although this time frame was not specified by
25 regulations.
26
27 40 CFR Part 191, promulgated in 1985, set release limits at defined boundaries. Therefore,
28 determining possible contamination of areas far from the repository was no longer an
29 objective of consequence modeling. Instead, quantities of actinides released from the disposal
30 system, a defined volume, became the primary measure for assessing performance, although
31 dose calculations to humans were still of interest to many groups and required for certain
32 regulatory criteria. The probabilistic methodology suggested in 40 CFR Part 191 led to an
33 appreciation of the possible interactions among multiple boreholes, assessment of the
34 probabilities of defined events, and formal assessment of the performance impact of
35 uncertainty in estimates of physical quantities. The standard also established a regulatory time
36 period, during which actinide transport and system performance must be modeled. The EPA
37 has become increasingly prescriptive about how the DOE should incorporate the uncertainty
38 associated with projecting human actions into the future (for example, 40 CFR Parts 191 and
39 194, and the Compliance Application Guidance). In addition, expectations about the quantity
40 and quality of supporting information used to support analyses of repository performance have
41 gradually escalated.
42
43 Interactions between the DOE and external groups have played an important role in
44 developing the current understanding of the disposal system performance. Interactions with

1   the National Academy of Sciences (NAS) and interactions with the Environmental Evaluation
2   Group (EEG) have been the most important of these. Interactions with the state of New
3   Mexico and with the EPA have also contributed. At various times through the years, the DOE
4   has convened expert panels and working groups to obtain advice on certain issues; for
5   example, an expert working group met for many years to advise on the treatment of
6   uncertainty in characterizing the Culebra (Zimmerman and Gallegos 1993).
7
8   *MASS.2.1 Conceptual Models Used During Site Selection (1975-1976)*
9
10   The Oak Ridge National Laboratory (ORNL) selected the site for the WIPP in the early 1970s.
11   At that time, the concept of long-term performance of the WIPP was based on an
12   understanding that bedded salt deposits were dry, natural creep of the salt would encapsulate
13   waste, salt had good heat-dissipation properties, and the northern Delaware Basin had
14   predictable geology that was amenable both to repository construction and to predictions of
15   performance. Site-selection criteria were strongly influenced by experience at the abandoned
16   bedded-salt site near Lyons, Kansas, and consequently focused strongly on isolating the
17   repository from potential breach mechanisms associated with resource exploitation and
18   dissolution. Accordingly, buffer zones of two miles between the site and existing deep
19   boreholes and of five miles between the site and any existing potash mines were established as
20   criteria for siting, and interest in fluid flow in aquifers and abandoned boreholes was chiefly
21   related to its potential for dissolving salt in the Salado Formation.
22
23   During site selection in the early 1970s, several ideas about the Salado and processes
24   associated with radioactive waste disposal in it were accepted. The formation was known to
25   contain anhydrite layers; the DOE wanted to choose a repository horizon without anhydrite
26   beds in close proximity because they would interfere with creep and waste encapsulation.
27   Project staff recognized that a disturbed rock zone (DRZ) would develop around the
28   repository; but because of salt creep, the long-term effects of the DRZ were assumed to be
29   negligible as the waste was encapsulated and the disturbed salt healed (that is, as its properties
30   became similar once again to those of intact salt). The generation of gas by microbial
31   degradation of waste constituents was recognized as a possible pressure-building mechanism.
32   Because the Salado was thought to be dry, corrosion of steel in the waste was not considered
33   to be important. It was known that intragranular brine inclusions could migrate toward waste
34   as a result of the thermal effects of heat-emitting waste. This possibility for brine migration
35   was of considerable concern because at the time it was intended that the WIPP would have
36   two excavations for waste disposal: one at a shallower horizon for relatively cold transuranic
37   (TRU) waste and one at a deeper horizon for heat-emitting spent nuclear fuel.
38
39   The ORNL identified a candidate site northeast of the present WIPP site in 1974. As
40   discussed in Chapter 2.0 and Appendix GCR, drilling of U.S. Energy Research and
41   Development Administration (ERDA)-6 in 1974 at that site revealed steeply dipping beds,
42   missing units, and brine containing hydrogen sulfide near the deeper planned repository
43   depths. The dipping beds and missing units indicated that a level, minable repository horizon
44   free of anhydrite could not be expected. Hydrogen sulfide in the brine posed a potential

1 hazard to mine workers. Thus, the discovery of the deformed beds and associated brine at the
2 ORNL site changed the concept of uniform evaporite stratigraphy throughout the northern
3 Delaware basin.
4
5 The ORNL site was deemed unacceptable, and a search for a new site with acceptable
6 conditions was initiated in late 1975. The new search was conducted by SNL. SNL used
7 selection criteria similar to ORNL's. The present site was identified in December 1975.
8 Examination of petroleum exploration data, primarily seismic reflection surveys, indicated
9 that deformation was limited largely to a zone paralleling the buried Capitan reef. A region in
10 which Castile deformation is absent was identified and borehole ERDA-9 was drilled through
11 the Salado near the center of the proposed site, confirming that its beds were flat-lying and
12 that no brine was present in it or immediately below the potential repository elevations.
13 Consequently, because the site satisfied this and other criteria, it was accepted as suitable in
14 1976, and site characterization began.
15
16 At the end of site selection and with the current site identified, the following concepts were
17 accepted by the DOE and shaped thinking about the consequences of repository development:
18
19 • the Salado is dry, with no mobile intergranular liquid,
20
21 • intragranular fluid inclusions could migrate in thermal fields,
22
23 • gas could be generated by microbial action,
24
25 • salt would creep and encapsulate waste,
26
27 • there are deformed areas and brine-producing areas in the Delaware Basin evaporites,
28 but the present site was free of deformation and brine at the potential repository
29 horizons, and
30
31 • natural dissolution fronts would not threaten the repository, as a result of either
32 vertical or lateral dissolution, for more than 250,000 years.
33
34
35 *MASS.2.2* *Conceptual Models Developed During Site Characterization and Repository*
36 *Design (1976-1981)*
37
38 Experimental activities conducted at the site immediately after site selection focused on
39 characterizing the encapsulation properties of the Salado, the migration of intragranular brine
40 in a thermal gradient, microbial gas generation, and the hydrologic properties of the units
41 above the Salado.
42
43 After site selection, interest in fluid flow in water-bearing units of the area shifted from its
44 effects on dissolution to the role of these units as potential pathways for radionuclide release.

The Magenta and Culebra Members of the Rustler Formation and the Rustler-Salado contact zone were recognized from regional experience to be potential pathways. At the time, the relative importance of these units was unknown, so the first tests targeted all three. The Rustler-Salado contact was confirmed to be transmissive in Nash Draw but did not yield significant quantities of water at the site and did not represent a significant pathway for fluid movement for either radionuclide transport or dissolution. The Culebra was more transmissive than the Magenta, and the transmissivities of these units varied by several orders of magnitude. In time, characterization of groundwater pathways for radionuclide release became the principal characterization activity pursued at the WIPP site.

The hydrologic properties of the Salado were characterized by surface testing (drill-stem tests) during this period. These tests indicated measurable permeabilities over substantial thicknesses of the Salado, suggesting that the permeability of the Salado was sufficiently high that gas generated by microbial action would dissipate into the rock without reaching high pressure. Accordingly, the program to characterize gas generation, which had been progressing through the late 1970s, was canceled.

Many repository breach mechanisms by natural processes were postulated during this period, and investigations began to evaluate their likelihood and consequences. These investigations examined volcanism, tectonism, karst hydrology, deep dissolution, and other processes. In time, all such naturally occurring processes for breaching the repository were resolved as not likely to occur or not likely to occur in a manner that would impair WIPP performance.

MASS.2.3 Repository Design

The design of the repository—the dimensions and geometry of the rooms, pillars, and accessways—was conducted by Bechtel, Inc., in the late 1970s. The design sought to ensure long-term encapsulation of the waste by salt creep and to provide enough volume to dispose of the projected 6.2 million cubic feet (176,000 cubic meters) of waste. Given these performance criteria, the physical dimensions of the repository were determined with primary consideration given to mine safety during waste-disposal operations. Because the repository was designed prior to underground access, the basis for the design drew on experience gained from potash mines in the Delaware Basin.

The initial repository design placed the shafts at the south end of the repository, an area for experimental activities north of the shafts, and the waste-disposal region north of the experimental area. From early on, the DOE viewed the WIPP as a research and developmental facility that would conduct experiments that were of interest to a wide variety of disposal programs and concepts. Accordingly, the original purpose of the experimental area was to house experiments to support development of models of rock mechanics and salt creep, experiments on seal behavior, and experiments of interest to high-level waste disposal concepts, such as canister design and fluid-inclusion brine movement. It was not intended at first that the experimental region would support studies of phenomena that had been previously characterized from the surface, such as the permeability of the Salado.

1　The repository design did not initially include constructed barriers to separate the waste into
2　modules. Early discussions with the NAS oversight panel led to concern that fire in
3　combustible portions of the waste could pose a hazard to mine workers. Modularization of
4　the waste was proposed to enhance mine safety. Because constructing closures is expensive
5　and time-consuming, separating waste at the panel scale was considered the best of several
6　options for balancing concerns about safety, cost, and mine operations.
7
8　In November 1981, the WIPP-12 borehole was deepened into the Castile and encountered
9　large quantities of brine that flowed freely into the borehole and to the surface. The discovery
10　of a Castile brine reservoir at WIPP-12 prompted the rotation of the waste panels from their
11　planned location north of the experimental area to south of the shafts, the current
12　configuration, and eventually led to a geophysical program in the 1980s to investigate the
13　possibility of brine reservoirs under the panels. Both the DOE and the EEG conducted
14　consequence analyses of a drilling encounter with a brine reservoir like that at WIPP-12 and
15　concluded that the health consequences were minor (Woolfolk 1982; Channell 1982).
16
17　In 1980, Congressional legislation limited the WIPP to the disposal of TRU waste, and plans
18　for a spent-fuel disposal level in the Infra-Cowden salt near the base of the Salado were
19　abandoned. Because TRU waste generates relatively little heat, migration of brine in fluid
20　inclusions was of little concern for the WIPP after 1980, although tests were conducted of this
21　phenomenon because of continued interest in high-level-waste disposal in salt beds elsewhere.
22
23　Thus prior to underground access at the WIPP in the early 1980s, several conceptual models
24　shaped the thinking about the performance of the WIPP repository:
25
26　　• the Salado is dry with no mobile intergranular liquid,
27
28　　• intergranular fluid inclusions are unimportant,
29
30　　• the Salado has permeability high enough that gas generated by microbial action will
31　　　dissipate, and pressure will not build up,
32
33　　• fluid flow and transport of radionuclides in Salado are negligible,
34
35　　• natural processes are not likely to release radionuclides,
36
37　　• the Culebra is the most important unit above the Salado,
38
39　　• the Culebra hydrology is relatively simple,
40
41　　• based on available batch K_d measurements and the assumption of porous-medium
42　　　flow, retardation in Culebra is assumed, and
43
44　　• WIPP-12 leads to rotation of panels away from encountered brine reservoir.

MASS.2.4 Conceptual Models Developed During Site Characterization and Development (1982 - Present)

The repository horizon was selected in 1982 after the initial shaft was sunk and after design of the repository had been established. The horizon was selected based on the preliminary design of the repository, salt thickness above and below the excavations, and ease of mining. The DOE wanted (a) the mine to be at least 300 feet (91 meters) below the McNutt Potash Zone (hereafter referred to as McNutt) to provide isolation from possible mining, (b) anhydrite bed or clay seams within the back (roof) to be at least 2 to 3 feet (0.6 to 0.9 meters) above the repository to reduce the possibility of roof fall, and (c) the mine to be as shallow as possible to minimize mining costs. The horizon selected between Marker Bed (MB) 138 and MB139 was deemed to best satisfy all of these criteria.

Experiments to investigate rock mechanics and salt creep were started in the initial underground excavations. Some brine was observed seeping into the repository from boreholes drilled upward into the back and collected in downward boreholes. Some brine was also observed on some freshly excavated surfaces. These observations led to significant changes in the conceptual models of WIPP performance.

The concern was raised that the waste would not become encapsulated in a solid mass by salt creep, because brine that had seeped in would impede such consolidation. Information about the rate of brine flow showed that concerns about the waste becoming fluidized were unrealistic because consolidation to a sufficiently low porosity would occur before significant amounts of brine could accumulate. However, a new series of tests was executed to validate beliefs about the hydraulic properties of the Salado that had been based on surface-based testing conducted in the late 1970s. This series of tests included the Small-Scale Brine Inflow, Brine Sampling and Evaluation Program (BSEP), Room Q, in-situ permeability tests, and laboratory flow tests. Some of these test programs continued until their conclusion in 1995.

The in-situ permeability tests showed that intergranular fluids were involved in flow and also demonstrated that the drill-stem tests conducted in the 1970s had overestimated the permeability of the Salado. These results led to the realization in the late 1980s that gas dissipation in the Salado would not be sufficient to avoid the potential for high pressures. Brine seepage into the repository raised the possibility of gas generation by corrosion of steel in addition to microbial gas generation. A new program to characterize gas generation began in the late 1980s.

Because of gas generation and low permeabilities in the far-field Salado, it was thought that high pressure in the repository could induce the Salado to fracture. This topic had been of concern in the 1970s when microbial gas generation was investigated. The renewed concern about gas generation led to a program to investigate hydrofracturing of the Salado interbeds by high pressure, and eventually to the adoption of a fracturing model in performance assessment.
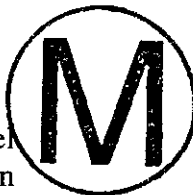
1   Inadvertent penetration of the repository by deep drilling and the resultant release of
2   radionuclides directly to the surface were treated deterministically in early evaluations of
3   long-term performance. The promulgation of 40 CFR Part 191 made it necessary to consider
4   the possibility of multiple boreholes and their interactions. The combination of brine
5   saturation in the repository and possible high gas pressures led eventually to two new
6   postulated mechanisms for release to the surface—gas spall (release of fine particulates
7   caused by high gas pressures and flows from the waste to the penetrating borehole) and direct
8   brine release to the surface during drilling—in addition to the cuttings and cavings releases
9   that had been modeled previously.

10

11 Actinide solubilities were not considered important until the mid-to-late 1980s. Before this
12 time, the DOE's expectation that the repository would be dry made aqueous concentrations
13 seem unimportant. From early on, the DOE had considered adding getters (materials that act
14 to remove radionuclides) to the repository, not so much to control actinide mobility as to
15 assure performance (for example, Tyler et al. 1988). From the mid-to-late 1980s, however,
16 the importance of actinide solubilities has been increasingly recognized in conjunction with
17 the importance of release pathways involving fluid flow from the repository. Direct control of
18 repository chemistry is more effective in controlling actinide solubilities than getters.

19

20 Transport of actinides in colloidal forms was recognized as potentially important by the late
21 1980s, but, because of lack of understanding, no allowance for the possible impact of actinide
22 transport was made in the ranges chosen for actinide solubilities in early performance
23 assessments. The effect of transport of actinides in colloidal forms was not explicitly modeled
24 until the calculations for this application.

25

26 From the time of the initial conceptual design and the 1980 Final Environmental Impact
27 Statement (FEIS) (DOE 1980), it was assumed that backfill would be emplaced in the
28 repository to help fill the void space and reduce the magnitude of subsidence in overlying
29 units, in addition to eliminating any potential risk of underground fire propagation. The WIPP
30 Final Safety Analysis Report (DOE 1990) showed that there was no significant chance of fire
31 propagation in the waste disposal region even in the absence of backfill. The Backfill
32 Engineering Analysis Report (Westinghouse Electric Corporation, 1996) showed that addition
33 of backfill would have negligible impact on the subsidence of overlying units. For a time,
34 therefore, backfill was not considered as part of the baseline design for the repository.
35 Recently, the addition of a carefully designed backfill to control chemical conditions in the
36 repository has been shown to have significant benefit in assuring lower actinide solubilities.

37

38 Because of the possibility of high gas pressure in the repository and the associated possibility
39 of fracturing of the Salado, it became apparent in the late 1980s that effective isolation of
40 radionuclides from the anhydrite interbeds close to the repository could not be fully assured.
41 Because the anhydrite interbeds were known to be relatively more permeable than the halite-
42 rich horizons of the Salado, recognizing that the DRZ was not likely to heal effectively
43 increased the potential importance of interbeds passing through the DRZ with respect to fluid
44 flow in the Salado.

1   Panel closures were designed to isolate panels from each other during waste operations. For a
2   time, in recognition of the concept that DRZ healing could not be relied upon to isolate
3   interbeds from the repository and that fluids might flow around panel closures, these closures
4   were essentially assumed not to exist for evaluations of long-term performance. This
5   treatment was unrealistic, however, and the more reasonable idea that panel closures should
6   be modeled with properties similar to those assigned to the imperfectly healed DRZ emerged.
7
8   The conceptual design of shaft seals evolved during the 1980s. The long-term ability of the
9   shaft seals to isolate the repository from overlying units had been credited to a salt component
10   to be emplaced throughout much of the Salado. The salt-based component would consolidate
11   under the pressure of salt creep and, over a period of a hundred to several hundred years,
12   would develop properties similar to that of intact salt. However, control of brine flow to the
13   salt seal from upper units was of concern because significant volumes of brine could delay or
14   even prevent creep consolidation of the long-term seal components of crushed salt. The early
15   concepts of shaft construction, which used a concrete and concrete-grout plug to protect the
16   salt component, were not thought to be robust enough to control downward brine flow and,
17   possibly in the long term, might be susceptible to damage by the flow. This concern led to a
18   design and testing program to develop the present shaft seal concept, which is based on the
19   principle that multiple components and multiple materials provide demonstrable protection of
20   long-term components from downward brine flow and support a high level of confidence in
21   the expected behavior of shaft seals.
22
23   Test programs in the units above the Salado have been in progress continuously since site
24   selection. The preeminent importance of the Culebra as a lateral pathway for transport has
25   been recognized by the DOE. The Rustler and Salado contact was demonstrated to be
26   unimportant, and the Magenta was demonstrated to have generally lower conductivity than the
27   Culebra and not to have hydraulically significant fractures that could channel flow. Although
28   the Rustler was characterized to some extent throughout its thickness, in the 1980s the interest
29   focused on the Culebra. Transport in the Culebra has been demonstrated to be controlled by
30   the variation in hydraulic conductivity and by interaction between flow in fractures and flow
31   in matrix. Increasingly complex tests were conducted to characterize the Culebra, including
32   multi-well tracer tests and regional pumping tests, culminating in the recent seven-well tracer
33   test conducted at H-19, multiwell retesting at H-11, and distinctive single-well injection and
34   withdrawal tests at both H-19 and H-11. Testing at these localities provided new, high-quality
35   test results at two relatively high-permeability locations in the Culebra. Increasingly complex
36   modeling techniques were used to represent the characterized variability and residual
37   uncertainty in the transmissivity of the Culebra, assisted by review and advice from the
38   Geostatistics Expert Group, a panel convened by the DOE, and INTRAVAL, an international
39   model validation review group. Effective chemical and physical retardation was no longer
40   assumed but became the subject of study, and by the early 1990s several alternative
41   conceptual models had been advanced and were implemented in the preliminary performance
42   assessments (WIPP Performance Assessment Department 1993, 8-27 to 8-56). One of these
43   has since been identified as superior to the others (see Section MASS.15).
44

1 In the Dewey Lake, above the Rustler, boreholes occasionally produce groundwater but,
2 because it had long been assumed that groundwater in the Dewey Lake is in discontinuous
3 lenses and that regional flow does not occur, characterizing groundwater in the Dewey Lake
4 was a low priority for the DOE. When performance assessments in 1994 showed that long-
5 term releases to the Dewey Lake are unlikely because the Culebra captures all fluids moving
6 upward through the Rustler in a borehole, further characterization of the Dewey Lake was
7 perceived as unimportant. Recently, the DOE has recognized that a continuous water table
8 may exist in the Dewey Lake, but it is observed only in areas where permeabilities are
9 relatively higher than average. Nevertheless, if releases into the Dewey Lake occur, they will
10 be of little consequence, because, as a red bed, the Dewey Lake has a uniformly distributed
11 and large sorption capacity as the result of the widespread occurrence of both hydrated iron
12 oxides and clays.
13
14 In the Castile, geophysical techniques were used to help resolve whether brine reservoirs like
15 that encountered at WIPP-12 might exist under the waste panels. In the late 1980s, these
16 techniques indicated a zone of lower resistivity that can be interpreted as brine. This zone
17 exists under a portion of the waste disposal area.
18
19 In addition to experimental programs, the development of probabilistic performance
20 assessments for the WIPP also led to a considerable effort to characterize the consequences of
21 combinations of events and processes. One notable development was the identification of the
22 need to model the effects of multiple intrusions into the repository, some of which might
23 penetrate brine reservoirs, and the possible interactions among these intrusions in a partially
24 saturated repository. This development led to the identification of the scenarios currently in
25 use.
26
27 Thus, by the late 1980s, the conceptual model for the disposal system had changed
28 considerably from that of the late 1970s to mid-1980s. Rather than a fairly simple repository
29 horizon that encapsulated waste rapidly and was thereafter relatively stable, as envisioned
30 through 1985, the first WIPP preliminary performance assessment in 1989 recognized that the
31 long-term conditions in the disposal system depended critically on the interplay between
32 various natural, excavation-induced, and waste-related processes, and the final condition
33 depended closely on the relative rates of these processes. Although some changes have
34 occurred since 1989—for example, uncertainty about many aspects of the disposal system has
35 been substantially reduced through experimental programs and some new release processes
36 have been identified and incorporated—the overall conceptual model recognized in the late
37 1980s remains valid today:
38
39   • the waste horizon is not effectively isolated from nearby interbeds,
40
41   • the repository is partially to fully saturated with liquid,
42
43   • gas generation is closely linked to other processes,
44

- creep closure occurs but does not assure complete consolidation,

- brine inflow from the Salado is likely,

- high gas pressures in the repository could induce fracturing of Salado interbeds,

- actinide solubilities and colloid actinides are important,

- borehole-repository-brine reservoir intersections are possible,

- multiple intrusions allow the possibility of cross-borehole flow,

- the Culebra is the most transmissive upper unit, and releases through other units are unlikely, and

- Culebra transport is complex, fractures are important, and retardation is sensitive.

This list of the major concepts developed in the late 1980s has driven the selection of subsequent experimental programs and determined the types of modeling done in performance assessment from 1989 onward. Since 1989, details have changed, but the overall concept of long-term performance has remained stable. The models described in Chapter 6.0 (Section 6.4) of this application and further described in this appendix are based on this overall conceptual understanding of disposal system interactions.

MASS.3 General Assumptions in Performance Assessment Models

Several assumptions are applied generally to the disposal system through the conceptual and mathematical models implemented in the major computer codes used in this performance assessment. Several major assumptions are discussed here. A table of general assumptions is also presented in Section MASS.3.4.

MASS.3.1   Darcy's Law Applied for Fluid Flow Calculated by BRAGFLO, SECOFL2D, and SECOTP2D

A mathematical relationship expressing the flux of fluid as a function of hydraulic head gradients applied, commonly known as Darcy's Law, is applied to geologic media for all fluid flow calculations. For details about the specific formulation of Darcy's Law used, refer to Appendix BRAGFLO for the disposal system modeling, and Appendices SECOFL2D and SECOTP2D for Culebra modeling. Darcy's Law is not applied for flow up a borehole that is being drilled (see Section MASS.16.2 and Chapter 6.0, Section 6.4.7.1.1, for more discussion of this topic).
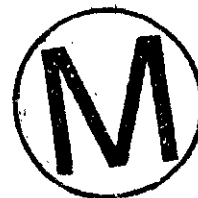
1   Darcy's Law generally applies for flow models if certain conditions are satisfied: (1) the flow
2   occurs in a porous medium with interconnected porosity, (2) flow velocities are low enough
3   that viscous forces dominate inertial forces, and (3) a threshold hydraulic gradient is exceeded.
4
5   Hydraulic tests in the Salado (Beauheim et al. 1991; 1993) were carefully designed to limit the
6   effects of outside influences on the tested interval and provide the best evidence for the
7   controlling flow mechanism in the Salado. The tests influence rock as far as 33 feet
8   (10 meters) from the test zone and are not thought to significantly alter the pretest conditions
9   of most of the tested region. The stratigraphic intervals tested include halite (both pure and
10   impure) and anhydrite with associated clay seams at distances from 3 to 75 feet (1 to 23
11   meters) from the repository. Because tests close to the repository are within the DRZ, tests
12   farthest from the repository are considered more representative of undisturbed conditions.
13
14   The tests are interpreted using potentiometric flow models incorporating Darcy's Law.
15   Successful interpretations using these models are obtained and indicate a continuous porous
16   medium that can be hydraulically characterized with permeability, pore compressibility, and
17   porosity parameters. Tests in pure halite yield ambiguous interpretations, indicating either
18   very low permeability or no flow whatsoever (a potential violation of the applicability of
19   Darcy's Law). However, the effects of the pure halite layers on the performance of the
20   repository have been demonstrated to be small (see below). Thus, the regions of importance
21   to the performance of the repository have been tested, appear to meet the criteria for Darcy
22   flow, and can be assumed to behave as continuous porous media that obey Darcy's Law.
23
24   Bear (1972, 125) discusses the balance of viscous and inertial forces in fluid flow. The
25   Reynold's number, Re, is the ratio of inertial to viscous forces. For porous media, Re is
26   calculated as

$$Re = \frac{qd}{v} ,$$

27   where q is the specific discharge in units of length per time, d is some length dimension of the
28   porous matrix, and v is the kinematic viscosity of the fluid in units of length squared per time
29   ($v = \mu/\rho$, where ρ is fluid density and μ is dynamic viscosity). In principle, d is related to the
30   length of elementary channels in the porous medium. Because of the difficulty of establishing
31   this length, however, it is customary to use some measure of the pore grain size for d.
32   Alternatively, Collins (1961) suggests $d = (k/n)^{1/2}$, where k is permeability in units of length
33   squared, and n is porosity. The upper limit for application of Darcy's Law is not exceeded if
34   Re is less than some number between 1 and 10 (Bear 1972, 126).
35
36   The specific discharge above which the models of fluid flow might be invalid can be
37   estimated for the WIPP. The maximum d in the BRAGFLO domain, by Collins' method, is
38   approximately 2×10^{-4} centimeters (calculated for the waste disposal region, using an assumed
39   permeability of 1×10^{-12} square meters $= 1 \times 10^{-8}$ square centimeters and an assumed porosity
40   of 0.2). Salado brine has a dynamic viscosity of 2.1×10^{-2} grams per centimeter per second; a

density of 1.22 grams per cubic centimeter, for a kinematic viscosity of 0.017 grams per cubic centimeter per second. Taking Re equal to 1 as the critical indicator, the critical specific discharge is the ratio of v to d, and has a value approaching 100 centimeters per second. As all specific discharges of brine in the BRAGFLO model are significantly less than this value, viscous forces dominate brine flow in the model and the upper limit of the validity of Darcy's Law is not exceeded.

For gas in the WIPP, assumed to have the properties of hydrogen for this calculation, density is about 8.2×10^{-5} grams per cubic centimeter and dynamic viscosity is about 89.2×10^{-6} grams per centimeter per second, for a kinematic viscosity of about 1.1 square centimeter per second. The critical specific discharge for gas in the BRAGFLO model is greater than 5,000 centimeters per second. In WIPP simulations of gas flow, q for gas remains below this value, indicating that the upper limit for the validity of Darcy's Law for gas is not exceeded.

Bear (1972, 128) proposes that a minimum hydraulic gradient, the threshold hydraulic gradient, exists below which flow in porous media does not occur. The minimum gradient may be required to overcome countercurrents that may occur at very low velocities, or may be required to overcome the slight nonNewtonian behavior of the viscosity of water. In general, this behavior is evident in fine-grained, low permeability rock such as clay. Because the WIPP is situated in the low-permeability Salado, flow may not be able to occur through the Salado unless a minimum hydraulic gradient is exceeded. Testing for a minimum hydraulic gradient is extremely difficult, however, and therefore has not been attempted at the WIPP.

Except for pure halite, Salado intervals tested at the WIPP have responded to hydraulic testing, and test results can be interpreted to high certainty using models based on Darcy's Law without correcting for the existence of minimum hydraulic gradients. This is strong evidence that the standard Darcy's Law is applicable in these units. In hydraulic tests of the pure halite, no hydraulic response to induced pressure change in the test zone was observed. Two explanations are offered for the results observed during the test. Either (1) the pure halite has a permeability low enough that a hydraulic response could not be measured over the duration of the test, or (2) a high threshold gradient for fluid flow exists in pure halite and was not exceeded during the test in rock around the test interval.

Although the reason for the lack of response in pure halite during flow tests is not established conclusively, its behavior can be approximated in continuum models of fluid flow based on Darcy's Law by assigning it an extremely low permeability relative to other rocks units, which effectively prevents flow through the volume that represents pure halite. This technique assumes the gradients calculated during modeling in the pure halite interval will not exceed the threshold gradient for flow, if it exists. For performance assessment modeling, this assumption is sound given that relatively large gradients were imposed on the unit during hydraulic testing and did not induce flow. Christian-Frear and Webb (1996) analyzed the effects of the variation in lithologic types, including pure halite, in a model of the Salado surrounding the repository. In their study, they found that the hydrologic response of the Salado to the presence of the repository was adequately represented by the simplified

1 stratigraphic representation that is implemented in BRAGFLO. Thus, even though the lack of
2 hydraulic response in pure halite units is not conclusively explained, the hydraulic
3 characterization of pure halite intervals is adequate for an accurate assessment of WIPP
4 performance.
5
6 Darcy's Law assumes laminar flow, that is, there is no motion of the fluid at the fluid/solid
7 interface. For liquids, it is reasonable to assume laminar flow under most conditions. For
8 gases at low pressure, however, gas molecules near the solid interface may not have intimate
9 contact with the solid and may have finite velocity, not necessarily zero. This effect, which
10 results in additional flux of gas above that predicted by application of Darcy's Law, is known
11 as the slip phenomenon, or Klinkenberg effect (Bear 1972, 128). A correction to Darcy's Law
12 for the Klinkenberg effect is incorporated into the BRAGFLO model (see Appendix
13 BRAGFLO, Section 4.12, for additional details).
14
15 Darcy flow for one and two phases implies that values for certain parameters must be
16 specified. Some principal parameters relate to the properties of the fluid, others to the rock.
17 Fluid properties in the Darcy flow model used for the WIPP are its density, viscosity, and
18 compressibility. Rock properties in Darcy flow models are porosity, permeability, and
19 compressibility (pore, bulk, or rock). In BRAGFLO, other parameters are required to describe
20 the interactions or interference between the two phases present in the model, gas and brine,
21 because they can occupy the same pore space. In the WIPP application of Darcy flow models,
22 compressibility of both the liquid and rock are related to porosity through a dependence on
23 pressure. Fluid density, viscosity, and compressibility are functions of fluid composition,
24 pressure, and temperature. In BRAGFLO, fluid viscosity is a function of pressure, but its
25 density and compressibility are held constant. Fluid composition for the purposes of modeling
26 flow and transport is assumed to be constant.
27
28 *MASS.3.2   Hydrogen Gas as Surrogate for Waste-Generated Gas Physical Properties in*
29 *   BRAGFLO*
30
31 The gas phase in the BRAGFLO model is assigned the properties of hydrogen because
32 hydrogen will, under most conditions reasonable for the WIPP, be the dominant component of
33 the gas phase.
34
35 Hydrogen gas is produced by the corrosion of steel in the repository by water or brine.
36 Because of the surface area, the total mass of steel emplaced, and the quantity of brine that is
37 reasonably expected to flow into the repository from the Salado, as much as 0.3×10^6 moles
38 of hydrogen per year can be generated in the repository and 2×10^9 total moles of hydrogen
39 (Wang 1995).
40
41 Other gases may be produced by processes occurring in the repository. If microbial
42 degradation occurs, a significant amount of CO_2 and CH_4 will be generated by microbial
43 degradation of cellulosics, and, perhaps, plastics and rubbers in the waste. CO_2 produced,
44 however, will react with MgO backfill and cementitious materials to form $MgCO_3$ and

1    $CaCO_3$, thus resulting in very low CO_2 fugacity in the repository. Although other gases exist
2   in the disposal system, for BRAGFLO calculations it is assumed these gases are insignificant
3   and are not included in the model.
4
5   With the average stoichiometry gas generation model, the total number of moles of gas
6   generated will be the same whether the gas is considered to be pure H_2 or a mixture of several
7   gases, because the generation of other gases is accounted for by specifying the stoichiometric
8   factor y. Therefore, considering the moles of gas generated alone, the pressure buildup in the
9   repository will be approximately the same, because the expected gases behave similarly to an
10   ideal gas, even up to lithostatic pressures.
11
12   The effect of assuming pure H_2 instead of a mixture of gases (including H_2, CO_2, H_2S and
13   CH_4) on flow behavior, and its resulting impact on the WIPP repository pressure is presented
14   as follows:
15
16   Radial flow of a 100 percent saturated rock with nonideal gas is described by Darcy's Law
17   (Amyx et al. 1960):

$$q_b = 1.988 \times 10^{-5} \left[\frac{T_b z_b}{P_b} \frac{kh \left(P_e^2 - P_w^2\right)}{\mu_{avg} z_{avg} \ln\left(\dfrac{r_e}{r_w}\right)} \right], \tag{2}$$

18   which can be rewritten:
19

$$P_e^2 - P_w^2 = \frac{q_b}{1.988 \times 10^{-5}} \left[\frac{P_b}{T_b z_b} \frac{\mu_{avg} z_{avg} \ln\left(\dfrac{r_e}{r_w}\right)}{kh} \right], \tag{3}$$

20   where:
21   q   =   gas flow rate, cubic feet per day at base (reference) conditions
22   T   =   temperature, K
23   P   =   pressure, pounds per square inch atmosphere
24   k   =   permeability, millidarcys
25   h   =   height, feet
26   μ   =   viscosity, centipoises
27   z   =   gas compressibility factor (a function of gas pressure and temperature)
28   r   =   radius, consistent units
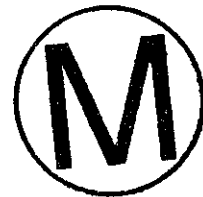
1　e　=　external boundary (repository)
2　w　=　internal boundary (wellbore)
3　b　=　base or reference conditions for gas (temperature, pressure, compressibility factor)
4　avg　=　average properties between external and internal boundaries because u and z are
5　　　　　functions of pressure which change with time.
6
7　This expression is very useful for looking at the relationships of gas properties (specifically μ
8　and z [which is a function of the gas temperature and pressure]) and rock properties (namely
9　k) on defining q and P.
10
11　In order to evaluate the effect of gas composition on q and P, a computer program developed
12　by the National Institute of Standards and Technology (NIST) entitled SUPERTRAPP was
13　used (NIST 1992). This computer program allows calculations of gas properties for 116 pure
14　fluids and mixtures of up to 20 components for temperatures to 1,000 K and pressures to 300
15　megapascals. The computer program currently can evaluate hydrogen, CO_2, and water but
16　does not have the capacity to evaluate brine (Friend and Huber 1994). In analyzing gas flow, it
17　is assumed that CH_4 will behave similarly to CO_2. Because such small quantities of H_2S are
18　anticipated at the WIPP, its impact will be neglected. Therefore, for this evaluation only the
19　impact of CO_2 is considered.
20
21　Figure MASS-1 shows the relationship between gas viscosity for various mole fractions of H_2
22　at pressures of 7 megapascals and 15 megapascals as determined from SUPERTRAPP. The
23　viscosity at 50 percent mole fraction H_2 is 2.3 times greater than for 100 percent mole fraction
24　H_2. As shown in Equation 2, viscosity has an inverse relationship to flow rate and, as shown
25　in Equation 3, a direct relationship to the square of the repository pressure. Hence viscosity
26　differences that would result if gas properties other than those of hydrogen were incorporated
27　would result in a decrease in flow rate and potentially higher pressures.
28
29　As shown in Figure MASS-2, the gas compressibility at 50 percent mole fraction H_2 is about
30　0.9 times that at 100 percent mole fraction H_2. Like viscosity, the gas compressibility factor is
31　inversely related to flow rate and directly related to the square of the repository pressure.
32　Hence changing composition from 100 percent to 50 percent H_2 would result in a slight
33　increase in flow rate and a decrease in pressure. Therefore, the impact of variation in gas
34　compressibility caused by composition is considered minor and so is neglected.
35
36　The absolute permeability of the surrounding formation plays a significant part with respect to
37　both flow rate and pressure determinations. Because marker bed permeabilities range over
38　four orders of magnitude (see Appendix PAR, Parameter 20), these primary flow pathways
39　will have a greater influence on pressure and flow rate determinations compared to either
40　uncertainty in viscosity or gas compressibility effects.
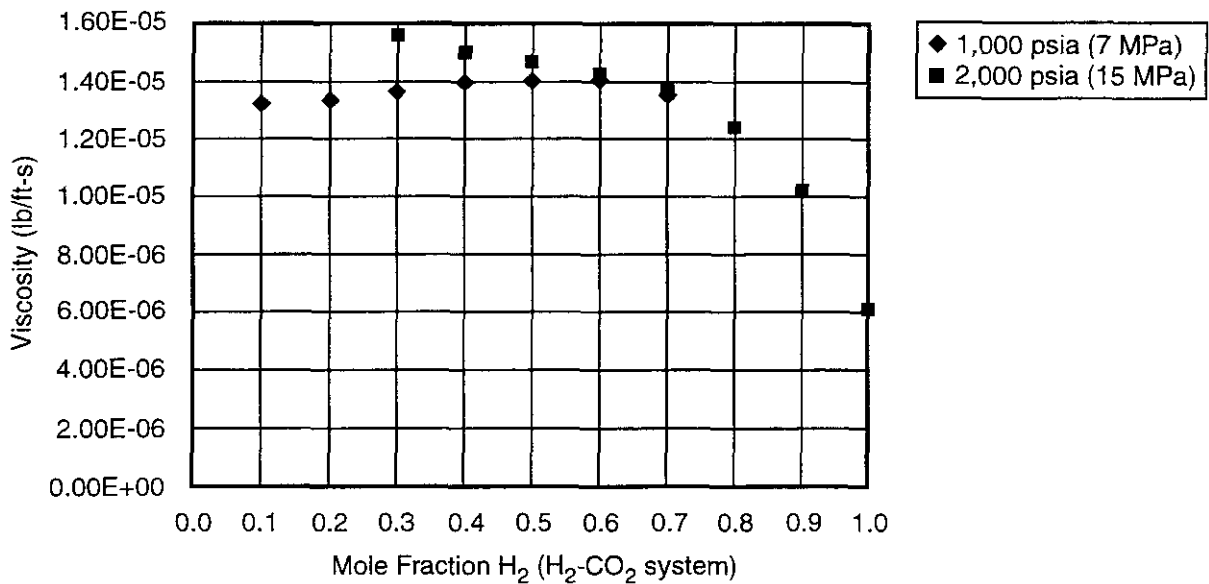
CCA-MAS003-0

Figure MASS-1. Gas Viscosity as a Function of Mole Fraction H_2 at 7 Megapascals and 15 Megapascals Pressure

1 **THIS PAGE INTENTIONALLY LEFT BLANK**
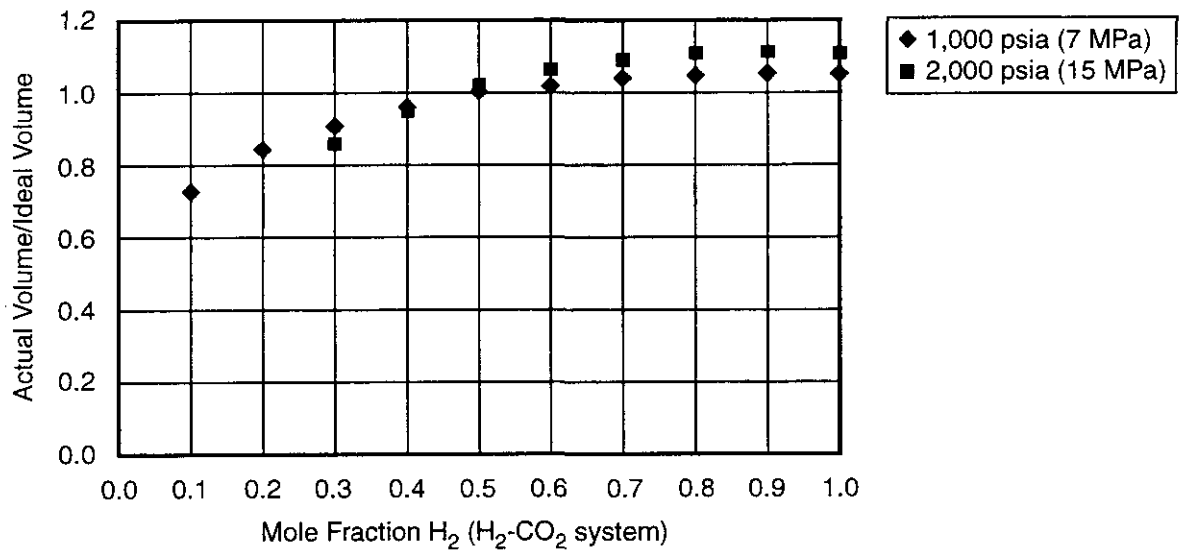
CCA-MAS002-0

Figure MASS-2. Gas Compressibility as a Function of Mole Fraction H₂

1
2

THIS PAGE INTENTIONALLY LEFT BLANK
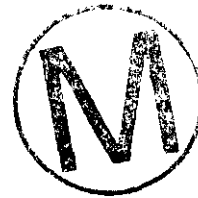
1   *MASS.3.3 Salado Brine as Surrogate for Liquid Phase Physical Properties in BRAGFLO*
2
3   BRAGFLO models physical properties for all liquids as Salado brine properties. However,
4   liquid in the modeled region may consist of (1) brine originally in the Salado, (2) liquid
5   introduced in the excavation during construction, maintenance, and ventilation during the
6   operational phase, (3) a very small amount of liquid introduced as a component of the waste,
7   (4) liquid from overlying units, and (5) liquid from the Castile brine reservoir. However, for
8   BRAGFLO modeling it is assumed that the properties of all of these liquids are similar
9   enough to Salado brine properties that the effect of variation in properties that may occur from
10 liquids mixing is negligible. The properties required by BRAGFLO, and the subject of the
11 discussion here, are density, viscosity, and compressibility.
12
13 Following repository closure, Salado brine will flow toward the repository at a rate that
14 depends on the properties of the rock and brine, as well as hydraulic gradients. Brine flowing
15 into the repository from the Salado is an important, sometimes dominant, source of liquid in
16 the repository following closure. Because Salado brine is the only important source of brine
17 that is present in all scenarios, it is assumed that the properties of brine important in the
18 BRAGFLO model are the same as those of Salado brine.
19
20 During construction of the repository, water was spread for dust control. This water
21 principally consisted of groundwater from the Culebra collected in the sumps and
22 manufactured brine purchased from a local vendor. The physical properties of Salado brine as
23 a surrogate for this Culebra brine are adequate because (1) the two brines have similar original
24 physical properties, (2) the introduced brine will have equilibrated with liquid in the Salado
25 and by dissolution, (3) some of the introduced liquid has evaporated, and (4) the volume
26 introduced is relatively small.
27
28 Introduction of liquid through respiration in the repository is also considered insignificant.
29 Because of the dry climate in the region, air drawn in from the surface and circulated through
30 the repository is normally undersaturated in water vapor. In addition, the relative humidity of
31 mine air is less than the equilibrium humidity of water in the mine environment. Thus, this
32 liquid vapor remains in the vapor state until it is removed from the repository through forced
33 circulation up the ventilation shaft.
34
35 The density difference among Salado brine, Castile brine, and brine from overlying units is
36 the result of varying dissolved mineral content. Castile brine contains essentially sodium
37 chloride (NaCl), while the Salado brine is saturated with approximately one-half sodium
38 chloride and one-half magnesium chloride. Brine from overlying units is consistently fresher.
39 Densities for WIPP brines were measured and reported by Brush (1990). The specific gravity
40 of Salado and Castile brines are very similar and vary between 1.215 to 1.23 grams per cubic
41 centimeter. Brines from the units above the Salado have lower specific gravity (for example,
42 the specific gravity of Culebra brine is about 1.09 grams per cubic centimeter [WIPP
43 Performance Assessment Division 1991]).
44

1 The viscosity of Salado brine is approximately 1.8×10^{-3} cp; for Culebra brine, the viscosity is
2 approximately 1×10^{-3} cp (WIPP Performance Assessment Division 1991). Because of their
3 similar specific gravity, it is expected that the viscosity of Castile and Salado brines is similar.
4
5 The ratio of density to viscosity appears in flow equations. The maximum difference of these
6 is close to a factor of two for the three types of brines. Compressibilities range from
7 approximately 2×10^{-10} per pascal for Culebra brine (for this discussion the range is assumed
8 to be similar to that of water) to 2.5×10^{-10} per pascal for Salado brine and 9×10^{-10} per pascal
9 for Castile brine (WIPP Performance Assessment Division 1991). The differences in the
10 physical properties among these brines are considered insignificant with regard to the position
11 of complementary cumulative distribution functions (CCDFs) because the variability of these
12 values is relatively small (factors of two or three, without considering blending effects of
13 mixing), and CCDFs are typically plotted in log-log format with many log cycles. Therefore,
14 these differences are assumed negligible in the performance assessment. (Note that variability
15 in chemical properties of these brines is accounted for, as discussed in Chapter 6.0, Sections
16 6.4.3.4 and 6.4.3.5, and Appendix SOTERM, Section SOTERM.2.2.1.)
17
18 *MASS.3.4 Table of General Modeling Assumptions*
19
20 This section presents Table MASS-1, which lists modeling assumptions used in the
21 performance assessment. Table MASS-1 is a guide to general modeling assumptions used
22 and provides some guidance for integrating the assumptions made with (a) the chapters or
23 appendices in which they are discussed and (b) the code(s) that implement these assumptions.
24 The features, events, and processes (FEPs) discussed in Appendix SCR that are relevant to the
25 assumptions are also indicated. The final column in the table indicates whether the DOE
26 considers the assumption described to be reasonable or conservative. As discussed in Chapter
27 6.0 (Section 6.5), the DOE has not attempted to bias the overall results of the performance
28 assessment toward a conservative outcome. However, where data or models are infeasible to
29 obtain, or where effects on performance are not expected to be significant enough to justify
30 development of a more complicated model, the DOE has chosen to use conservative
31 assumptions. The designator R (reasonable) in the final column indicates that the DOE
32 considers the assumption to be reasonable based on WIPP-specific data or information, data
33 and information considered analogous to the WIPP disposal system, expert judgment, or other
34 reasoning. The designator C (conservative) indicates the DOE considers the assumption made
35 may overestimate a process or effect that may contribute to releases to the accessible
36 environment. The regulatory designator (Reg) indicates that the assumption is based on
37 regulations in 40 CFR Part 191, criteria in 40 CFR Part 194, or other regulatory guidance.
38
39 **MASS.4 Model Geometries**
40
41 This section presents supplementary information on the disposal system geometry presented in
42 Chapter 6.0 (Section 6.4.2), as modeled by the code BRAGFLO, and the Culebra flow and
43 transport geometries used, as modeled by the codes SECOFL2D and SECOTP2D.
44

Table MASS-1. General Modeling Assumptions

CCA Section and Appendix	Code	Modeling Assumption	Related FEP in Appendix SCR	Assumption Considered*
MASS.3 Some General Assumptions in Performance Assessment Models				
MASS.3.1 Darcy's Law Applied for Fluid Flow calculated by BRAGFLO, SECOFL2D, and SECOTP2D				
1	BRAGFLO SECOFL2D	Flow is governed by mass conservation and Darcy's Law in porous media. Flow is laminar and fluids are Newtonian.	Saturated groundwater flow Unsaturated groundwater flow Brine inflow	R
2	BRAGFLO	Two-phase flow in the porous media is by simultaneous immiscible displacement.	Fluid flow caused by gas production	R
3	BRAGFLO	The Brooks-Corey or Van Genuchten/Parker equations represent interaction between brine and gas.	Fluid flow caused by gas production	R
4	BRAGFLO	The Klinkenberg effect is included for flow of gases at low pressures.	Fluid flow caused by gas production	R
5	BRAGFLO	Threshold displacement pressure for flow of gas into brine is constant.	Fluid flow caused by gas production	R
6	BRAGFLO SECOFL2D SECOTP2D	Fluid composition and compressibility are constant.	Saturated groundwater flow Fluid flow caused by gas production	R
MASS.3.2 Hydrogen Gas as Surrogate for Waste-Generated Gas Physical Properties in BRAGFLO				
7	BRAGFLO	The gas phase is assigned the density and viscosity properties of hydrogen.	Fluid flow caused by gas production	R
MASS.3.3 Salado Brine as Surrogate for Liquid Phase Physical Properties in BRAGFLO				
8	BRAGFLO	All liquid physical properties are assigned the properties of Salado brine.	Saturated groundwater flow	R

Table MASS-1. General Modeling Assumptions (Continued)

CCA Section and Appendix	Code	Modeling Assumption	Related FEP in Appendix SCR	Assumption Considered*
6.4.2 Model Geometries MASS.4 Model Geometries				
6.4.2.1 Disposal System Geometry MASS.4.1 Disposal System Geometry as Modeled in BRAGFLO				
	BRAGFLO	The disposal system is represented by a two-dimensional, north-south, vertical cross section.	Stratigraphy Physiography	R
	BRAGFLO	Flow in the disposal system is radially convergent or divergent centered on the repository, shaft, and borehole for disturbed performance.	Saturated groundwater flow Unsaturated groundwater flow	R
	BRAGFLO	Variable dip in the Salado is approximated by a 1° dip to the south.	Stratigraphy	R
	BRAGFLO	Stratigraphical layers are parallel.	Stratigraphy	R
	BRAGFLO	The stratigraphy consists of units above the Dewey Lake, the Dewey Lake, the Forty niner, the Magenta, the Tamarisk, the Culebra, the Unnamed Lower Member, and the Salado (comprising impure halite, MB138, anhydrites a and b [lumped together], and MB139). The dimensions of these units are constant. A Castile brine reservoir is included in all scenarios.	Stratigraphy	R
6.4.2.2 Culebra Geometry MASS.4.3 Historical Context of Culebra Geometries as Modeled in SECOFL2D and SECOTP2D				
	SECOFL2D SECOTP2D	The Culebra is represented by a two-dimensional, horizontal geometry for groundwater flow and radionuclide transport simulation.	Stratigraphy	R
	SECOFL2D GRASPINV	Transmissivity varies spatially. There is no vertical flow to or from the Culebra.	Groundwater recharge Groundwater discharge	R

Table MASS-1. General Modeling Assumptions (Continued)

CCA Section and Appendix	Code	Modeling Assumption	Related FEP in Appendix SCR	Assumption Considered*
	SECOTP2D	The regional flow field provides boundary conditions for local transport calculations.	Advection	R
6.4.3 The Repository				
MASS.5 BRAGFLO Geometry of the Repository				
	BRAGFLO	The repository comprises five regions: a waste panel, the panel closures, the remainder of the panels and the access drifts, the operations region, and the experimental region. Also, a single shaft region is modeled, and a borehole region is included for a borehole that intersects the separate waste panel. The dimensions of these regions are constant.	Disposal geometry	R-C
	BRAGFLO	Long-term flow up plugged and abandoned boreholes is modeled as if all intrusions occur into a downdip (southern) panel.	Disposal geometry	C
	BRAGFLO	For each repository region the model geometry preserves design volume.	Disposal geometry	R
	BRAGFLO	Pillars and individual drifts and rooms, and panel closures in the nine lumped panels, are not modeled for long-term performance, and containers provide no barrier to fluid flow.	Disposal geometry	C
	BRAGFLO	The distance from the south end of the modeled waste panel to the modeled shaft is the true distance from the south end of the waste disposal region to the waste handling shaft.	Disposal geometry	R
	BRAGFLO	Long-term flow is radial to and from the borehole that intersects the waste disposal panel during disturbed performance.	Waste-induced borehole flow	R
	BRAGFLO	Panel closures are modeled with the same properties as the surrounding DRZ.	Disposal geometry	C

Table MASS-1. General Modeling Assumptions (Continued)

CCA Section and Appendix	Code	Modeling Assumption	Related FEP in Appendix SCR	Assumption Considered*
6.4.3.1 Creep Closure MASS.6 Creep Closure Appendix PORSURF				
	SANTOS	Creep closure is modeled using a two-dimensional model of a single room. Room interactions are insignificant.	Salt creep Changes in the stress field Excavation-induced changes in stress	R
	SANTOS	Creep closure causes a decrease in room volume which decreases waste porosity. The amount of creep closure is a function of time, gas pressure, and waste matrix strength.	Salt creep Changes in the stress field Consolidation of waste Pressurization	R
	BRAGFLO	Porosity of operations and experimental areas is fixed at a value representative of consolidated material.	Salt creep	R
6.4.3.2 Repository Fluid Flow MASS.7 Repository Fluid Flow				
	BRAGFLO	General assumptions 1 to 8.		See above
	BRAGFLO	The waste disposal region is assigned a constant permeability representative of average consolidated waste without backfill.	Saturated groundwater flow Unsaturated groundwater flow	R
MASS.7.1 Flow Interactions with the Creep Closure Model				
	BRAGFLO	The experimental and operations regions are assigned a constant permeability representative of unconsolidated material and a constant porosity representative of consolidated material.	Saturated groundwater flow Unsaturated groundwater flow Salt creep	R

Table MASS-1. General Modeling Assumptions (Continued)

CCA Section and Appendix	Code	Modeling Assumption	Related FEP in Appendix SCR	Assumption Considered*
MASS.7.2 Flow Interactions with the Gas Generation Model				
	BRAGFLO	For gas generation calculations, the effects of wicking are accounted for by assuming that brine in the repository contacts waste to an extent greater than that calculated by the Darcy flow model used.	Wicking	R
6.4.3.3 Gas Generation MASS.8 Gas Generation Appendix WCA				
	BRAGFLO	Gas generation occurs by anoxic corrosion of steel containers, and Fe and Fe-base alloys in the waste, giving H_2, and microbial degradation of cellulosics and, perhaps, plastics and rubbers, giving mainly CO_2 and CH_4. Radiolysis, oxic reactions, and other gas generation mechanisms are insignificant. Gas generation is calculated using the Average Stoichiometry model, and is dependent on brine availability.	Container material inventory Waste inventory Degradation of organic material Gases from metal corrosion	R
	BRAGFLO	The anoxic corrosion rate is dependent on liquid saturation. Anoxic corrosion of steel continues until all the steel is consumed. Steel corrosion will not be passivated by microbially-generated gases CO_2 or H_2S. Brine is consumed by the corrosion reaction.	Brine inflow Gases from metal corrosion Degradation of organic material	R
	BRAGFLO	Laboratory-scale experimental measurements of gas generation rates at expected room temperatures are used to account for the effects of biofilms and chemical reactions.	Effects of biofilms on microbial gas generation Effects of temperature on microbial gas generation Chemical effects of corrosion	R

Table MASS-1. General Modeling Assumptions (Continued)

CCA Section and Appendix	Code	Modeling Assumption	Related FEP in Appendix SCR	Assumption Considered*
	BRAGFLO	The rate of biodegradation is dependent on the amount of liquid present. It is assumed that biodegradation neither produces nor consumes water. Gas generation by microbial degradation takes place in half the simulations. In half of the simulations with microbial gas generation, microbes consume all of the cellulosics but none of the plastics and rubbers. In the other half of the simulations with microbial gas generation, microbes consume all of the cellulosics and all of the plastics and rubbers. Microbial gas generation will continue until all biodegradable organic materials are consumed if brine is present. The MgO backfill will react with CO_2 and remove it from the gas phase.	Brine inflow Degradation of organic material Waste inventory	R
	BRAGFLO	Gas dissolution in brine is of negligible consequence.	Fluid flow caused by gas production	R
	BRAGFLO	The gas phase is assigned the properties of hydrogen (general assumption 8).	Fluid flow caused by gas production	See above
6.4.3.4 Chemical Conditions in the Repository SOTERM.2 Conceptual Framework of Chemical Conditions				
	NUTS PANEL	Chemical conditions in the repository will be constant. Chemical equilibrium is assumed for all reactions that occur between brine in the repository, waste, and abundant minerals, with the exceptions of gas generation and redox reactions.	Speciation Redox kinetics	R
	NUTS PANEL	Brine and waste in the repository will contain a uniform mixture of dissolved and solid-state species. No microenvironments that influence the overall chemical environment will persist.	Heterogeneity of waste forms Speciation	C

Table MASS-1. General Modeling Assumptions (Continued)

CCA Section and Appendix	Code	Modeling Assumption	Related FEP in Appendix SCR	Assumption Considered*
	NUTS PANEL	For the undisturbed performance and E2 scenarios, brine in the waste panels has the composition of Salado brine. For E1 and E1E2 scenarios, all brine in the waste panel intersected by the borehole has the composition of Castile brine.	Speciation	R
	NUTS PANEL	Chemical conditions in the waste panels will be reducing. However, a condition of redox disequilibrium will exist between the possible oxidation states of the actinide elements.	Redox kinetics Speciation Effects of metal corrosion	R
	NUTS PANEL	The pmH and pCO_2 in the waste panels will be controlled by the equilibrium between brucite and magnesite. (A result of this assumption is low pCO_2 and alkaline conditions).	Speciation Backfill chemical composition	R

6.4.3.5 Dissolved Actinide Source Term
SOTERM.3.3 The FMT Computer Code

	NUTS PANEL	Radionuclide dissolution to solubility limits is instantaneous.	Dissolution of waste	C
	NUTS PANEL	Six actinides (Th, U, Np, Pu, Cm, and Am) are considered for calculations of radionuclide transport of brine. Choice of radionuclides is discussed in Appendix WCA.	Waste inventory	R
	NUTS PANEL	The reducing conditions in the repository will eliminate significant concentrations of Am(V), Pu(V), Pu(VI), and NP(VI) species. Am and Cm will exist predominantly in the III oxidation state, Th in the IV oxidation state. It is assumed that the solubilities and K_ds of Pu, Np, and U will be dominated by one of the remaining oxidation states: Pu(III) or Pu(IV), Np(IV) or NP(V), U(IV) or U(VI).	Speciation Redox kinetics	R

Table MASS-1. General Modeling Assumptions (Continued)

CCA Section and Appendix	Code	Modeling Assumption	Related FEP in Appendix SCR	Assumption Considered*
	NUTS PANEL	For a given oxidation state, the different actinides exhibit similar chemical behavior and thus have similar solubilities.	Speciation	R
	NUTS PANEL	Organic ligands will not significantly affect solubility.	Waste inventory Dissolution of waste Organic ligands Organic complexation	R
	NUTS PANEL	For undisturbed performance and for all aspects of disturbed performance except for cuttings and cavings releases, radionuclide-bearing compounds are distributed evenly throughout the disposal panel.	Waste inventory Heterogeneity of waste forms	R
	NUTS PANEL	Mobilization of actinides in the gas phase is negligible.	Dissolution of waste	R
	NUTS PANEL	Actinide concentrations in the repository will be inventory limited when the mass of an actinide becomes depleted such that the predicted solubilities cannot be achieved.	Dissolution of waste	R
6.4.3.6 Source Term for Colloidal Actinides				
	NUTS PANEL	Four types of colloids comprise the source term for colloidal actinides; microbes, humic substances, intrinsic colloids, and mineral fragments.	Colloid formation and stability Humic and fulvic acids	R
	NUTS PANEL	The only intrinsic colloids that will form are those of the plutonium Pu(IV) polymer.	Colloid formation and stability	R
	NUTS PANEL	Concentrations of intrinsic colloids and mineral fragment colloids are modeled as constants that were based on experimental observations. Humic and microbe colloid actinide concentrations are modeled as proportional to dissolved actinide concentrations.	Colloid formation and stability	R

Table MASS-1. General Modeling Assumptions (Continued)

CCA Section and Appendix	Code	Modeling Assumption	Related FEP in Appendix SCR	Assumption Considered*
	NUTS PANEL	The maximum concentration of each actinide associated with each colloid type is constant.	Actinide sorption	R
6.4.4 Shafts and Shaft Seals MASS.12 Shafts and Shaft Seals				
	BRAGFLO	General Assumptions 1 to 8.		See above
	BRAGFLO	The four shafts connecting the repository to the surface are represented by a single shaft with a cross-section and volume equal to the total volume of the four real shafts and separated from the waste by the distance of the nearest real shaft.	Disposal geometry	R
	BRAGFLO	The seal system is represented by nine materials occupying eleven model regions.	Seal geometry Seal physical properties	R
	BRAGFLO	The shaft is surrounded by a DRZ which heals with time. The DRZ is represented through the permeabilities of the shaft system itself, rather than as a discrete zone. The effective permeability of shaft salt, clay and concrete seals are adjusted several times after closure to reflect consolidation and possible degradation. Permeabilities are constant for asphalt and earthen fill components.	Salt creep Consolidation of seals Disturbed rock zone Microbial growth on concrete Chemical degradation of seals Mechanical degradation of seals	R
	BRAGFLO	Concrete shaft components are modeled as if they degrade 400 years after emplacement.	Mechanical degradation of seals	C
	NUTS	Radionuclides are not retarded by the seals.	Actinide sorption Speciation	C

Table MASS-1. General Modeling Assumptions (Continued)

CCA Section and Appendix	Code	Modeling Assumption	Related FEP in Appendix SCR	Assumption Considered*
6.4.5 The Salado MASS.13 Salado				
	BRAGFLO	General Assumptions 1 to 8.		See above
6.4.5.1 Impure Halite MASS.13.1 High Threshold Pressure for Halite-Rich Salado Rock Units				
	BRAGFLO	Rock and hydrologic properties are constant.	Stratigraphy	R
6.4.5.2 Salado Interbeds MASS.13.3 The Anhydrite Interbed Fracture Model				
	BRAGFLO	Interbeds have a fracture-initiation pressure above which local fracturing and changes in porosity and permeability occur in response to changes in pore pressure. A power function relates the permeability increase to the porosity increase. A pressure is specified above which porosity and permeability do not change.	Disruption caused by gas effects	R
	BRAGFLO	Interbeds have identical physical properties; they differ only in position, thickness, and some fracture parameters.	Saturated groundwater flow	R
6.4.5.3 Disturbed Rock Zone MASS.13.4 Flow in the Disturbed Rock Zone				
	BRAGFLO	The permeability of the DRZ is constant and higher than intact Salado. The DRZ porosity is equal to the porosity of impure halite to plus 0.29 percent.	Disturbed rock zone Roof falls Gas explosions Seismic activity Underground boreholes	C-R

Table MASS-1. General Modeling Assumptions (Continued)

CCA Section and Appendix	Code	Modeling Assumption	Related FEP in Appendix SCR	Assumption Considered*
6.4.5.4 Actinide Transport in the Salado MASS.13.5 Actinide Transport in the Salado				
	NUTS	Dissolved actinides and colloidal actinides are transported by advection in the Salado. Diffusion and dispersion are assumed negligible.	Advection Diffusion Matrix diffusion	R
	NUTS	Sorption of actinides in the anhydrite interbeds, colloid retardation, colloid transport at higher than average velocities, co-precipitation of minerals containing actinides, channeled flow, and viscous fingering are not modeled.	Actinide sorption Colloid transport Colloid filtration Colloid sorption Fluid flow caused by gas production Fracture flow	R
	NUTS	Radionuclides having similar half lives are grouped as discussed in Appendix WCA.	Radioactive decay and ingrowth	R
	NUTS	Sorption of actinides in the borehole is not modeled.	Actinide sorption	C
6.4.6 Units Above the Salado MASS.14 Geologic Units above the Salado				
	SECOTP2D	Above the Salado, lateral actinide transport to the accessible environment can occur only through the Culebra.	Saturated groundwater flow Unsaturated groundwater fkow Solute transport	R
6.4.6.1 Unnamed Lower Member				
	SECOFL2D BRAGFLO	The unnamed lower member, Tamarisk, and Forty-niner are assumed to be impermeable.	Saturated groundwater flow	C
6.4.6.2 The Culebra MASS.15 Culebra Appendix TFIELD				
	SECOFL2D SECOTP2D	General Assumptions 1, 6, and 8.		See above

1
2

Table MASS-1. General Modeling Assumptions (Continued)

CCA Section and Appendix	Code	Modeling Assumption	Related FEP in Appendix SCR	Assumption Considered*
	SECOFL2D SECOTP2D	For fluid flow the Culebra is modeled as a uniform (single-porosity) porous medium. For radionuclide transport a double-porosity model is used (advection in high permeability features and diffusion and sorption in low-permeability features).	Saturated groundwater flow Fracture flow Advection Diffusion	R
	SECOFL2D	The Culebra flow field is determined from the observed hydraulic conditions and estimates of the effects of climate change and potash mining outside the controlled area, and does not change with time unless mining is predicted to occur in the disposal system in the future.	Saturated groundwater flow Climate change Precipitation (for example, rainfall) Temperature Changes in groundwater flow caused by mining	R
	BRAGFLO	The Culebra is assigned a single permeability to calculate brine flow into the unit from an intrusion borehole.	Natural borehole fluid flow Waste-induced borehole flow	R
	SECOFL2D	Gas flow in the Culebra is not modeled. Gas from the repository does not affect fluid flow in the Culebra.	Saturated groundwater flow Fluid flow caused by gas production	R
	BRAGFLO SECOFL2D SECOTP2D	Different thicknesses of the Culebra are assumed for BRAGFLO, SECOFL2D, and SECOTP2D calculations, although the transmissivities are consistent.	Effects of preferential pathways	R
	GRASP-INV	Uncertainty in the spatial variability of the Culebra transmissivity is accounted for by statistically generating many transmissivity fields.	Saturated groundwater flow Fracture flow Shallow dissolution	R
	SECOFL2D BRAGFLO	Potentiometric heads are set on the edges of the regional grid to represent flow in a portion of a much larger hydrologic system.	Groundwater recharge Groundwater discharge Changes in groundwater recharge and discharge Infiltration	R

5

6

7

8

9

10

11

12

Table MASS-1. General Modeling Assumptions (Continued)

CCA Section and Appendix	Code	Modeling Assumption	Related FEP in Appendix SCR	Assumption Considered*
6.4.6.2.1 Transport of Dissolved Actinides in the Culebra				
MASS.15.2 Dissolved Actinide Transport and Retardation in the Culebra				
	SECOTP2D	Dissolved actinides are transported by advection in high-permeability features and diffusion in low permeability features.	Solute transport Advection Diffusion Matrix diffusion	R
	SECOTP2D	Sorption occurs on dolomite in the matrix. Sorption on clays present in the Culebra is not modeled.	Actinide sorption Changes in sorptive surfaces	C
	SECOTP2D	Sorption is represented using a linear isotherm model.	Actinide sorption Kinetics of sorption	R
	SECOTP2D	The possible effects on sorption of the injection of brines from the Castile and Salado into the Culebra are accounted for in the distribution of actinide K_ds.	Actinide sorption Groundwater geochemistry Natural borehole fluid flow	R
	SECOTP2D	Hydraulically-significant fractures are assumed to be present everywhere in the Culebra.	Advection	C
6.4.6.2.2 Transport of Colloidal Actinides in the Culebra				
MASS.15.3 Colloidal Actinide Transport and Retardation in the Culebra				
	SECOTP2D	Humic actinides are chemically retarded identically to dissolved actinides and are treated as dissolved actinides.	Advection Diffusion Colloid transport Microbial transport	R
	SECOTP2D	The concentration of intrinsic colloids is sufficiently low to justify elimination from performance assessment transport calculations.		R
	SECOTP2D	Microbial colloids and mineral fragments are too large to undergo matrix diffusion. Filtration of these colloids occurs in high permeability features (which is modeled using a decay approach). Attenuation is so effective that associated actinides are assumed to be retained within the disposal system and are not transported in SECOTP2D.	Microbial transport Colloid sorption	R

Table MASS-1. General Modeling Assumptions (Continued)

CCA Section and Appendix	Code	Modeling Assumption	Related FEP in Appendix SCR	Assumption Considered*
6.4.6.2.3 Subsidence Due to Potash Mining				
MASS.15.4 Subsidence Caused by Potash Mining in the Culebra				
	SECOFL2D	The effect of potash mining is to increase the hydraulic conductivity in the Culebra by a factor from 1 to 1,000.	Potash mining Changes in groundwater flow caused by mining	Reg.
6.4.6.3 The Tamarisk				
	SECOFL2D BRAGFLO	The Tamarisk is assumed to be impermeable.	Saturated groundwater flow	R
6.4.6.4 The Magenta				
	BRAGFLO	General Assumptions 1 to 8.		See above
	BRAGFLO	The Magenta permeability is set to the lowest value measured near to the center of the WIPP site. This increases the flow into the Culebra.	Saturated groundwater flow	R
	NUTS	No radionuclides entering the Magenta will reach the accessible environment. However, the volumes of brine and actinides entering and stored in the Magenta are modeled.	Solute transport	R
6.4.6.5 The Forty-niner				
	BRAGFLO	The Forty-niner is assumed to be impermeable.	Saturated groundwater flow	R
6.4.6.6 Dewey Lake				
	BRAGFLO	General Assumptions 1 to 8.		See above
	NUTS	The sorptive capacity of the Dewey Lake is sufficiently large to prevent any release over 10,000 years.	Saturated groundwater flow Actinide sorption	R
6.4.6.7 Supra-Dewey Lake Units				
	BRAGFLO	General Assumptions 1 to 8.		See above

Table MASS-1. General Modeling Assumptions (Continued)

CCA Section and Appendix Code		Modeling Assumption	Related FEP in Appendix SCR	Assumption Considered*
	BRAGFLO	The units above the Dewey Lake are a single hydrostratigraphic unit.	Stratigraphy	R
	BRAGFLO	The units are thin and predominantly unsaturated.	Unsaturated groundwater flow Saturated groundwater flow	R
6.4.7 The Intrusion Borehole MASS.16 Intrusion Borehole				
6.4.7.1 Releases During Drilling				
	CUTTINGS_S BRAGFLO_DBR	Any actinides that enter the borehole are assumed to reach the surface.	—	C
MASS.16.1 Cuttings, Cavings, and Spall Releases during Drilling				
	BRAGFLO PANEL CUTTINGS_S	Future drilling practices will be the same as they are at present.	Oil and gas exploration Potash exploration Oil and gas exploitation Other resources Enhanced oil and gas recovery	Reg.
	CUTTINGS_S	Releases of particulate waste material are modeled (cuttings, cavings, and spallings). Releases are corrected for radioactive decay until the time of intrusion.	Drilling fluid flow Suspension of particles Cuttings Cavings Spallings	R
	CUTTINGS_S	Particle waste shear based on properties of marine clays, considered a worst case	Cavings	C
6.4.7.1.1 Direct Brine Release During Drilling MASS.16.2 Direct Brine Releases during Drilling				
	BRAGFLO PANEL	Brine containing actinides may flow to the surface during drilling. Direct brine release will have negligible effect on the pressure and saturation in the waste panel.	Blowouts	R

Table MASS-1. General Modeling Assumptions (Continued)

CCA Section and Appendix	Code	Modeling Assumption	Related FEP in Appendix SCR	Assumption Considered*
	BRAGFLO	A two-dimensional grid (one degree dip) on the scale of the waste disposal region is used for direct brine release calculations.	Blowouts	R
	BRAGFLO	Calculation of direct brine release from several different locations provides reference results for the variation in release associated with location.	Blowouts	R
6.4.7.2 Long-Term Releases Following Drilling MASS.16.3 Long-Term Properties of the Abandoned Intrusion Borehole				
	BRAGFLO	Plugging and abandonment of future boreholes are assumed to be consistent with practices in the Delaware Basin.	Natural borehole fluid flow Waste-induced borehole flow	Reg.
6.4.7.2.1 Continuous Concrete Plug through the Salado and Castile				
	BRAGFLO	A continuous concrete plug is assumed to exist throughout the Salado and Castile. Long-term releases through a continuous plug are analogous to releases through a sealed shaft.	Natural borehole fluid flow Waste-induced borehole flow	Reg-R
6.4.7.2.2 The Two-Plug Configuration				
	BRAGFLO	A lower plug is located between the Castile brine reservoir and underlying formations. A second plug is located immediately above the Salado. The brine reservoir and waste panel are in direct communication though an open cased hole.	Natural borehole fluid flow Waste-induced borehole flow	Reg.-R
	BRAGFLO	The casing and upper concrete plug are assumed to fail after 200 years, and the borehole is assumed to be filled with silty-sand like material. At 1,200 years after abandonment the permeability of the borehole below the waste panel is decreased by one order of magnitude as a result of salt creep.	Natural borehole fluid flow Waste-induced borehole flow	R

Table MASS-1. General Modeling Assumptions (Continued)

CCA Section and Appendix	Code	Modeling Assumption	Related FEP in Appendix SCR	Assumption Considered*
6.4.7.2.3 The Three-Plug Configuration				
	BRAGFLO	In addition to the two plug configuration, a third plug is placed within the Castile above the brine reservoir. This third plug behaves in a similar manner to the lower plug in the two-plug configuration.	Natural borehole fluid flow Waste-induced borehole flow	Reg.-R
6.4.8 Castile Brine Reservoir MASS.18 Castile Brine Reservoir				
	BRAGFLO	The Castile region is assigned a low permeability, which prevents fluid flow. Brine occurrences in the Castile are bounded systems. Brine reservoirs under the waste panels are assumed to have limited extent and interconnectivity, with effective radii on the order of several hundred meters.	Brine reservoirs	R
6.4.9 Climate Change MASS.17 Climate Change				
	SECOFL2D	Climate-related factors are treated through recharge. A parameter called the Climate Index is used to scale the Culebra flux field.	Climate change Temperature Precipitation (for example, rainfall)	R
6.4.10 Initial and Boundary Conditions for Disposal System Modeling				
6.4.10.1 Disposal System Flow and Transport Modeling (BRAGFLO and NUTS)				
	BRAGFLO	There are no gradients for flow in the far-field of the Salado, and pressures are above hydrostatic, but below lithostatic. Excavation and waste emplacement result in partial drainage of the DRZ.	Saturated groundwater flow Brine inflow	R

1 **Table MASS-1. General Modeling Assumptions (Continued)**
2

CCA Section and Appendix	Code	Modeling Assumption	Related FEP in Appendix SCR	Assumption Considered*
5	BRAGFLO	An initial water-table surface is set in the Dewey Lake at an elevation of 3,215 feet (980 meters) above mean sea level. The initial pressures in the Salado are extrapolated from a sampled pressure in MB139 at the shaft and are in hydrostatic equilibrium. The excavated region is assigned an initial pressure of one atmosphere. The liquid saturation of the waste-disposal region is consistent with the liquid saturation of emplaced waste. Other excavated regions are assigned zero liquid saturation, except the shaft which is fully saturated.	Saturated groundwater flow	R
6	NUTS	Molecular transport boundary conditions are no diffusion or dispersion in the normal direction across far-field boundaries. Initial actinide concentrations are zero everywhere except in the waste.	Radionuclide decay and ingrowth Solute transport	R

7
8 6.4.10.2 Culebra Flow and Transport Modeling (SECOFL2D, SECOTP2D)
9

10	SECOFL2D	Constant head boundary conditions are set on the far-field boundaries of the regional flow model. Constant head boundary conditions are also set on the boundaries of the local domain, and are derived by interpolating the solution of the regional domain..	Saturated groundwater flow	R
11	SECOFL2D	Initial actinide concentrations in the Culebra are zero.	Solute transport	R

12
13 6.4.10.3 Initial and Boundary Conditions for Other Computational Models
14

15	NUTS PANEL BRAGFLO (direct brine release) CUTTINGS_S	Initial and boundary conditions interpolated from previously executed BRAGFLO calculation.		R

16
17
18
19

Table MASS-1. General Modeling Assumption (Continued)

CCA Section and Appendix	Code	Modeling Assumption	Related FEP in Appendix SCR	Assumption Considered*
6.4.12 Sequences of Future Events				
	CCDFGF	Each 10,000 year future (random sequence of future events) is generated by randomly and repeatedly sampling: the time between drilling events; the location of drilling events; the activity level of the waste penetrated by each drilling intrusion; the plug configuration of the borehole, and the penetration of a Castile brine reservoir, and by randomly sampling the occurrence of mining in the disposal system.	Oil and gas exploration Potash exploration Oil and gas exploitation Other resources Enhanced oil and gas recovery Natural borehole fluid flow Waste-induced borehole flow	Reg.-R
6.4.12.1 Active and Passive Institutional Controls in Performance Assessment Chapter 7.0				
	CCDFGF	Active institutional controls are effective for 100 years and completely eliminate possibility of incompatible activities. Passive institutional controls are effective for 600 years and reduce rate of incompatible events to 0.01 of the rate during the following uncontrolled period.		Reg.-R
6.4.12.2 Number and Time of Drilling Intrusions				
	CCDFGF	Drilling may occur after 100 years according to a Poisson process.	Loss of records Oil and gas exploration Potash exploration Oil and gas exploitation Other resources	Reg.-R
6.4.12.3 Location of Intrusion Boreholes				
	CCDFGF	The waste disposal region is discretized with 144 regions with the probability of each region being intersected equal. A borehole can penetrate only one region.	Disposal geometry	R

Table MASS-1. General Modeling Assumptions (Continued)

CCA Section and Appendix	Code	Modeling Assumption	Related FEP in Appendix SCR	Assumption Considered*
6.4.12.4 Activity of the Intersected Waste Appendix WCA				
	CCDFGF	569 waste streams identified for contact-handled (CH)-TRU and all the remote-handled (RH)-TRU waste was grouped (binned) together into one equivalent or average (WIPP-scale) RH-TRU waste stream.	Heterogeneity of waste form	R
6.4.12.5 Diameter of the Intrusion Borehole Appendix DEL				
	CUTTINGS_S	The diameter of the intrusion borehole is constant at 12.25 inches (31.12 centimeters).		Reg.-R
6.4.12.6 Probability of Intersecting a Brine Reservoir				
	CCDFGF	One brine reservoir is assumed to exist below the waste panels. The probability that a deep borehole intersects a brine reservoir below the waste panels is 0.08. Brine reservoirs may be depleted by boreholes drilled in the waste disposal region that do not intersect waste (for example, through intact rock).	Brine reservoirs	R
6.4.12.7 Plug Configuration in the Abandoned Intrusion Borehole				
	CCDFGF	The two-plug configuration has a probability of 0.68. The three-plug configuration has a probability of 0.30. The continuous concrete plug has a probability of 0.02.		Reg.-R
6.4.12.8 Probability of Mining Occurring in the Land Withdrawal Area				
	CCDFGF	Mining in the disposal system occurs a maximum of once in 10,000 years (a 10^{-4} probability per year).		Reg.-R

Table MASS-1. General Modeling Assumptions (Continued)

| CCA Section and Appendix	Code	Modeling Assumption	Related FEP in Appendix SCR	Assumption Considered*
6.4.13 Construction of a Single CCDF				
	CCDFGF	Deterministic calculations are executed with BRAGFLO, NUTS, SECOFL2D, SECOTP2D, CUTTINGS_S, and PANEL to generate reference conditions. These reference conditions are used to estimate the consequences associated with random sequences of future events. These are in turn used to develop CCDFs.		R
	CCDFGF	10,000 random sequences of future events are generated for each CCDF plotted.		R
6.4.13.1 Constructing Consequences of the Undisturbed Performance Scenario				
	CCDFGF	A BRAGFLO and NUTS calculation with undisturbed conditions is sufficient for estimating the consequences of the undisturbed performance scenario.		R
6.4.13.2 Scaling Methodology for Disturbed Performance Scenarios				
	CCDFGF	Consequences for random sequences of future events are constructed by scaling the consequences associated with deterministic calculations (reference conditions) to other times, generally by interpolation but sometimes by assuming either similarity or no consequence.		R
6.4.13.3 Estimating Long-Term Releases from the E1 Scenario				
	CCDFGF NUTS	Reference conditions are calculated or estimated for intrusions at 100, 350, 1,000, 3,000, 5,000, 7,000, and 9,000 years.	Waste-induced borehole flow	R
	SECOTP2D	Reference behavior for actinide transport in the Culebra is calculated for intrusions at 350 and 1,000 years.	Solute transport	R

Table MASS-1. General Modeling Assumptions (Continued)

CCA Section and Appendix	Code	Modeling Assumption	Related FEP in Appendix SCR	Assumption Considered*
6.4.13.4 Estimating Long-Term Releases from the E2 Scenario				
	CCDFGF NUTS SECOTP2D	The methodology is similar to the methodology for the E1 scenario. For multiple intrusions, the additional source term to the Culebra for the second and subsequent intrusions is assumed to be negligible.	Waste-induced borehole flow Waste inventory	R
6.4.13.5 Estimating Long-Term Releases from the E1E2 Scenario				
	CCDFGF PANEL	The concentration of actinides in liquid moving up the borehole assumes homogeneous mixing within the panel.	Waste-induced borehole flow	C
	PANEL	Any actinides that enter the borehole reach the Culebra.	Waste-induced borehole flow	C
6.4.13.6 Multiple Scenario Occurrences				
	CCDFGF PANEL	The panels are assumed not to be interconnected for long term brine flow.	Saturated groundwater flow Unsaturated groundwater flow	R
6.4.13.7 Estimating Releases During Drilling for All Scenarios				
	PANEL NUTS	Repository conditions will be dominated by Castile brine if any borehole connects to a brine reservoir.	Brine reservoirs Natural borehole fluid flow	R
	CUTTINGS_S	Depletion of actinides in parts of the repository that have been penetrated by boreholes is not accounted for in calculating the releases from subsequent intrusions at such locations.	Waste-induced borehole flow Waste inventory	C
6.4.13.8 Estimating Releases in the Culebra and the Impact of the Mining Scenario				
	CCDFGF SECOFL2D SECOTP2D	Releases from intrusions at random times in the future are scaled from releases calculated at 100 years with a unit source of radionuclides in the Culebra.		R

Table MASS-1. General Modeling Assumptions (Continued)

CCA Section and Appendix	Code	Modeling Assumption	Related FEP in Appendix SCR	Assumption Considered*
	CCDFGF	Actinides in transit in the Culebra when mining occurs are transported in the flow field used for the undisturbed case. Actinides introduced subsequent to mining are transported in the flow field used for the disturbed case (that is, mined case).		R

* R = Reasonable
C = Conservative
Reg. - Based on regulatory guidance
See above - Refers to assumptions 1 through 8 listed at the beginning of this table.
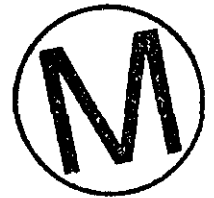
MASS.4.1 Disposal System Geometry as Modeled in BRAGFLO

Overall, the conceptual model of the geometry of the disposal system is that the spatial effects of process interactions can be represented in two dimensions. The geometry used to represent the processes of long-term fluid flow in the Salado, flow between a borehole and overlying units, and flow within the repository (where processes coupled to fluid flow occur, such as creep closure and gas generation), is a vertical cross-section through the repository on a north-south axis. The dimension of this geometry in the direction perpendicular to the plane of the cross-section varies so that spatial effects of certain processes can be better represented, as discussed below.

Three other two-dimensional model geometries are used in performance assessment. For fluid flow and transport modeling in the Culebra, the geometry is a horizontal two-dimensional plane (see Sections 6.4.2 and 6.4.6.2). For modeling brine flow from the intruded panel to the borehole during drilling, the geometry is a two-dimensional, horizontal representation of a waste panel (see Section 6.4.7). For modeling brine flow that might occur between an E-type borehole and other boreholes penetrating the repository, the geometry used is a two-dimensional, horizontal representation of the entire repository (see Section 6.4.13.6). These geometries are mentioned here but not discussed in detail because they are components of other conceptual models requiring geometric assumptions.

The two-dimensional geometry developed for the Salado is based on the assumption that brine and gas flow will converge upon and diverge from the repository horizon. The impact of this conceptual model and its implementation in a two-dimensional grid has been compared to a model that does not make the assumption of convergent and divergent flow (see Attachment 4-1 for additional information). The conceptual model for the Salado includes the slight and variable dip of beds in the vicinity of the repository, which might affect fluid flow.

1 Above and below the repository, it is assumed that any flow between the borehole or shaft
2 (see Section 6.4.3) and surrounding materials will converge or diverge. With respect to flow
3 in units overlying the Salado, the only purpose of this conceptual model is to determine the
4 quantity (flux) of fluid leaving or entering the borehole or shaft. Fluid movement through the
5 units above the Salado is treated in a different conceptual model (see Section 6.4.6). Below
6 the repository, the possible presence of a brine reservoir is considered to be important, so a
7 hydrostratigraphic layer representing the Castile and a possible brine reservoir in it is
8 included.
9
10 *MASS.4.2 Historical Context of the Disposal System Geometry*
11
12 The geometry used in the disposal-system model has seen numerous changes since the 1991
13 preliminary performance assessment (WIPP Performance Assessment Division 1991), in
14 which undisturbed performance used different geometrical assumptions than for disturbed
15 performance, but all calculations used homogeneous waste regions. In gas and brine
16 migration calculations performed in 1992 prior to the 1992 performance assessment for
17 40 CFR Part 191 (WIPP Performance Assessment Department 1992a) several different
18 geometries were again used, however some of these explored discretizing the repository into
19 different waste and panel seal regions and explored the impact of the north end of the
20 repository. The 1992 performance assessment calculations used geometries similar in
21 principle to those used for the 1992 gas and brine migration calculations (Sandia WIPP
22 Project 1992; WIPP Performance Assessment Department 1992b).
23
24 The current disposal system geometry was chosen to allow simulations for both disturbed and
25 undisturbed scenarios to use the same grid description. The repository regions that contain
26 waste have been divided into two subregions: a panel region and the remainder of the
27 repository. Separating the panel region allows a more detailed representation of an intrusion
28 borehole penetrating a panel. The effects of inter-panel communication can be examined by
29 varying the permeability of the panel closure. In addition, the Culebra and other geologic
30 units extending to the surface are represented. The various shaft seal components are also
31 included in the modeling. The computational grid used in BRAGFLO is identical for all three
32 scenarios, and the distinction between scenarios is facilitated by introducing material changes
33 at specified time intervals. For example, at the time of an intrusion the material properties
34 corresponding to the borehole grid blocks are changed to those properties consistent with the
35 long-term behavior of a borehole and plug system.
36
37 *MASS.4.3 Historical Context of Culebra Geometries as Modeled in SECOFL2D and*
38 *SECOTP2D*
39
40 The geometries used in the SECOFL2D and SECOTP2D Culebra models are chosen to
41 provide a reasonable and realistic basis for two-dimensional simulations of groundwater flow
42 and radionuclide transport through the Culebra. This model, described in Sections 6.4.2 and
43 6.4.6.2, has been developed over many years. The development of the various modeling
44 domains and assumptions is documented in Section MASS.15.

MASS.5 BRAGFLO Geometry of the Repository

The purpose of this model is to provide a reasonable representation of the geometry of the WIPP repository with respect to the interactions between important processes that occur there.

This conceptual model represents the geometry of the repository for performance assessment. As with the geometry of the disposal system discussed in Chapter 6.0 (Sections 6.4.2.1) and Section MASS.4, the principal process considered in setting up the repository geometry is fluid flow. Several features considered to be important in fluid flow are included in the conceptual model. The first is the overall dimension of the repository along the north-south trend of the cross section, as well as the major divisions within the repository (waste disposal region, operations region, and experimental region). The second is the volume of a single panel, because fluid flow to a borehole penetrating the repository can potentially access only the volume in a waste panel directly and other regions of the repository only by flow through or around a panel closure. The third is the physical dimensions of panel closures separating the single panel and the other major divisions of the repository. In determining the appropriate way to represent these features, the important concepts applied are to preserve dimensions along the axis of the model, interface areas, and volumes excavated.

Notably absent from the conceptual model for the long-term performance of the repository are pillars and individual drifts and rooms. These are excluded from the model for simplicity, and it is assumed that they have either negligible impact on fluid flow processes or, alternatively, that including them in the conceptual model would be beneficial to long-term performance because their presence could make flow paths more tortuous and decrease fluxes. This assumption includes lumping nine of the 10 panels in the waste disposal region into a single region (see Sections 6.4.3 and 6.4.3.2).

The BRAGFLO model of the WIPP disposal system is a two-dimensional array of three-dimensional grid blocks. Each grid block has a finite length, width, height, volume, and surface area for its boundaries with neighboring grid blocks. The BRAGFLO two-dimensional grid is similar to any other two-dimensional grid used to treat flows, except that the grid-block dimension in the direction perpendicular (z-direction) to the plane of the grid varies from block to block as a function of the lateral direction (x-direction). This allows the BRAGFLO grid to treat important geometric aspects of the WIPP disposal system, such as the very small intrusion borehole, the moderate-size shaft, and the larger controlled areas.

MASS.5.1 Historical Context of the Repository Model

Several early models of repository fluid-flow behavior (models of radionuclide migration pathways, gas flow from the disposal area to the shaft, Salado brine flow through panel to borehole, effects of anhydrite layers on Salado brine flow through a panel, and flow from a brine reservoir through a disposal room) are summarized in a 1990 report (Rechard et al. 1990). In the preliminary performance assessment of 1992, all waste was lumped into a single region (WIPP Performance Assessment Department 1993). Because human intrusion

1 boreholes must be treated in detail for the 1996 performance assessment, it was necessary to
2 model a single waste panel with a borehole surrounded by two-dimensional radial-flaring
3 gridblocks. The remainder of the waste is modeled as the rest of the repository and is
4 separated from the waste panel by a panel closure.
5
6 **MASS.6 Creep Closure**
7
8 The model used for creep closure of the repository is discussed in Appendix PORSURF,
9 Chapter 6.0 (Section 6.4.3.1), and Appendix BRAGFLO (Section 4.11).
10
11 **MASS.7 Repository Fluid Flow**
12
13 This model represents the long-term flow behavior of liquid and gas in the repository and its
14 interaction with other regions in which fluid flow may occur, such as the Salado, shafts, or ·
15 intrusion borehole. This model is not used to represent the interaction of fluids in the
16 repository with a borehole during drilling.
17
18 There are at least three different alternative models that the DOE evaluated for explaining
19 brine inflow. One conceptual model, the far-field flow model, is for flow from the far field in
20 response to potentiometric gradients through naturally interconnected intergranular pore
21 spaces. There is experimental evidence supporting this model in anhydrite interbeds and some
22 non-anhydrite intervals. Experimental results from very pure halite are ambiguous with
23 respect to this model: results can be interpreted either as very low permeability (near-
24 complete absence of interconnected pore space); or as a lithology in which fluid is not
25 responsive to applied pressure gradients. In the first case, potentiometric flow models can be
26 used effectively with very low permeability values. In the second case, which would imply a
27 conditional exception to the potentiometric flow model, a potentiometric model would not be
28 appropriate for use.
29
30 Numerous parameters are necessary to describe flow in terms of potentiometric equations.
31 These include properties describing the rock formation: porosity, permeability, density, rock
32 compressibility; and properties describing fluid flow and fluid interactions: relative
33 permeability, capillary pressure, fluid compressibility, fluid density, and fluid viscosity.
34 Within the conceptual model, few limits are imposed on the spatial variability or functional
35 dependence of these properties. It is known, for example, that the pore structure and
36 composition of the Salado are not uniform, which leads to spatial heterogeneity in rock
37 properties both by layering and within each layer. Fluid properties are known to be functions
38 of pressure, temperature, chemical composition, and saturation.
39
40 A second conceptual model, the redistribution model, proposes that interconnected pore
41 spaces do not exist naturally in most lithologic units in the Salado. Interconnected networks
42 form as the result of fracturing and creep around excavations. Potentiometric flow occurs in
43 interconnected networks, but because the interconnectedness is of limited extent, the volume
44 of brine that can flow is severely limited compared to the naturally interconnected case. A

1   numerical model based on the redistribution concept was developed and applied to the small-
2   scale brine inflow (SSBI) data set (McTigue 1993). The redistribution-based model allowed
3   the use of a more realistic capacitance for the formation response than do far-field flow
4   models with far-field properties.

6   The third conceptual model for flow, the clay consolidation model, arises from observations
7   made as part of the BSEP. On the basis of observations recorded during more than nine years
8   of underground observations (Deal and Case 1987; Deal and Roggenthen 1989; Deal et al.
9   1987, 1989, 1991a, 1991b, 1993), this model proposes that the most significant source of
10 brine flowing into the repository is clay layers exposed by excavation. According to the
11 model, (1) clay layers compact and yield brine when stresses are relieved near the excavation
12 and (2) flow through other lithologic units is negligible.

14 Since definitive data do not exist to reconcile these three alternatives, the DOE has
15 implemented the far-field flow model because it results in a range of variability in brine
16 inflow that covers the other two alternative models. The first principle in the conceptual
17 model for fluid flow in the repository is that gas and brine can be both present and mobile
18 (two-phase flow), governed by conservation of energy and mass and by Darcy's Law for their
19 fluxes (see Appendix BRAGFLO, Sections 4.1 through 4.4). Consistent with typical concepts
20 of two-phase flow, the phases can affect each other by impeding flow caused by partial
21 saturation (relative permeability effects) and by affecting pressure caused by capillary forces
22 (capillary pressure effects).

24 The flow of brine and gas in the repository is assumed to behave as two-phase, immiscible,
25 Darcy flow (see Appendix BRAGFLO, Sections 4.8 and 4.9). BRAGFLO is used to simulate
26 brine and gas flow in the repository and to incorporate the effects of disposal room closure
27 and gas generation. Fluid flow in the repository is affected by the following factors:

29 •   the geometrical association of pillars, rooms, and drifts; panel closure caused by creep;
30   and possible borehole locations;

32 •   the varied properties of the waste areas resulting from creep closure and heterogeneous
33   contents;

35 •   flow interactions with other parts of the disposal system; and

37 •   reactions that generate gas.

39 The geometry of the panel around the intrusion borehole is consistent with the assumption that
40 fluid flow there will occur directly toward or directly away from the borehole. The geometry
41 represents a semi-circular volume north of the borehole and a semi-circular volume south of
42 the borehole (representing the assumption of radial flow in a subregion of a two-dimensional
43 representation of the repository). Around the shaft, the assumption of convergent or divergent
44 flow is made, and implemented with a similar gridding technique.

1 Approximating convergent and divergent flow around the intrusion borehole and the shaft
2 creates two narrow necks in the otherwise fairly uniform width grid in the region representing
3 the repository. In the undisturbed performance scenario and under certain conditions in other
4 scenarios, flow in the repository may pass laterally through these necks. In reality, these necks
5 do not exist. Their presence in the model is expected to have a negligible or conservative
6 impact on model predictions compared to predictions that would result from use of a more
7 realistic model geometry. The time scale involved and the permeability contrast between the
8 repository and surrounding rock are sufficient that lateral flow that may occur in the repository
9 is restricted by the rate at which liquid gets into or out of the repository, rather than the rate at
10 which it flows through the repository.

12 Gas generation is affected by the quantity of liquid in contact with metal. However, the
13 distribution of fluid in the repository can be only approximated. For example, capillary action
14 can create wicking that would increase the overall region in which gas generation occurs, but
15 this cannot be modeled at the necessary resolution to fundamentally stimulate processes
16 without undesirable effects on the duration of the model simulations. Therefore, as a
17 bounding measure for gas generation purposes, brine in the repository is distributed to an
18 extent greater than actually estimated by the Darcy flow models used and values of parameters
19 chosen.

21 Panel closures are represented with a permeability of 1×10^{-15} square meters, which is
22 equivalent to the DRZ permeability. This value is considered reasonable as verified by an
23 analysis, which is presented as Attachment 7-1 of this appendix.

25 Modeling of flow within the repository is based on homogenizing the room contents into
26 relatively large computational volumes. The approach ignores heterogeneities in disposal
27 room contents that may influence gas and brine behavior in the room by causing fluid flow
28 among channels or preferential paths in the waste, bypassing entire regions. Isolated regions
29 could exist for several reasons:

31 • they may be isolated by low-permeability regions of waste that serve as barriers,

33 • connectivity with the interbeds may occur only at particular locations within the
34   repository, or

36 • the repository dip may promote preferential gas flow in the upper regions of the waste.

38 The adequacy of the homogenization approach was examined in screening analyses DR-1
39 (Webb 1995) and DR-6 (Vaughn et al. 1995a). To address room heterogeneity, this analysis
40 used an additional parameter in BRAGFLO to specify the minimum active (mobile) brine
41 flow saturation (pseudo-residual brine saturation). Above this saturation, the normal
42 descriptions of two-phase flow apply (that is, either the Brooks and Corey or van Genuchten
43 and Parker relative permeability models). Below this minimum, brine is immobile, although
44 it is available for reaction and may still be consumed during gas-generation reactions. The

1   assumption of a minimum saturation limit is justified based on the presumed heterogeneity of
2   the waste and the fact that the repository dips slightly. The minimum active brine saturation
3   was treated as an uncertain parameter and sampled uniformly between values 0.1 and 0.8
4   during the analysis. This saturation limit was applied uniformly throughout the disposal room
5   in order to bound the impact of heterogeneities on flow (Webb 1995; Vaughn et al. 1995a).
6   Results of this analysis showed that releases to the accessible environment in the baseline case
7   (homogenization) are consistently higher.

9   The experimental and operations regions are represented in performance assessment by a
10   fixed porosity of 18.0 percent and a permeability of 10^{-11} square meters. This combination of
11   low porosity and high permeability will conservatively overestimate fluid flow through these
12   regions and limit the capacity of these regions to store fluids, thus potentially overestimating
13   releases to the environment. This conclusion is based on a screening analysis (Vaughn et al.
14   1995b) that examined the importance of permeability varying with porosity in closure regions
15   (waste disposal region, experimental region, and operations region). To perform this analysis,
16   a model for estimating the change in permeability with porosity in the closure regions (waste
17   disposal region, experimental region and operations region) was implemented in BRAGFLO.
18   A series of BRAGFLO simulations was performed to determine whether permeability varying
19   with porosity in closure regions could enhance contaminant migration to the accessible
20   environment. Two basic scenarios were considered in the screening analysis, undisturbed
21   performance and disturbed performance. To assess the sensitivity of system performance on
22   dynamic permeability in the closure regions, CCDFs of normalized contaminated brine
23   releases were constructed and compared with the corresponding baseline conditional CCDFs.
24   The baseline model treated permeabilities in the closure regions as fixed values. Results of
25   this analysis showed that the inclusion of dynamic closure of the waste disposal region,
26   experimental region, and operations region in BRAGFLO results in computed releases to the
27   accessible environment that are essentially equivalent to the baseline case.

29   *MASS.7.1 Flow Interactions with the Creep Closure Model*

31   The dynamic effect of halite creep and room consolidation on room porosity is modeled only
32   in the waste disposal region. Other parts of the repository, such as the experimental region
33   and the operations region, are modeled assuming fixed (invariant with time) properties. In
34   these regions, the permeability is held at a fixed high value representative of unconsolidated
35   material, while the porosity is maintained at relatively low values associated with highly
36   consolidated material. It is assumed that this combination of low porosity and high
37   permeability conservatively overestimates flow through these regions and minimizes the
38   capacity of this material to store fluids, thus maximizing the release to the environment. To
39   examine the acceptability of this assumption, a screening analysis (Vaughn et al. 1995c)
40   evaluated the effect of including closure of the experimental region and operations region. In
41   this analysis, consolidation of the experimental region and operations region was implemented
42   in BRAGFLO by relating pressure and time to porosity using a porosity-surface method. The
43   porosity surface for the experimental region and operations region differs from the one used
44   for consolidation of the disposal room and is based on an empty excavation (see Appendix
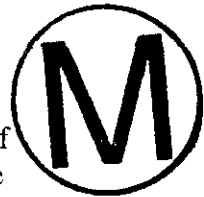
1 PORSURF). Results of the screening analysis showed that disregarding dynamic closure of
2 the experimental region is acceptable because it is conservative: lower releases occur when
3 closure of the experimental region and operations region is computed compared to simulations
4 with time-invariant high permeability and low porosity.

MASS.7.2 Flow Interactions with the Gas Generation Model

8 Gas generation affects repository pressure, which in turn is an important parameter in other
9 processes such as two-phase flow, creep closure, and interbed fracturing. Gas generation
10 processes considered in performance assessment calculations include anoxic corrosion and
11 microbial degradation. Radiolysis is excluded from performance assessment calculations on
12 the basis of laboratory experiments and a screening analysis (Vaughn et al. 1995d) that
13 concluded that radiolysis does not significantly affect repository performance.

15 In modeling gas generation, the effective liquid in a computational cell is the computed liquid
16 in that cell plus an adjustment to account for the uncertainty associated with wicking by the
17 waste (see Appendix BRAGFLO, Section 7.2.9). Capillary action (wicking) is the ability of a
18 material to carry a fluid by capillary forces above the level it would normally seek in response
19 to gravity. Because the current gas-generation model computes substantially different gas-
20 generation rates depending on whether the waste is wet or merely surrounded by water vapor,
21 the physical extent of wetting could be important. A screening analysis (Vaughn et al. 1995e)
22 examined wicking and concluded that it should be included in performance assessment
23 calculations. The baseline gas-generation model in BRAGFLO accounts for corrosion of iron
24 and microbial degradation of cellulosics. The net reaction rate of these processes depends
25 directly on brine saturation: an increase in brine saturation will increase the net reaction rate
26 by weighting the inundated portion more heavily and the slower humid portion less heavily.
27 To simulate the effect of wicking on the net reaction rate, an effective brine saturation, which
28 includes a wicking saturation contribution, is used to calculate reaction rates rather than the
29 actual brine saturation. To account for uncertainty in the wicking saturation contribution, this
30 contribution was sampled from a uniform distribution that ranged from 0.0 to 1.0 for each
31 BRAGFLO simulation in the analysis.

MASS.8 Gas Generation

35 This model represents the possible generation of gas in the repository by corrosion of steel and
36 microbial degradation of cellulosics, plastics, and rubbers. Additional discussion of this topic
37 may be found in Appendices WCA (Section WCA.5.1), BRAGFLO (Section 4.13), SOTERM
38 (Section SOTERM.2.2), and SCR (Section SCR.2.5.1).

40 Gas will be produced in the repository by a variety of chemical reactions—principally those
41 between brine, metals, microbes, cellulosics and similar materials, plastics, and rubber
42 materials—and by liberation of dissolved gases to the gaseous phase. The processes assumed
43 for long-term performance are anoxic corrosion of steel waste containers and metals in the
44 waste and microbial degradation of cellulosics and, perhaps, plastics and rubbers in the waste.

1   Anoxic corrosion reactions between brine and steel are expected to occur and produce H_2;
2   they are included in the conceptual model. Microbial degradation of cellulosics and perhaps,
3   plastics and rubbers, might occur. If it does, it may produce various gases, primarily CH_4 and
4   CO_2. However, by reaction with the MgO backfill that will be emplaced to control the
5   chemistry of the repository, CO_2 produced by microbial degradation will be rapidly removed
6   from the gaseous phase (see Appendix SOTERM, Section SOTERM.2.2.2, and Chapter 6.0,
7   Section 6.4.3.4). Other gases such as N_2 and H_2S produced by microbial degradation are
8   insignificant in quantity (see Attachment 8-1). Thus the conceptual model for gas generation
9   is that anoxic corrosion of steel will produce H_2; microbial degradation of cellulosics, plastics,
10   and rubbers might occur and might produce other gases, but any CO_2 produced is rapidly
11   removed by reaction with MgO backfill.

12

13   In the conceptual model, the rate of gas production in the repository by anoxic corrosion can
14   be limited by several factors. Anoxic corrosion cannot occur unless brine (water) is present
15   and in contact with steel. The corrosion rate is assumed to be dependent on brine saturation.
16   Because anoxic corrosion consumes steel, the rate of gas production can be limited by the
17   quantity of steel left in the repository. Because corrosion is a surface reaction, it proceeds at
18   quantifiable rates per unit surface area of steel. In addition, anoxic corrosion consumes water.
19   Because of these factors, the rate of gas generation in the repository can vary through time as
20   conditions change. It is assumed that anoxic corrosion can occur in the repository as soon as
21   the shafts are sealed.

22

23   Microbial degradation of cellulosics, plastics, and rubbers is limited by several factors, chiefly
24   the long-term viability of microbes in the repository. Whether microbes degrade plastics and
25   rubbers is also important. The rate of microbial degradation is dependent on brine saturation.
26   Because of uncertainty, however, it is assumed that there is no effect of microbial degradation
27   on brine (water) content in the repository.

28

29   A limited quantity of O_2 will be trapped in the panels after repository closure. However, this
30   O_2 will be consumed quickly by both oxic corrosion and microbial degradation, and the
31   reducing environment will be dominant in the repository over 10,000 years. The contribution
32   of oxic corrosion and biodegradation to overall gas production is negligible. Thus, oxic
33   reactions are not considered in the conceptual model for gas generation.

34

35   Addition of an MgO backfill significantly reduces the impact of microbial generation of CO_2
36   (see Attachment 8-2). As discussed in Section 6.4.3.4, the MgO backfill will react with
37   carbon dioxide produced by microbial degradation and remove it from the gaseous phase.

38

39   Because the conceptual model discusses the general processes and interactions assumed to
40   occur without direct reference to the mathematical equations used, no parameters are defined
41   by this conceptual model. The mathematical model used to implement it, the average
42   stoichiometry model, is discussed in Section 6.4.3.3 and Attachment 8-2. The most important
43   parameter in the average stoichiometry model is the rate at which gas generation occurs with
44   brine and steel present, because this is the principal control on the total quantity of gas

1   generated. The assumptions made about the principal reactions and their stoichiometry are
2   also important, however, because they affect the quantity of gas created per unit quantity of
3   steel and water reacted.
4
5   The feedback between the gas generation conceptual model and the repository fluid flow
6   conceptual model is important to understand. Gas generation cannot continue for long with
7   the low initial quantity of liquid present in the waste, as specified by waste acceptance criteria.
8   For gas generation to occur, brine must flow into the repository; for gas generation to be
9   sustained, brine consumed by gas generation must be replenished. Gas generation, however,
10 tends to increase repository pressure and keep brine from flowing into it. Thus the rates at
11 which various processes proceed are important in determining the conditions of the repository.
12 There is important feedback as well between the gas generation model and other conceptual
13 models through pressure effects, such as those calculating creep closure (Section 6.4.3.1),
14 interbed fracturing (Section 6.4.5.2), two-phase flow (Section 6.4.3.2), and the radionuclide
15 release associated with spalling and direct brine release during an inadvertent drilling
16 intrusion (Section 6.4.7).
17
18 Single-process laboratory studies of anoxic corrosion of steels and Al-based materials by
19 R. E. Westerman and his colleagues at Pacific Northwest Laboratory (PNL) from
20 November 1989 through September 1995 have shown that the factor with the greatest effect
21 on the rate of H_2 generation by anoxic corrosion is the quantity of brine in WIPP disposal
22 rooms (Attachment 8-2). This is because anoxic corrosion occurs rapidly under inundated
23 conditions, but not at all under humid conditions. The pressure difference between WIPP
24 disposal rooms and the far field and the porosity of the room contents also affect the extent of
25 brine inflow and outflow and, hence, the anoxic-corrosion rate. Because the average
26 stoichiometry model is incorporated in BRAGFLO, gas generation is coupled with brine and
27 gas inflow and outflow. Moreover, because BRAGFLO uses a porosity surface to simulate
28 room closure (Butcher and Mendenhall 1993), it also couples gas generation to room closure.
29 Telander and Westerman (1993) and subsequent studies of anoxic corrosion at PNL have
30 shown that pH, pressure, and the composition of the gaseous phase also affect the H_2-
31 generation rate.
32
33 The greatest uncertainty in modeling gas generation in WIPP disposal rooms is whether
34 microbial gas generation will occur and, if so, to what extent it will occur and what its effects
35 will be. The following sources of microbial uncertainty have been described:
36
37   •   whether microorganisms capable of carrying out the potentially significant respiratory
38   pathways identified by Brush (1990) (denitrification, SO_4^{2-} reduction, and
39   methanogenesis) will be present when the repository is filled and sealed,
40
41   •   whether these microbes will survive for a significant fraction of the 10,000-year period
42   of performance of the repository,
43
44   •   whether sufficient H_2O will be present in the waste or brine,

- whether sufficient electron acceptors (oxidants) will be present and available,

- whether enough nutrients, especially N and P, will be present and available,

- whether microbes will consume significant quantities of plastics and rubbers during the 10,000-year period of performance of the repository, and

- the stoichiometry of the overall reaction for each significant respiratory pathway, especially the number of moles of electron acceptors, nutrients, gases, and H_2O consumed or produced per mole of substrate consumed.

With regard to the first five of these uncertainties, it has been concluded that, although significant microbial gas production is possible, it is by no means certain. Therefore, it has been estimated that significant microbial gas generation in WIPP disposal rooms will occur half of the time; and in half of the cases that significant microbial degradation occurs, microbes will consume all of the plastics and rubbers in the repository after they consume all of the cellulosics (Attachment 8-3).

Single-process laboratory studies of microbial consumption of cellulosics by A.J. Francis and his colleagues at Brookhaven National Laboratory from May 1991 through September 1995 showed that if significant microbial activity occurs, the factor with the greatest effect on the microbial gas-generation rate is the quantity of brine in the repository (see Francis and Gillow 1994; Attachment 8-2). This is because microbial gas generation occurs rapidly under inundated conditions, but at much lower rates under humid conditions. Francis and Gillow (1994) also found that inoculation with halophilic microbes from the WIPP site and nearby lakes, amendment with NO_3^- (an electron acceptor), amendment with nutrients, and addition of bentonite (a previously proposed backfill material) affect the rate or extent of microbial gas generation. Other factors that could affect the rate or extent of microbial gas generation, but which Francis and Gillow (1994) did not quantify, are the pH; the dissolved or suspended concentrations of actinides or other heavy metals, which could inhibit or preclude microbial activity; and the concentrations of microbial byproducts, which could inhibit or preclude additional microbial activity. High pressure will not preclude or even inhibit microbial activity significantly, even when it increases to 150 atmospheres (lithostatic pressure at the depth of the repository).

Data summarized by Molecke (1979) imply that radiolysis of cellulosics, plastics, and rubbers will not be a significant, long-term gas-generation process in WIPP disposal rooms. (Radiolysis here refers to α radiolysis, the breaking of chemical bonds by α particles emitted during the radioactive decay of the actinide elements in TRU waste. Because molecular dissociation caused by other types of radiation will be insignificant in a TRU-waste repository such as the WIPP, this discussion considers only α radiolysis.) Based on calculations using the results of laboratory studies of brine radiolysis carried out for the WIPP by Reed et al. (1993) on estimates of the quantities of brine that could be present in the repository after filling and sealing, and on estimates of the solubilities of Pu, Am, Np, Th, and U summarized

1   by Trauth et al. (1992), it was concluded that radiolysis of H_2O will not significantly affect the
2   overall gas or H_2O content of the repository (see Appendix SCR, Section SCR.2.5.1.3.1).
3
4   *MASS.8.1 Historical Context of Gas Generation Modeling*
5
6   The DOE performed laboratory studies of gas generation during the late 1970s to support the
7   development of TRU waste acceptance criteria (Molecke 1978, 1979; Sandia National
8   Laboratories 1979). For the most part, these laboratory studies comprised single-process
9   experiments (one gas-generation process studied at a time) on microbial activity and radiolysis
10 with nonradioactive and some radioactive simulated TRU waste. There was very little work
11 on anoxic corrosion. Based on laboratory measurements on samples obtained by drilling from
12 the surface, the permeability of the Salado appeared to be high enough for rapid migration of
13 gas from the repository, even given the highest gas-generation rates summarized by Molecke
14 (1979). Therefore, the DOE concluded that further studies of gas generation were
15 unnecessary.
16
17 In 1987, preliminary performance assessment calculations on the effects of human intrusion
18 identified inflow of intergranular Salado brine as a concern for the long-term performance of
19 the repository. In early 1988, the DOE began to examine the possible effects of processes
20 such as anoxic corrosion of steels and microbial degradation of cellulosics on the H_2O content
21 of WIPP disposal rooms. Brush and Anderson (1989a) concluded that these processes could
22 affect the H_2O content as significantly as brine inflow. Furthermore, they concluded that these
23 processes could also produce significant quantities of gas. Meanwhile, in situ measurements
24 in the WIPP underground workings revealed that the permeability of the Salado was much
25 lower than believed in the late 1970s.
26
27 Systems analysis carried out by Lappin et al. (1989) to support the 1990 Supplemental
28 Environmental Impact Statement, which used gas-generation assumptions from Brush and
29 Anderson (1989a, 1989b, and 1989c), the rates-and-potentials gas-production model of
30 Lappin et al. (1989), and new in situ permeabilities, demonstrated that gas would affect the
31 overall performance of the repository if present in significant quantities.
32
33 Therefore, the DOE initiated laboratory studies of gas generation in February 1989. These
34 studies have comprised mainly single-process experiments on anoxic corrosion, microbial
35 activity, and radiolysis, mostly with nonradioactive, simulated CH-TRU waste (Brush 1990;
36 Brush et al. 1991a, 1991b, 1993; Reed et al. 1993; Telander and Westerman 1993; Francis and
37 Gillow 1994).
38
39 The DOE has also developed two additional gas-generation models since 1989. The WIPP
40 Performance Assessment Division (1991) developed the average stoichiometry gas-generation
41 model and incorporated it into BRAGFLO, which also simulates room closure. Incorporation
42 of the average stoichiometry model into BRAGFLO thus coupled this gas-generation model
43 with the hydrologic and geomechanical models used for performance assessment. The WIPP
44 Performance Assessment Division (1991) and Brush et al. (1994) developed the average

1 stoichiometry and the reaction-path gas-generation models, respectively, based on the results
2 of the single-process laboratory studies that were restarted in 1989. However, although these
3 laboratory studies considered only one gas-generation process at a time (anoxic corrosion,
4 microbial activity, or radiolysis), they did, at least to some extent, simulate some of the
5 possible interactions between these processes. For example, the study of anoxic corrosion by
6 Telander and Westerman (1993) considered the effects of the microbially produced gases CO_2
7 and H_2S on corrosion, and Brush et al. (1994) included passivation of steels and other Fe-
8 based metals by CO_2 and H_2S in the reaction-path model.
9
10 Work began on the reaction-path gas-generation model in 1992, which includes more gas-
11 generation processes than the average stoichiometry model and the interactions among these
12 processes (Brush et al. 1994). It was recommended to replace the average stoichiometry
13 model in BRAGFLO with the reaction-path model. However, in November 1995, the DOE
14 decided to terminate all work on the reaction-path model and to continue to use the average
15 stoichiometry model in BRAGFLO. The rationale for the decision is documented in
16 Attachment 8-1. The main advantage of the reaction-path model relative to the average
17 stoichiometry model is that the former includes passivation of steels by microbially produced
18 CO_2 and H_2S. However, the results from laboratory studies of anoxic steel corrosion fail to
19 support passivation of steels by CO_2. Therefore, the main advantage of the reaction-path
20 model no longer exists. In addition, the experimental results show that anoxic steel corrosion
21 does not stop at about 70 atm hydrogen pressure as predicted by the reaction-path model.
22 Because of these reasons, the reaction-path model is not used in BRAGFLO calculations.
23
24 **MASS. 9 Chemical Conditions**
25
26 Topics in the models used for chemical conditions in the repository are discussed in Appendix
27 SOTERM and Chapter 6.0 (Section 6.4.3.4).
28
29 **MASS.10 Dissolved Actinide Source Term**
30
31 Topics in the models used for the dissolved actinide source term in the repository are
32 discussed in Appendix SOTERM, Chapter 6.0 (Section 6.4.3.5), and Appendix SCR (Sections
33 SCR.2.5.2 and SCR.2.5.3).
34
35 **MASS.11 Colloidal Actinide Source Term**
36
37 Topics in the models used for the colloidal actinide source term are discussed in Appendix
38 SOTERM (Section SOTERM.6) and Chapter 6.0 (Section 6.4.3.6).
39
40 **MASS.12 Shafts and Shaft Seals**
41
42 The conceptual model for the shafts and shaft seals used in the performance assessment has
43 been chosen to provide a reasonable and realistic basis for simulating long-term fluid flow
44 through the shaft seal system and to allow evaluation of the effect that uncertainty about the

1 long-term properties of the shaft seal system may have on cumulative radionuclide releases
2 from the disposal system. The conceptual model is also discussed in Chapter 6.0 (Section
3 6.4.4) and Appendix SEAL (Section 2).

5 The conceptual model of the seals is based on results of detailed numerical models of the shaft
6 seal system design. These models were developed to evaluate the performance of the shaft
7 seal system under a range of conditions. Both fluid flow and structural response of the system
8 have been evaluated. The principal uncertainties associated with the detailed models follow:

10 • reconsolidation of the crushed salt component,

12 • construction, permeability, and gas threshold pressure of the clay components, and

14 • damage, permeability, healing, and character of the Salado and Rustler disturbed rock
15   zones.

17 These uncertainties are also present in the performance assessment model and have been
18 accounted for in the values specified for seal parameters. The consequences of uncertainty in
19 seal component performance were a primary motivation in the development of the proposed
20 seal system design. Although there is uncertainty in many of the materials and models, the
21 shaft will be completely filled with high density, low permeability materials. The use of
22 multiple materials and components for each sealing function results in a robust system. Time
23 dependency of the performance of seal components is incorporated directly into the model
24 through temporal variation in seal properties.

26 The processes that can affect the performance of the shaft seals—structural, hydraulic, and
27 coupled structural and hydrological—are discussed in some detail in Appendix SEAL
28 (Sections 7 and 8). Evaluation of these issues required the use of existing structural and both
29 single-and two-phase flow codes. In addition, development of conceptual and numerical
30 models for crushed salt reconsolidation, the disturbed rock zone, and the shaft seal system was
31 required. These models have been reviewed by independent, qualified experts, are well
32 documented, and have been developed within an accepted quality assurance program. Codes
33 used in the analyses include SPECTROM-32 (structural) (Callahan 1994), SWIFT II
34 (single-phase flow) (Reeves et al. 1986), and TOUGH2 (multi-phase flow) (Pruess 1991).
35 These codes were selected for their capability to simulate the processes thought to affect seal
36 performance. They are also well-documented, accepted, and widely used within the scientific
37 community. The codes were modified to implement the conceptual models specific to the
38 seals, and these modifications were made within a program that establishes criteria for
39 assuring software quality.

41 The BRAGFLO model of the seal system requires consistency with parameters associated
42 with the surrounding system. For example, the permeability of the crushed salt component
43 should always be greater than or equal to that of the intact halite. Similarly, the calculation of
44 the effective halite DRZ permeability requires the permeability of intact halite as input. As

1 discussed in Appendix SEAL (Section 1.4), procedures in performance assessment have been
2 implemented to ensure these parameter consistency concerns are met.
3
4 *MASS.12.1 Historical Development of the Shaft Seals*
5
6 The four shafts into the repository will be sealed after completion of disposal activities at the
7 WIPP. The shaft seal system design has evolved over time (Stormont 1988; Nowak et al.
8 1990; DOE 1995). The Initial Reference Seal System Design proposed a two component
9 design to achieve a sealing strategy with two phases: concrete and clay seals formed a short-
10 term seal, and a crushed salt seal formed long-term protection. The use of native rock (that is,
11 crushed salt) as a permanent sealing material is considered the most effective means to
12 eliminate the shafts as a preferred pathway for migration of hazardous constituents. Because
13 some interim period must pass for the crushed salt to reconsolidate to sufficiently high
14 densities, short-term seals were proposed as a means to prevent fluid migration during the
15 interim. Estimates of this interim period ranged from 100 to 200 years.
16
17 Seal design changes and refinements have been incorporated into the conceptual model of the
18 seals used by the DOE (Bertram-Howery et al. 1990; WIPP Performance Assessment
19 Department 1991; Sandia WIPP Project 1992). Performance assessments conducted prior to
20 1992 addressed general sealing issues but did not include specific seal components.
21
22 Results of the scoping calculations using the DCCA model demonstrated that low-
23 permeability materials were required for the shaft seals (DOE 1995, Appendix D). However,
24 the simplicity of the conceptual model limited the applicability of results to the detailed seal
25 system design.
26
27 The shaft seal design for the WIPP is presented in Appendix SEAL (Sections 4 and 5).
28
29 **MASS.13 Salado**
30
31 The purpose of this model is to reasonably represent the effects of fluid flow in the Salado on
32 long-term performance of the disposal system. The conceptual model is also discussed in
33 Chapter 6.0 (Section 6.4.5).
34
35 Fluid flow in the Salado is considered in the conceptual model of long-term disposal system
36 performance for several reasons. First, some liquid could move from the Salado to the
37 repository because of the considerable gradients that can form for liquid flow inward to the
38 repository. This possibility is important because such fluid can interact with creep closure,
39 gas generation, actinide solubility, and other processes occurring in the repository. Second,
40 gas generated in the repository is thought to be capable of fracturing the Salado interbeds
41 under certain conditions, creating increased permeability channels that could be pathways for
42 lateral transport. The pathway of lateral transport in intact Salado is also modeled, but it is
43 considered unlikely to result in any significant radionuclide transport to the accessible
44 environment boundary.
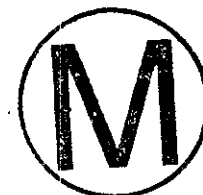
1   The fundamental principle in the conceptual model for fluid flow in the Salado is that it is a
2   porous medium within which gas and brine can be both present and mobile (two-phase flow),
3   governed by conservation of energy and mass, and by Darcy's Law for their fluxes (see
4   Appendix BRAGFLO, Sections 4.1 through 4.4). Consistent with typical concepts of two-
5   phase flow, each phase can affect the other by impeding flow because of partial saturation
6   (relative permeability effects) and by affecting pressure by capillary forces (capillary pressure
7   effects). It is assumed that no waste-generated gas is present initially, but gas can enter the
8   interbeds. It is expected that the low permeability of impure and pure halite intervals of the
9   Salado will prevent gas from penetrating because of the expected high capillary pressure for
10 these units.

11
12 Some variability in composition exists between different horizons of the Salado. The largest
13 differences occur between the anhydrite-rich layers called interbeds and those dominated by
14 halite. Within horizons dominated by halite, composition varies from nearly pure halite to
15 halite plus several percent other minerals, in some instances including clay (see Chapter
16 2.0, Section 2.1.3.4). The Salado is modeled as impure halite except for those interbeds that
17 intersect the DRZ near the repository. This conceptual model and an alternative model that
18 explicitly represented all stratigraphically distinct layers of the Salado near the repository
19 (Christian-Frear and Webb 1996) produced similar results.

20
21 From other modeling and theoretical considerations, flow between the Salado and the
22 repository is expected to occur primarily through interbeds that intersect the DRZ. Because of
23 the large surface areas between the interbeds and surrounding halite, the interbeds serve as
24 conduits for the flow of brine in two directions: from halite to interbeds to the repository, or,
25 for brine flowing out of the repository, from the repository into interbeds and then into halite.
26 Because the repository is modeled as a relatively porous and permeable region, brine is
27 considered most likely (but not constrained) to leave the repository through MB139 below the
28 repository because of the effect of gravity. Gas is considered most likely (but not constrained)
29 to leave the repository through anhydrite interbeds above the repository.

30
31 The effect of gravity may also be important in the Salado because of the slight and variable
32 natural stratigraphic dip. For long-term performance modeling, the dip in the Salado within
33 the domain is taken to be constant and 1 degree from the north to south.

34
35 Fluid flow in the Salado is conceptualized as occurring either convergently upon the
36 repository, or divergently from it, as discussed in detail in Section 6.4.2.1. Because the
37 repository is not conceptualized as homogeneous, implementing a geometry for the conceptual
38 model of convergent or divergent flow in the Salado is somewhat complicated and is
39 discussed in Section 6.4.2.1.

40
41 The conceptual model for Salado fluid flow has primary interactions with three other
42 conceptual models. The interbed fracture conceptual model allows porosity and permeability
43 of the interbeds to increase as a function of pressure. The repository fluid flow model is
44 directly coupled to the Salado fluid flow model by the governing equations of flow in

1   BRAGFLO (in the governing equations of the mathematical model, they cannot be
2   distinguished), and it differs only in the region modeled and the parameters assigned to
3   materials. The Salado model for actinide transport is directly coupled to the conceptual model
4   for flow in the Salado through the process of advection.
5
6   *MASS.13.1 High Threshold Pressure for Halite-Rich Salado Rock Units*
7
8   A parameter used to describe the effects of two-phase flow is threshold pressure. The
9   threshold pressure is important because it helps determine the ease with which gas can enter a
10 liquid-saturated rock unit. For a brine-saturated rock, the threshold pressure is defined as
11 "equal to the capillary pressure at which the relative permeability to the gas phase begins to
12 rise from its zero value, corresponding to the incipient development of interconnected gas
13 flow paths through the pore network" (Davies 1991, 9).
14
15 The threshold pressure, as well as other parameters used to describe two-phase characteristics,
16 has not been measured for halite-rich rocks of the Salado. The Salado, however, is thought to
17 be similar in pore structure to rocks for which threshold pressures have been measured
18 (Davies 1991). Based on this observation, Davies (1991) postulated that the threshold
19 pressure of the halite-rich rocks in the Salado could be estimated if an empirical correlation
20 exists between rocks postulated to have similar pore structure.
21
22 Davies developed a correlation between threshold pressure and intrinsic permeability
23 applicable to the Salado halites. (A similar correlation was developed for Salado anhydrites;
24 subsequent testing confirmed that the correlation predicted threshold pressures accurately.)
25 The correlation developed by Davies predicts threshold pressures in intact Salado halites on
26 the order of 20 megapascals or greater (Davies 1991). This threshold pressure predicted by
27 correlation is so high that for all practical and predictive purposes, no gas will flow into intact
28 Salado halites (see Section 6.4.5.1).
29
30 Because threshold pressure helps control the flow of gas, and because the greatest volume of
31 rock in the Salado is rich in halite, a high threshold pressure effectively limits the volume of
32 gas that can be accommodated in the pore spaces of the host formation. Thus high threshold
33 pressure is considered conservative as well as realistic, because if gas could flow into the pore
34 spaces of Salado halite, repository pressures could be reduced dramatically.
35
36 *MASS.13.2 Historical Context of the Salado Conceptual Model*
37
38 In the 1980 FEIS (documented in Lappin et al. 1989, Table 1-1, 1-7 to 1-8), the Salado was
39 assumed to be a confining bed, containing no circulating groundwater (Lappin et al. 1989,
40 7 – 87). Brine was thought to be present only in fluid inclusions and hydrous minerals and
41 was assumed not to be present along grain boundaries. Gas permeability was estimated to be
42 adequate to dissipate the volumes of gas potentially generated by the waste. There was no
43 explicit recognition of any differing hydrologic role for the nonhalite interbeds.
44

1   Based on the results of early in situ permeability testing, the conceptual model of the Salado
2   had changed by the time of publication of Lappin et al. (1989, Table 1-1, 1-7 to 1-8). Grain
3   boundary brines were known to be present and were distinct compositionally from fluid
4   inclusions. The Salado was interpreted to be brine saturated. The major contribution to fluid
5   flow was interpreted to be movement of grain-boundary fluids, as a result of pore pressure
6   gradients resulting from excavation. Darcy flow, assuming atmospheric boundary conditions
7   within the repository (which was all that could be modeled at the time), probably over-
8   predicted brine inflow. Far-field permeability (not distinguished between halites and
9   anhydrites) was thought to be less than 10^{-21} to 10^{-22} square meters and possibly even
10   effectively zero in undisturbed regions. Because gas would have to displace brines in the
11   Salado, dissipation of significant volumes of gas would be difficult. The combination of gas-
12   generation rates and low permeability would have led to pressures exceeding lithostatic unless
13   these pressures were relieved: numerical models for altered anhydrites did not exist at that
14   time. Except at seal locations, MB139 was thought to be a relatively high-permeability flow
15   path directly under the excavations because of the development of open excavation-related
16   fractures.
17
18   In the preliminary performance assessment completed in December 1992 (WIPP Performance
19   Assessment Department 1992, 2-41 to 2-45), anhydrite interbeds provided the dominant
20   pathway for fluid migration because of their relatively high permeability. New test data
21   indicated permeabilities of 10^{-16} to 10^{-21} square meters for anhydrites and 10^{-20} to 10^{-24} square
22   meters for halite. (The DOE interpreted the low ends of these ranges to be far-field
23   permeabilities and the higher ends to results from excavation effects; see Sandia WIPP Project
24   1992, 2-56 to 2-57). It was newly recognized that there would be coupling between fluid
25   flow, creep closure, and brine-dependent gas generation. No altered-anhydrite model was
26   implemented in this preliminary performance assessment.
27
28   In 1994, the DOE concluded that the regional 1-degree stratigraphic dip could have an effect
29   on fluid flow into and out of the repository. An altered-anhydrite model for interbed fracture
30   under elevated gas pressures was implemented. Flow simulations incorporating detailed
31   stratigraphy confirmed that simplifications considering only a lumped impure halite were
32   adequate (Christian-Frear and Webb 1996). The potential for preferential brine outflow
33   caused by channeling, fingering, updip flow, or fracturing was also recognized. Concern
34   about the adequacy of the two-dimensional modeling simplification to provide reasonable
35   estimates of three-dimensional brine inflow and outflow was thought to be potentially
36   important, because of the addition of both dip and altered-anhydrite fracturing models. These
37   concerns led to a number of modeling and analysis efforts to investigate the adequacy of
38   performance assessment assumptions.
39
40   In 1995 and 1996, final analyses of the Room Q experiments showed experimental results to
41   be consistent with a Darcy flow model.
42

1 *MASS.13.3 The Anhydrite Interbed Fracture Model*
2
3 The purpose of this model is to alter the porosity and permeability of the anhydrite interbeds if
4 their pressure approaches lithostatic, simulating some of the hydraulic effects of fractures with
5 the intent that unrealistically high pressures (much in excess of lithostatic) do not occur in the
6 repository or disposal system. The conceptual model is also discussed in Section 6.4.5.2.
7
8 In the 1992 preliminary performance assessment, repository pressures were shown to greatly
9 exceed lithostatic pressure if a large quantity of gas was generated. Pressures within the waste
10 repository and surrounding regions were predicted to be roughly 20 to 25 megapascals. It was
11 expected that fracturing within the anhydrite marker beds would occur at pressures slightly
12 below lithostatic pressure. An expert panel on fractures was convened to develop the
13 conceptual bases for the fracturing within the anhydrite marker beds.
14
15 The porosity and permeability increases are conceptualized as occurring vertically throughout
16 the affected interbed; in other words, throughout the porous medium as a whole rather than on
17 discrete portions. This simplification facilitates numerical implementation and execution.
18
19 Two parametric behaviors must be quantified in the conceptual model. First, the change of
20 porosity with pressure in the anhydrite marker beds must be specified. This is done with a
21 relatively simple equation, described in Appendix BRAGFLO (Section 4.10), that relates
22 porosity change to pressure change using an assumption that the fracturing can be thought of
23 as increasing the compressibility of interbeds. Parameters in the model are treated as fitting
24 parameters and have little relation to physical behavior except that they affect the porosity
25 change. The second parametric behavior is the change of permeability with pressure, which is
26 incorporated by a functional dependence on the porosity change. It is assumed that a power
27 function is appropriate for relating the magnitude of permeability increase to the magnitude of
28 porosity increase. The parameter in this power function, an exponent, is also treated as a
29 fitting parameter and can be set so that the behavior of permeability increase with porosity
30 increase fits the desired behavior.
31
32 The fracture enhancement model assumes fracture propagation is uniform in the lateral
33 direction to flow within the marker beds in the absence of dip. The 1-degree dip modeled in
34 BRAGFLO may affect fracture propagation direction. That is, within the accuracy of the
35 finite difference grid, a fracture will develop radially outward. This would not account for
36 fracture fingering or a preferential fracturing direction; however, no existing evidence
37 supports heterogeneous anhydrite properties that would contribute to preferential fracture
38 propagation. This evidence is discussed in Attachment 13-2.
39
40 The maximum enhanced fracture porosity controls the storativity within the fracture. The
41 extent of the migration of the gas front into the marker bed is sensitive to this storativity. The
42 additional storativity caused by porosity enhancement will mitigate gas migration within the
43 marker bed. The enhancement of permeability by marker-bed fracturing will make the gas
44 more mobile and will contribute to longer gas-migration distances. Thus the effects of

1   porosity enhancement at least partially counteract the effects of permeability enhancement in
2   affecting the gas-migration distances.
3
4   Because intact anhydrite is partially fractured, the pressure at which porosity or permeability
5   changes are initiated is close to the initial pressure within the anhydrite. The fracture
6   treatment within the marker beds will not contribute to early brine drainage from the marker
7   bed, because the pressures at these times are below the fracture initiation pressure.
8
9   The input data to the interbed fracture model (see Appendix PAR, Table PAR-36) were
10   chosen deterministically to produce the appropriate pressure and porosity response as
11   predicted by a linear elastic fracture mechanics (LEFM) model, as discussed in Mendenhall
12   and Gerstle (1993). Results from this performance assessment show that repository pressures
13   do not exceed the full fracture pressure of approximately 16.5 megapascals, a value slightly
14   higher than lithostatic pressure.
15
16   *MASS.13.4 Flow in the Disturbed Rock Zone*
17
18   The conceptual model for the DRZ around the waste disposal, operations, and experimental
19   regions has been chosen to provide a reasonably conservative estimate of fluid flow between
20   the repository and the intact halite and anhydrite marker beds. The conceptual model is also
21   discussed in Section 6.4.5.3 of this application.
22
23   The conceptual model implemented in the performance assessment uses values for the
24   permeability and porosity of the DRZ that do not vary with time. A screening analysis
25   examined an alternative conceptual model for the DRZ in which permeability and porosity
26   changed dynamically in response to changes in pressure (Vaughn et al. 1995). This analysis
27   implemented a fracturing model in BRAGFLO for the DRZ. This fracturing model is
28   identical to the existing anhydrite interbed alteration model. In this model, formation
29   permeability and porosity depend on brine pressure as described by Freeze et al. (1995, 2-16
30   to 2-19) and Appendix BRAGFLO (Section 4.10). This model permits the representation of
31   two important formation alteration effects. First, pressure build-up caused by gas generation
32   and creep closure within the waste will slightly increase porosity within the DRZ and offer
33   additional fluid storage with lower pressures. Second, the accompanying increase in
34   formation permeability will enhance fluid flow away from the DRZ. Because an increase in
35   porosity tends to reduce outflow into the far field, parameter values for this analysis were
36   selected so that the DRZ alteration model greatly increases permeability while only modestly
37   increasing porosity.
38
39   Two basic scenarios were considered in the screening analysis by Vaughn et al. (1995),
40   undisturbed performance and disturbed performance. Both scenarios included a 1-degree
41   formation dip downward to the south. Intrusion event E1 is considered in the disturbed
42   scenario and consists of a borehole that penetrates the repository and pressurized brine in the
43   underlying Castile. Two variations of intrusion event E1 were examined, E1 updip and E1
44   downdip. In the E1 updip event, the intruded panel region was located on the updip (north)

end of the waste disposal region, whereas in the E1 downdip event, the intruded panel region is located on the downdip (south) end of the disposal region. These two different geometries permitted evaluation of the possibility of increased brine flow into the panel region caused by higher brine saturations downdip from the borehole and the potential for subsequent impacts on contaminant migration. To incorporate the effects of uncertainty in each case (E1 updip, E1 downdip, and undisturbed), a Latin hypercube sample size of 20 was used, for a total of 60 simulations. To assess the sensitivity of system performance on formation alteration of the DRZ, conditional CCDFs of normalized contaminated brine releases were constructed and compared with the corresponding baseline model conditional CCDFs that were computed with constant DRZ permeability and porosity values. Based on comparisons between conditional CCDFs, computed releases to the accessible environment were determined to be essentially equivalent between the two treatments.

Preliminary performance assessments considered alternative conceptual models that allowed for some lateral extent of the DRZ into the halite surrounding the waste disposal region and for the development of a transition zone between anhydrites a and b and MB138 (WIPP Performance Assessment Department 1993, Figures 4.1-2 and 5.1.2; Davies et al. 1993; Gorham et al. 1992). The transition zone was envisioned as a region that had experienced some hydraulic depressurization and perhaps some elastic stress relief because of the excavation, but probably no irreversible rock damage and no large permeability changes. Modeling results indicated that including the lateral extent of the DRZ had no significant effect on fluid flow. Communication vertically to MB138 was a potentially important process, however, and the model adopted for the performance assessment conservatively assumes that the DRZ extends upward to MB138 without an intervening transition zone.

MASS.13.5 Actinide Transport in the Salado

The purpose of this model is to represent the transport of actinides in the Salado. This model is also discussed in Section 6.4.5.4.

Actinide transport in the Salado is conceptualized as occurring only by advection through the porous medium described in the Salado hydrology conceptual model. Advection is the movement of material with the bulk flow of fluid. Other processes that might disperse actinides, such as diffusion, hydrodynamic dispersion, and channeling in discrete fractures, are not included in the conceptual model.

Advection is a direct function of fluid flow, which is discussed in the conceptual model for Salado fluid flow.

This application of NUTS treats the transport of radionuclides within all the regions for which BRAGFLO computes brine and gas flow. The brine must pass through some part of the repository at some period in its history to become contaminated. While there, it is assumed to acquire radioactive constituents, which it then transports by advection to other regions outside the repository. NUTS uses BRAGFLO's velocity field, pressures, porosities, saturations, and other model parameters (including geometrical grid, residual saturation, material map, brine

1 compressibility, and time step) averaged over a given number of time steps (20 for this
2 performance assessment calculation), which it takes as input for its transport calculations.
3 Consequently, the results of NUTS are subject to all the uncertainties associated with
4 BRAGFLO's conceptual model and parameterization, which will not be repeated here.
5 Details of the source term are discussed in Appendix SOTERM.

7 This application of NUTS disregards sorptive and other retarding effects throughout the entire
8 flow region, even though retardation must occur at some level within the repository, the
9 marker beds, and the anhydrite interbeds, and especially in zones with clay layers or clay as
10 accessory minerals.

12 This application of NUTS neglects molecular dispersion, which leads to uncertainty. For
13 materials of interest in the WIPP repository system, molecular diffusion coefficients are at a
14 maximum on the order of 4×10^{-10} square meters per second. Thus, the simplest scaling
15 argument using a time scale of 10,000 years leads to a molecular diffusion (that is, mixing)
16 length scale of approximately 33 feet (10 meters), which is negligible compared to the lateral
17 advection length scale of roughly 7,874 feet (2,400 meters) (the lateral distance from the
18 repository to the accessible environment).

20 This application of NUTS also neglects mechanical dispersion, which leads to additional
21 uncertainty (see Section 6.4.5.4.2). Dispersion is quantified by dispersivities, which are
22 empirical (tensor) factors that are proportional to flow velocity (to within geometrical factors
23 related to flow direction). They account for both the downstream and cross-stream spreading
24 of local extreme values in concentration of dissolved constituents. Physically, the spreading is
25 caused by the fact that both the particle paths and velocity histories of once-neighboring
26 particles can be vastly different because of material heterogeneities characterized by
27 permeability variations. These variations arise from the irregular cross-sectional areas and
28 tortuous nonhomogeneous, nonisotropic connectivity between pores. Because of its velocity
29 dependence, the transverse component of mechanical dispersivity tends to transport dissolved
30 constituents from regions of relatively rapid flow (where mechanical dispersion has a larger
31 effect) to regions of slower flow (where mechanical dispersion has a smaller effect). In the
32 downstream direction, dispersivity merely spreads constituents in the flow direction.
33 Conceptually, ignoring lateral spreading assures that dissolved constituents will remain in the
34 rapid part of the flow field, which assures their transport toward the boundary. Similarly,
35 ignoring longitudinal dispersivity ignores the elongation of a feature in the flow direction,
36 which ignores foreshortening (or lengthening) of arrival times. However, because the EPA
37 release limits are time-integrated measures, the exact times of arrival are unimportant for
38 constituents that arrive at the accessible environment within the assessment period (10,000
39 years).

41 Advection is therefore the only transport mechanism considered important, which underscores
42 NUTS' reliance on BRAGFLO. Because the Darcy flows are given to NUTS as input, the
43 maximum solubility limits for combined dissolved and colloidal components are the most
44 important NUTS parameters. They are described in Appendix SOTERM (Section
45 SOTERM.7).

MASS.14 Geologic Units above the Salado

The model for geologic units above the Salado was developed to provide a reasonable and realistic basis for simulations of fluid flow within the disposal system and detailed simulations of groundwater flow and radionuclide transport in the Culebra. The conceptual model for these units is also discussed in Chapter 6.0 (Section 6.4.6) of this application.

The conceptual model used in performance assessment for the geologic units above the Salado is based on the overall concept of a groundwater basin, as introduced in Chapter 2.0 (Section 2.2.1.1) of this application, and developed further in Section MASS.14.2. The computer code SECOFL3D was used to evaluate the effect on regional-scale fluid flow by recharge and rock properties in the groundwater basin above the Salado. However, simpler models for this region are implemented in codes used in performance assessment. For example, in the BRAGFLO model, layer thicknesses, important material properties including porosity and permeability, and hydrologic properties such as pressure and initial fluid saturation are specified, but the model geometry and boundary conditions are not suited to groundwater basin modeling (nor is the BRAGFLO model used to make inferences about groundwater flow in the units above the Salado). In performance assessment the Culebra is the only subsurface pathway modeled for radionuclide transport above the Salado, although the groundwater basin conceptual model includes other flow interactions. The Culebra model implemented in performance assessment includes spatial variability in hydraulic conductivity and uncertainty and variability in physical and chemical transport processes. Thus, the geometries and properties of units in the different models applied to the units above the Salado by the DOE are chosen to be consistent with the purpose of the model.

The groundwater basin model incorporated into the code SECOFL3D is the most general and least limited model available to the DOE for investigating how fluid flow in the units above the Salado is affected by variation in regional rock properties, basin geometries, and boundary conditions (including recharge changes and climate change). This code is used for calculations in support of this application but not in performance assessment *per se*. Studies performed with this code provide support for the performance assessment assumption of a confined Culebra and quantify the possible effects of future change in climate on the performance of the WIPP.

The SECOFL2D and SECOTP2D codes are used directly in performance assessment to model fluid flow and transport in the Culebra. The assumptions made in these codes are discussed in Section 6.4.6.2 and Section MASS.15.

With respect to the units above the Salado, the BRAGFLO model is used only for determination of fluid fluxes between the shaft or intrusion borehole and hydrostratigraphic units. For this purpose, it does not need to resolve regional or local flow characteristics.

The basic stratigraphy and hydrology of the units above the Salado are described in Sections 2.1.3.5 through 2.1.3.10, and Section 2.2.1.4, respectively. Additional supporting

1 information is contained in Appendices GCR, HYDRO, and SUM. Details of the conceptual
2 model for each unit are described in Sections 6.4.6.1 through 6.4.6.7.
3
4 ## MASS.14.1 Historical Context of the Units above the Salado Model
5
6 The model used in the WIPP FEIS in 1980 (documented in Lappin et al. 1989, Table 1-1, 1-14
7 to 1-16) recognized three water-bearing zones within the Rustler, that is, the Magenta,
8 Culebra, and the Rustler-Salado-interface (Lappin et al. 1989, 7 – 87). The Culebra and
9 Magenta, although known to be separate units, were combined for regional-scale transport
10 modeling into a Rustler aquifer and assigned a uniform hydraulic conductivity, except in Nash
11 Draw. In the modeling, the Rustler aquifer was assumed to be an isotropic porous medium
12 with a uniform porosity of 0.10 (Lappin et al. 1989, Table K-2, K-18). Regional flow was
13 assumed to be toward the southwest, with discharge at Malaga Bend on the Pecos River.
14 Numerical modeling was not able to consider the possible impact of variations in brine
15 density within the Rustler; instead, modeling used an equivalent freshwater head. Steady-state
16 flow directions and rates were assumed. Fluid flow in units above the Rustler was not
17 considered because the limited available information suggested that these units were
18 unsaturated. Units below the Castile were assumed to have no effect on performance and
19 were not included in the analysis.
20
21 Several developments had taken place by 1989 (Lappin et al. 1989). Most importantly,
22 interest in fluid flow within the Rustler became strongly focused on the Culebra. The Culebra
23 is at least one order of magnitude more permeable than the Magenta, except in Nash Draw.
24 Modeling by Barr et al. (1983) showed no potential for significant transport or fluid
25 movement through the Magenta, and none of the hydraulic tests in the Magenta shows
26 anything but porous-medium behavior. All other units within the Rustler (unnamed lower
27 member, Tamarisk, Forty-niner) were even less permeable than the Magenta. Testing at
28 DOE-2 had shown that permeability of the lower Dewey Lake was significantly lower than in
29 the Magenta (Beauheim 1986). In the Draft Supplemental Environmental Impact Statement
30 (DSEIS) (DOE 1989) and the December 1992 preliminary performance assessment
31 calculations, all fluid flow and transport was assumed to be concentrated in the Culebra; this
32 was thought to be a conservative approach because it did not allow flow in units in which
33 release to the accessible environment was not possible.
34
35 Other important changes were in place by 1989. The potential for vertical fluid flow within
36 the Rustler was recognized, on the basis of limited data, although for flow and transport
37 calculations, the Culebra was assumed to be perfectly confined. Long-term flow transients
38 within the system, related to climate change, were considered to be likely. Finally, the
39 possibility of vertical fluid flow in an open borehole between the Rustler and the Bell Canyon
40 was considered, but it was concluded that such fluid flow would be directed downward and
41 was therefore of no physical or regulatory concern (Lappin et al. 1989).
42
43 Use of the groundwater basin conceptual model to gain an understanding of regional flow in
44 the units above the Salado was initiated in a modeling study performed by Davies (1989). He

1 selected boundaries to coincide with hydrologic features and used geologic data to infer
2 hydraulic conductivity values for areas in which conductivity measurements were not
3 available. Recognizing the three-dimensional nature of the regional groundwater system,
4 Davies oriented two-dimensional simulations in both vertical and horizontal planes. The
5 vertically oriented simulations were performed because it was recognized that the transient
6 nature of the system is related to movement of the water table and the consequent change in
7 the amount of water stored in the rocks. Davies confirmed that the hypothesis that the
8 modern-day flow system might be a transient response to recharge during the last glacial
9 pluvial period (Lambert 1987; Lambert and Carter 1987; Lambert and Harvey 1987) is
10 physically possible. He also concluded that as much as 25 percent of the total inflow to the
11 Culebra could be entering as vertical flux, and that fluid pressures in the Culebra are less than
12 hydrostatic because the Culebra is well connected to the discharge area and poorly connected
13 to the source of recharge. He suggested that the results of his study could be expanded by,
14 among other things, using a fully three-dimensional approach and additional study of the role
15 of long-term transient changes in flow.

16

17 As a first step in extending the work of Davies, Corbet and Wallace (1993) developed a fully
18 three-dimensional model with an adaptive upper boundary condition to approximately
19 simulate movement of the water table. These simulations were performed using a version of
20 the United States Geological Survey (USGS) code MODFLOW (McDonald and Harbaugh
21 1988) that was modified to include seepage faces. The modified MODFLOW model was
22 limited in its capabilities in that it only approximately calculated the position of the water
23 table and did not account for lateral variations in hydraulic conductivity. Nonetheless, the
24 simulation results provided the first information about possible recharge rates at a regional
25 scale and the sensitivity of groundwater flow patterns to changes in recharge. Specifically, the
26 results suggested that rates of recharge to the saturated zone do not exceed several millimeters
27 per year and that flow patterns in confined units are sensitive to small changes, perhaps only a
28 few tenths of a millimeter per year, in rates of recharge.

29

30 A new numerical code, SECOFL3D (Knupp 1996), was used to perform the most recent
31 three-dimensional simulations (Corbet 1994; Corbet and Swift 1996 [see Attachment 17-1]).
32 The algorithm implements a rigorous treatment of the free-surface and seepage-face boundary
33 conditions (Bear and Verruijt 1987; Dagan 1989; de Marsily 1986) and is designed to be
34 robust even if extremely large contrasts in hydraulic conductivity are present within the model
35 domain. A moving mesh that adaptively deforms so that its upper surface conforms to the
36 moving water table is used to ensure that the entire computational domain remains saturated.

37

38 *MASS.14.2 Groundwater-Basin Conceptual Model*

39

40 The conceptual model that emerged from taking a groundwater-basin approach represents a
41 significant advance in understanding (Section 2.2.1.1). It differs from previous conceptual
42 models in that it includes a description of the geometry of the groundwater basin, the
43 distribution of rock hydraulic properties, and the physical mechanisms that drive groundwater
44 flow. Previous conceptual models were limited to describing current flow conditions. They
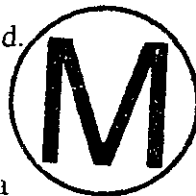
1   provided little basis to extrapolate backward or forward in time or to predict the impact of
2   human-induced disturbances to the hydrologic system.
3
4   An objective of groundwater basin modeling was to use numerical simulations to enhance
5   conceptual understanding of the hydrogeology of the Culebra in the context of regional
6   groundwater flow (Corbet and Knupp 1996). A conceptual model is considered to be a
7   qualitative description of the hydrologic processes, the geometry of the hydrogeologic system,
8   the hydrostratigraphy, and the pattern of groundwater flow. In short, a conceptual model is an
9   interpretation of reality. The rest of this section presents aspects of the conceptual model of
10   groundwater flow in the Culebra that was formulated by integrating the previous conceptual
11   understanding with the new information that these numerical simulations provided.
12   Simulation results are incorporated without specifically identifying them as such.
13
14   Groundwater flow in the Culebra in the vicinity of the WIPP is a portion of a larger
15   hydrologic system that includes the rock units that overlie the Salado. This system extends
16   laterally well beyond the WIPP site to the boundaries of a groundwater basin. The basin
17   boundary is not fixed in time; the basin is more extensive during dry periods in which the
18   water table is at depth and less extensive during wet periods in which the water table is near to
19   the land surface. The boundaries of the numerical model (Figure 2-29 in Chapter 2.0)
20   approximately represent the basin boundaries for dry periods. These boundaries, therefore,
21   outline the minimum region that must be considered to conceptually understand the evolution
22   of modern-day flow conditions and their extrapolation into the future.
23
24   There is a continuous water table across the groundwater basin. It is probably in the Dewey
25   Lake within the WIPP-site boundary. In places the hydraulic conductivity of the Dewey Lake
26   is small enough that groundwater inflow to an open drill hole penetrating the saturated portion
27   of this unit is too slow to be easily observed. It is also possible that some saturated portions of
28   the Dewey Lake might be perched, that is, that they overlie an unsaturated region. Perched
29   regions, if they exist, are part of the percolation process. They might affect the distribution of
30   percolation at the water table but do not directly affect flow in the saturated zone.
31
32   A fundamental aspect of the conceptual model that has evolved from groundwater basin
33   modeling is that the groundwater system is dynamic and is responding to the drying of the
34   climate that has occurred since the end of the Pleistocene. Recharge rates at the end of the
35   Pleistocene were sufficient to maintain the modeled water table near the land surface over
36   much of the model domain. Groundwater flow, at that time, was controlled by the
37   intermediate features of the land-surface topography. The gentle east to west slope of the land
38   surface in the vicinity of the WIPP, for example, caused groundwater in the Culebra to flow
39   toward and discharge into Nash Draw. As the amount of moisture available to recharge the
40   groundwater system decreased after the last glacial pluvial period, the elevation of the water
41   table declined. The decline occurred first in areas of high topography. As the water table
42   dropped, groundwater flow began to increasingly reflect the land-surface topography at the
43   scale of the entire groundwater basin. That is, the flow was away from the areas along the
44   north and north-east boundaries of the basin where land-surface elevations are greater than

1   3,609 feet (1,100 meters) and toward areas below 2,789 feet (850 meters) in the Pecos River
2   valley along the south boundary of the basin.
3
4   Dissolution of the upper Salado and associated processes has generated a zoned distribution of
5   hydraulic conductivity at the basin scale. Hydraulic conductivities in the region in which
6   dissolution is assumed to have disrupted stratigraphic layering (zone 1 of Figure MASS-3) are
7   orders of magnitude larger than the region in which the strata are intact (zone 4). A transition
8   interval separates these regions. Flow magnitudes and directions are quite different in these
9   regions. Lateral flow in the intact strata is slow and, regardless of the elevation of the water
10   table, is directed toward the disrupted region in areas that are within about a kilometer of the
11   transition interval. In contrast, flow in the disrupted region is relatively rapid and its direction
12   depends on the elevation of the water table. Flow is toward topographic depressions along the
13   west and south boundaries of the model domain if the water table is near the land surface.
14   Flow is directed toward the portion of the Pecos River valley along the south boundary if the
15   water table is at depth.
16
17   Within the region of intact strata, the contrast in hydraulic conductivities plays an important
18   role in determining flow patterns. The Dewey Lake and Triassic rocks are more permeable
19   than the anhydrites at the top of the Rustler. Consequently most of the water that recharges
20   the groundwater basin flows only in these rocks above the Rustler. The rest leaks vertically
21   through the upper anhydrites and is available for flow through the rest of the Rustler.
22   Gradients of hydraulic head along the base of the Dewey Lake provide the driving force for
23   flow in the Rustler.
24
25   Groundwater flow in the Rustler is characterized by very slow vertical leakage through
26   confining units and faster lateral flow in conductive units. Specific discharges (flow rates per
27   unit area) in the Culebra are two to three orders of magnitude greater than the vertical specific
28   discharges across the top of the Culebra. However, vertical leakage can contribute a
29   significant portion of the total inflow to portions of the Culebra that are extensive enough that
30   the upper surface is very much larger than the area available for lateral flow. It is difficult to
31   quantify the relative contribution of vertical leakage because the hydraulic conductivity of the
32   anhydrite confining layers at a regional scale is not well known.
33
34   As discussed in Chapter 2.0 (Section 2.2.1.4.1.2), studies of the isotopic composition of
35   groundwater above the Salado (for example, Chapman 1986, 1988; Siegel et al. 1991) have
36   generated debate about where and when the groundwater that is currently in the Culebra
37   within the WIPP site was recharged. Conceptually, the sites of recharge can be found in a
38   groundwater basin model by tracing various flowpaths from the WIPP site upstream to the
39   water table. Flow paths were not identified as such as part of the simulation study, but some
40   understanding can be reached by examining a large number of velocity distributions for the
41   Culebra, Magenta, and Dewey Lake and Triassic units. These results suggest that flowpaths
42   would have reached the water table in areas that are north and northeast of the WIPP site. The
43   various flowpaths to the WIPP site would include relatively rapid lateral flow in the
44   conductive units and slow vertical flow through the Rustler confining units. Flow paths that

1   enter the WIPP site portion of the Culebra by vertical leakage across its upper surface
2   originated outside of the WIPP site but closer to the WIPP site than the flow paths that enter
3   the WIPP site by lateral flow within the Culebra. None of the water in the Culebra within the
4   WIPP site is conceptualized as having been recharged in areas where the Culebra is at or near
5   to the land surface. It is also noted that the travel times along the various flowpaths to the
6   Culebra probably vary greatly. Therefore, the water currently in the Culebra is a mix of water
7   with much different residence times.

9   The modern-day pattern of groundwater flow has not equilibrated to the present climate.
10   There are two aspects to this disequilibrium. First, the position of the water table has not yet
11   adjusted to past changes in recharge rates. A decrease in recharge that started at the end of the
12   Pleistocene was complete by 8,000 years ago. The water table, however, is still in the process
13   of adjusting to this change in recharge. Second, hydraulic heads in rocks with small
14   conductivities are not adjusted to the current position of the water table. The base-case
15   transient simulation shows, for example, that closed regions of maximum head occur in the
16   Culebra at the present time. These maxima are in regions where the Culebra's conductivity is
17   believed to have been reduced by precipitation of halite in pore space. Groundwater flows out
18   of these regions too slowly for heads to remain in equilibrium with a falling water table. The
19   persistence of these regions of high head delays the transition of the flow field to one that fully
20   reflects the basin-scale topography.

22   The slow response of the water table to long-term changes in recharge is the dominant aspect
23   of the transient nature of the groundwater system. However, superimposed on long-term
24   changes in the flow system are short-term changes caused by alternating wet and dry periods
25   during the Holocene. Each wet-and-dry cycle results in a rise and fall of the water table. The
26   amount of change in the water table depends on the peak recharge rate and the rock properties.
27   The simulated change is typically 16 to 49 feet (5 to 15 meters). Changes in hydraulic head in
28   the Culebra lag behind changes in the water table and have a smaller amplitude. The overall
29   effect of the Holocene wet periods is to slow the long-term decline of the water table and to
30   superimpose short-term, and relatively small, variations to long-term flow velocities.

32   The new contributions to the conceptual understanding of the regional hydrogeology of the
33   Culebra resulting from modeling from a groundwater basin perspective include the following:

35   •   The shape and elevation of the water table largely determine rates and directions of
36   groundwater flow in the Culebra.

38   •   Groundwater inflow to the portion of the Culebra within the WIPP site boundary is by
39   a combination of lateral flow within the Culebra and extremely slow vertical leakage
40   from the overlying Tamarisk.
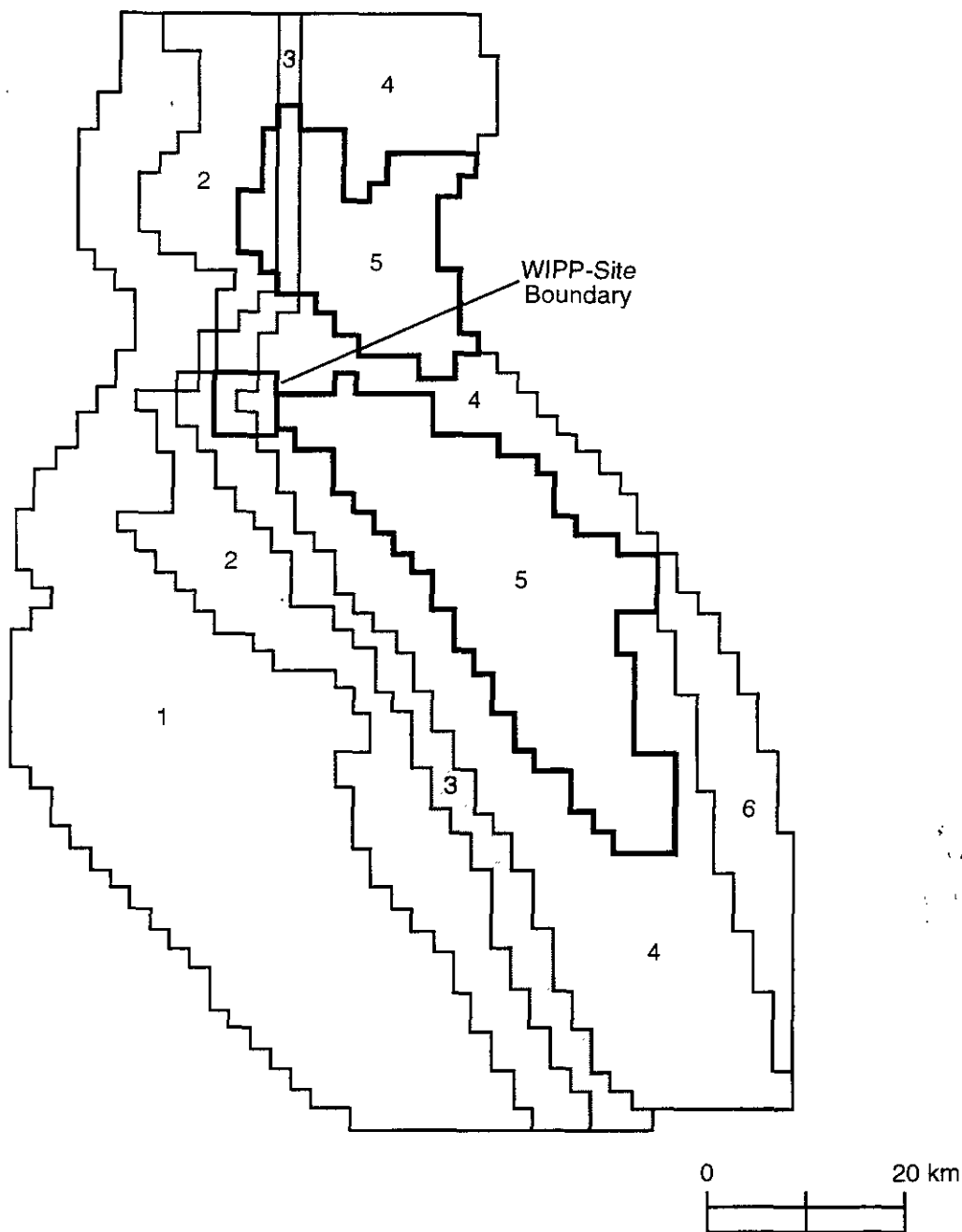
NOTE: Zonation approach used to represent the effects of depositional setting and post-depositional processes. Zone 1 ia a region in which dissolution of the upper Salado has fractured and disrupted overlying strata to the extent that stratigraphic layering is not preserved over long distances. In Zone 2, dissolution of the upper Salado is thought to have fractured the Rustler, but did not disrupt layering. Fractures that predate dissolution of the upper Salado are mostly filled with gypsum. These fracture fillings have been removed in Zone 3. Zone 4 represents intact strata. The region occupied by the halite facies of the mudstone/halite layers is indicated by Zone 5. A graben structure is shown as Zone 6.

CCA-MAS001-0

Figure MASS-3. Zonation Approaches Used in SECOFL3D Studies of Regional Groundwater Flow

1

THIS PAGE INTENTIONALLY LEFT BLANK

- The term recharge refers to a process that occurs at the water table. The inflow to the Culebra originated as recharge distributed over large areas of the groundwater basin. Recharge that eventually reaches the Culebra within the WIPP site does not occur where the Culebra crops out or where overlying confining units have been removed or fractured. The paths that water follows as it flows from the water table to the Culebra at the WIPP site necessarily include vertical leakage across confining layers. The travel time to reach the Culebra varies greatly along the various paths. The travel times are probably thousands or tens of thousands of years.

- Climate change alters recharge rates. Consequently the position of the water table changes and groundwater velocities at depth adjust accordingly.

- Modern-day flow velocities in the Culebra at the WIPP site can be understood and simulated using the groundwater basin conceptual model. The generally north-to-south flow is a result of the modern-day depth of the water table and the basin-scale distribution of hydraulic conductivity. Flow in wetter climates would rotate toward Nash Draw to the west. Flow in the Culebra directed away from Nash Draw is not supported by this model.

- The size and shape of the hydrogeologic system that determines groundwater flow velocities in the Culebra at the WIPP site have been tentatively identified.

MASS.15 Culebra

The conceptual model for groundwater flow in the Culebra (a) provides a reasonable and realistic basis for simulating radionuclide transport in the Culebra and (b) allows evaluation of the extent to which uncertainty about groundwater flow in the Culebra may contribute to uncertainty in the estimate of cumulative radionuclide releases from the disposal system. See Chapter 6.0 (Section 6.4.6.2) for additonal references to other relevant discussions on this conceptual model.

The conceptual model used in performance assessment for groundwater flow in the Culebra treats the Culebra as a confined two-dimensional aquifer with constant thickness and spatially varying transmissivity (see Attachment 15-7). Flow is modeled as single-phase (liquid) Darcy flow in a porous medium.

Basic stratigraphy and hydrology of the units above the Salado are described in Chapter 2.0 (Sections 2.1 and 2.2). Additional supporting information is contained in Appendices GCR, HYDRO, and SUM.

The conceptual model for flow in the Culebra is discussed in Chapter 6.0 (Section 6.4.6.2). Details of the calibration of the transmissivity field, based on available field data, are given in Appendix TFIELD (Section TFIELD.4). Initial and boundary conditions used in the model

1   are given in Section 6.4.10.2. A discussion of the adequacy of the two-dimensional
2   assumption for performance assessment calculations is included as Attachment 15-7.
3
4   The principal parameter used in the performance assessment to characterize flow in the
5   Culebra is an index parameter (the transmissivity index) used to select a single transmissivity
6   field for each Latin hypercube sample element from a set of calibrated fields, each of which is
7   consistent with available data (see Appendix PAR, Parameter 35).
8
9   *MASS.15.1 Historical Context of the Culebra Model*
10
11   Since the FEIS in 1980, the model used to describe flow and transport within the Culebra has
12   changed significantly. In the FEIS, the Culebra and Magenta were combined and modeled as
13   one layer referred to as the Rustler aquifers. In the modeling, the Rustler aquifers were
14   assumed to be an isotropic porous medium with a uniform porosity of 0.10 (Lappin et al.
15   1989, Table K-2, K-18). A uniform transmissivity field was assumed across the model
16   domain except in Nash Draw. Regional flow was assumed to be toward the southwest
17   discharging at Malaga Bend on the Pecos River. (There was no regulatory framework or
18   boundary defined at this time.) Numerical modeling was not able to consider the possible
19   effect of variations in brine density within the Rustler, so modeling used an equivalent
20   freshwater head. Steady-state flow directions and rates were assumed. As for physical-
21   transport characteristics, the Culebra was incorporated into the Rustler aquifers and assumed
22   to be an isotropic, homogeneous porous medium.
23
24   Haug et al. (1987) calibrated a flow model to the H-3 pumping test (Beauheim 1987a) and the
25   effects from the excavation of the shafts. Data from numerous new boreholes installed and
26   tested since the 1980 study were included in this model. The boundaries of the model were
27   not much larger than the extent of the WIPP site. Brine densities were also used as a
28   calibration target. The brine densities were assigned at the boundaries and subsequently
29   modified to match the observed fluid densities. Vertical leakage was included in an attempt to
30   calibrate the brine densities. This attempt led to the recommendation that future modeling
31   studies treat the Culebra as a leaky-confined aquifer. The transmissivity field was estimated by
32   kriging and modified by the addition of pilot points, which were located by trial and error. In
33   this model, single- and double-porosity effects on the flow field were investigated. At the
34   regional scale, the use of a double-porosity vs. single-porosity (matrix-only) conceptual model
35   had little effect on the flow field.
36
37   A modeling study (LaVenue et al. 1990) conducted to support the DSEIS only slightly
38   modified the conceptual model used by Haug et al. (1987). The differences in the conceptual
39   model were the assumptions that brine density varied spatially but was held constant through
40   time, and vertical leakage was not included. It was assumed that the brine concentrations
41   could be considered to have changed little over the period of time modeled. The boundaries
42   of the 1989 study were much larger than those of the 1987 study, extending approximately
43   18.6 miles (30 kilometers) north and south and 12.4 miles (20 kilometers) in east and west.
44   The model grid was centered on the WIPP site. The boundaries were selected to include the
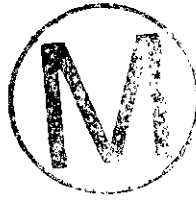
region for which head data were available and to minimize the boundary effects during transient simulation of the H-3, WIPP-13, and H-11 pumping tests. Fixed heads were assigned around all four boundaries based upon the regional head values. Transmissivities were estimated by kriging and ranged over seven orders of magnitude in this study. Pilot points were added to modify the transmissivity field during steady-state and transient calibration. Pilot-point locations were selected using an adjoint sensitivity analysis technique. The Culebra transmissivity field was calibrated on the basis of 41 test locations. Transmissivity was recognized to vary by approximately three orders of magnitude within the WIPP site. Modern flow in Culebra was recognized as being predominantly north to south on the WIPP site, and strongly affected by a high-transmissivity zone in the southeastern portion of the WIPP site. Flow was calculated on the basis of a fully confined Culebra and boundary conditions applied at the WIPP site scale. As discussed in Lappin et al. (1989), local flow and transport behavior were affected by fracturing where the transmissivity is greater than approximately 10^{-6} square meters per second. For physical transport, a double-porosity (matrix-diffusion) transport model for off-site transport from waste panels was assumed. Transport parameters were based on best estimates from nonsorbing tracer tests at three locations (Jones et al. 1992). It was assumed that the effective thickness was equal to the total thickness. Contaminant-transport calculations were one-dimensional.

The initial conditions for the Culebra flow field have been taken from the hydrographs of the WIPP boreholes. Prior to excavation of the salt handling shaft, the hydrographs showed little evidence of head change over the ten years preceding the shaft excavations. Head values were selected for each borehole with a hydrograph that preceded shaft excavation or that was located far from the shaft effects on the flow field. These data provided an estimate of the undisturbed head field and were subsequently used as initial conditions for the Culebra model's transient simulation.

In modeling the hydrologic characteristics of the Culebra, SNL (1992-1993) generated multiple transmissivity fields conditioned on hydraulic test data (point transmissivity data and transient head data) and then sampled those fields. This procedure addressed uncertainties in the location-specific values of the Culebra transmissivity. The geologic conceptual model was further revised to indicate that the degree of fracture flow was related to the degree of gypsum cement in the fractures. Contaminant-transport calculations were two-dimensional. The effective thickness of the Culebra was taken to be equal to the total thickness. A range of physical-transport parameters was used, as opposed to best estimates, to address the variability of physical-transport properties within the Culebra. The maximum fracture spacing was assumed to be equal to the total thickness of the Culebra (approximately 26 feet [8 meters]). The fracture spacing used in modeling was a convenient modeling simplification based on the concept of through-going parallel fractures. Representing fracturing in terms of fracture spacing is a mechanism to ensure that the proper surface-to-volume ratios are used in estimating the role of matrix diffusion. Calculations considered the possibility of both single-porosity (fracture-flow-only) and double-porosity (matrix diffusion) behavior.

1   The main differences between the 1989 and 1992 models were the model boundary locations,
2   boundary conditions, and the geostatistical approach used to develop and modify the
3   transmissivity field (LaVenue and RamaRao 1992). The 1992 model boundaries were rotated
4   38 degrees east to align with the axis of Nash Draw. This permitted the specification of a no-
5   flow boundary condition along a portion of the western boundary, which was selected to
6   coincide with the axis of Nash Draw. In addition, the northeastern corner of the model was
7   treated as a no-flow boundary because of the low transmissivities in the area and the lack of
8   any nearby regional heads to provide boundary head estimates. Transmissivities were
9   simulated by conditional simulation. Pilot points were automatically located and assigned
10 transmissivity values using an optimization routine during steady-state and transient-state
11 calibration.
12
13 By 1994, the model of the Culebra's hydrologic characteristics was unchanged from that of
14 December 1992. For the physical-transport characteristics, double-porosity transport was
15 assumed, but the base case had large fracture spacing, effectively the same as the Culebra
16 thickness. A single block size was assumed in each realization. Calculations still assumed an
17 effective thickness equal to the total thickness.
18
19 Since 1994, the model of the Culebra's regional hydrologic characteristics has not changed,
20 although additional large-scale information from pumping at H-19 and small-scale
21 information at Water Quality Sampling Program (WQSP) wells has been incorporated into the
22 calibration. Existing borehole-transmissivity interpretations have been refined. The model of
23 the physical-transport characteristics has changed on the basis of analysis of new data from
24 H-19 and H-11 and reanalysis of previous tests of H-3, H-11, H-6. The Culebra is now
25 conceived of as a fractured porous medium with inherent local variability in the degree and
26 scale of fracturing. Examination of core and shaft exposures has revealed that there are
27 multiple scales of porosity within the Culebra including fractures from microscale to large,
28 vuggy zones, and inter-particle and inter-crystalline porosity. This variability leads to both
29 lateral and vertical variations in permeability. Advection is believed to occur largely through
30 fractures; however, in some areas it may also occur through vugs connected by small fractures
31 and interparticle porosity. Diffusion occurs into all connected porosity. Performance
32 assessment, rather than conceiving of transport in terms of fracture and matrix porosities,
33 conceives the Culebra as being composed of advective and diffusive porosities. Matrix
34 diffusion is still believed to be effective and significant. The effective transport thickness is
35 thought to be less than the total stratigraphic thickness. The available data suggest that the
36 permeability of the upper portion of the Culebra is relatively low. Therefore the DOE has
37 concluded that the Culebra is adequately represented by a double-porosity continuum model
38 on the scale of performance assessment calculations, and it is not necessary to use a discrete-
39 fracture model on this scale.

1 *MASS.15.2 Dissolved Actinide Transport and Retardation in the Culebra*
2
3   The purpose of this model is to represent the effects of advective transport, physical
4   retardation, and chemical retardation on the movement of actinides in the Culebra. This
5   conceptual model is also discussed in Section 6.4.6.2.1.
6
7   The properties of the Culebra have been characterized by direct observation in outcrop,
8   boreholes, and shafts (Holt and Powers 1984, 1986, 1988, 1990), field hydraulic testing and
9   analysis (Beauheim 1987b), field tracer testing and analysis (Attachment 15-6; Jones et al.
10 1992; Mercer and Orr 1979), and laboratory testing and analysis (Papenguth and Behl 1996a,
11 1996b). The conceptual model for dissolved actinide transport in the Culebra is based on
12 these observations, tests, and analyses.
13
14 The conceptual model for actinide transport in the Culebra has three principal components:
15 advective transport, physical retardation, and chemical retardation. Two types of porosity are
16 present—porosity in which advective transport occurs, and porosity that is relatively inactive
17 in advective transport. This type of behavior is typically referred to as double porosity.
18 Because testing and analysis of the Culebra suggest that its upper portion does not play a
19 significant role in transport, transport is modeled only for the lower portion of the Culebra.
20
21 Advective transport refers to the transport of actinides in those pores of the Culebra where the
22 principal fluid flow occurs. This flow primarily occurs in fractures, but may also occur in
23 microfractures connecting vugs in vuggy regions or other portions of the porosity of the
24 Culebra that contain large pore-throat apertures (that is, high permeability regions). This
25 mechanism includes the effects of diffusion and dispersion in advective porosity as well as the
26 movement of actinides with the bulk fluid flow. Advective transport is thought to be
27 controlled by hydraulic gradient, hydraulic conductivity, thickness, and advective porosity.
28
29 Physical retardation refers to the process of diffusion from advective porosity into diffusive
30 porosity, that is, those portions of the porosity of the Culebra that are relatively inactive in
31 advective transport. Once in the diffusive porosity, the actinides are no longer carried along
32 by the most rapidly moving liquids, and their rate of movement is controlled by diffusion and
33 sorption. Diffusion can be an important process for effectively retarding solutes by
34 transferring mass from the porosity where advection (flow) is the dominant process into other
35 portions of the rock. The properties that control the diffusion of actinides into the diffusive
36 porosity are the surface area to volume ratio between advective porosity and the diffusive
37 porosity, the tortuosity of the diffusive porosity, and free-water diffusion coefficients (see
38 Attachment 15-3).
39
40 Chemical retardation refers to the sorption of actinides on minerals present in the Culebra.
41 The sorption is thought to occur on dolomite grains, but will also occur on clay or other
42 minerals. In the conceptual model, chemical retardation occurs only in the diffusive porosity,
43 and adds to the effects of the physical retardation. The governing properties for sorption are
44 described in a parametric expression of the degree to which dissolved actinides tend to sorb or

1 remain in solution (in the mathematical model, a K_d for a linear isotherm is used), which
2 requires the concentration of actinides in solution and the abundance of minerals on which
3 sorption can occur (see Attachment 15-1).
4
5 Advective porosity is thought to be a small percentage of the total volume of the Culebra
6 involved in transport. This porosity is interconnected and contains high-permeability features
7 such as fractures or vuggy pore structures. In this advective porosity, little actual rock
8 material is considered to exist (in other words, it is the fracture apertures and pore volumes
9 without surrounding rock). In contrast, diffusive porosity makes up the major portion of the
10 Culebra pore volume. It comprises lower-permeability features and most of the rock material.
11 The rate at which diffusion removes solutes from advective porosity is a function of the
12 surface area to volume ratio between the advective and diffusive porosity. For a given
13 geometry of advective porosity assumed in a model (for example, parallel-plate fractures), this
14 surface area to volume ratio can be expressed as a characteristic length which is known as the
15 matrix block length (for example, the thickness of a matrix slab between two parallel-plate
16 fractures).
17
18 In summary, the conceptual model for dissolved actinide transport in the Culebra includes two
19 types of porosity: advective porosity associated with high-permeability features of the
20 Culebra, and diffusive porosity associated with lower-permeability features. These two types
21 of porosity are distributed throughout the Culebra and are intertwined on a small scale; hence,
22 mapping their regional extent or boundaries between them is not feasible. Advection,
23 diffusion, and dispersion of dissolved actinides occur within the advective porosity. Diffusion
24 (physical retardation) and sorption (chemical retardation) occur within the diffusive porosity.
25 Advective porosity makes up a small portion of the overall pore volume of the Culebra;
26 diffusion is an important process for transferring mass into other portions of the rock mass
27 where there is a larger surface area for sorption. Because the upper portion of the Culebra has
28 been observed to be relatively inactive in solute transport in tests, it is assumed to be
29 unimportant and is not included in the conceptual model. Attachment 15-6 contains
30 additional information on the transport properties of the Culebra.
31
32 Several parameters are referred to or implied in the conceptual model as discussed in
33 Section 6.4.6.2. For transport in advective porosity, the principal parameter is the porosity of
34 the network, but because of links to the Culebra fluid flow model, the hydraulic gradient and
35 hydraulic conductivity largely control the specific discharge calculated by SECOFL2D.
36 Within diffusive porosity, the porosity, tortuosity, and diffusion coefficients for various
37 actinides are important because of their effect on the rate of diffusion. A parameter called
38 matrix block length, a measure of the surface area between the advective and diffusive
39 porosities, is also important. The density of sorbing minerals and their sorption properties,
40 expressed by K_d (the distribution coefficient), are important in chemical retardation.
41
42 It is commonly assumed that there should be a relationship between the conductivity of
43 advective porosity and its porosity and distribution, that is, that the fracture permeability,
44 porosity, and aperture or spacing should be correlated. Data collected and analyzed at the

WIPP do not support this assumption. There are no meaningful trends among these parameters for the data that have been collected. Therefore, values of these parameters are not correlated in the performance assessment (see Attachment 15-6, 14; Attachment 15-10).

Transport of actinides in the Culebra is coupled to several other conceptual models. An important coupling is to models for features that can introduce actinides to the Culebra, for example, the exploratory borehole, shafts and shaft seals, and dissolved actinide source term. The most important coupling is to the model for flow in the Culebra. Because transport in the Culebra is one of the last processes to occur along this pathway prior to release, it does not feed back to other conceptual models in any significant manner. In a manner of speaking, this conceptual model falls at the downstream end of the overall disposal system model, and thus has little or no impact on models that come before it.

MASS.15.2.1 Current Studies of Sorption in the Culebra

Several factors affect the sorption of Pu, Am, U, Th, and Np, the elements for which K_d values are required in performance assessment for Culebra transport calculations (Ramsey 1996) including:

- the properties of the sorbents (solids) that will sorb actinides from solution,

- the composition of solutions that currently exist in the Culebra or could enter the Culebra after human intrusion into WIPP disposal rooms,

- the oxidation state of the sorbate (actinide elements) in the Culebra,

- dissolved actinide concentration,

- equilibration time, and

- direction of reaction (sorption versus desorption).
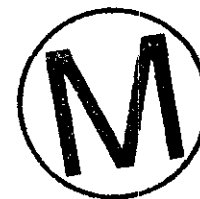
The two most important sorbents in the Culebra are dolomite, a carbonate mineral that constitutes most of the Culebra, and corrensite, an ordered mixture of chlorite and saponite associated with fracture surfaces and dispersed in the matrix (intact rock between the fractures) of the Culebra. Dolomite is important because it is by far the most abundant mineral in the Culebra. Corrensite is important because, although a minor constituent, it sorbs actinide elements more strongly than dolomite. The work of Sewards (1991) and Sewards et al. (1991, 1992) indicates that corrensite is associated with fracture surfaces and dispersed in the matrix at concentrations high enough to increase the retardation of Pu, Am, U, Th, and Np relative to that observed in laboratory studies with dolomite-rich rock. However, the DOE does not include K_ds for clay minerals in the ranges and probability distributions for the matrix K_ds for use in performance assessment calculations because laboratory data for clay-

1   rich rock under expected Culebra conditions are insufficient at this time. Furthermore, the
2   DOE does not take any credit for sorption by clay minerals associated with fracture surfaces.
3   Omitting K_ds for clays is conservative.

5   The experimental basis for the ranges and probabilities of matrix distribution coefficients is
6   documented in Attachment 15-1.

8   MASS.15.2.2   Historical Studies of Sorption in the Culebra

10   The DOE carried out several laboratory studies of sorption in the late 1970s and early 1980s
11   (Serne et al. 1977; Paine and Dosch 1992; Dosch and Lynch 1978; Dosch 1979, 1980, 1981;
12   Lynch and Dosch 1980; Lynch et al. 1981; Tien et al. 1983). These empirical studies used a
13   variety of sorbents and solutions—including dolomitic, anhydritic, and clay-rich rocks and
14   repository and Culebra brines—and in some cases included the effects of dissolved organics
15   on sorption. The DOE (1980) used some of these results for the 1980 WIPP Environmental
16   Impact Statement (EIS). According to Lappin et al. (1989), the sorption model used by the
17   DOE (1980) included a porous-medium approximation of the Culebra. Lappin et al. (1989)
18   and the DOE Office of Environmental Restoration and Waste Management (1990) also used
19   these results for the 1990 Supplemental EIS. For Pu, Am, U, Th, Np, and Cm, Lappin et al.
20   (1989) and the DOE Office of Environmental Restoration and Waste Management (1990)
21   included sorption by the matrix only, linear sorption isotherms, and instantaneous, reversible
22   equilibrium in their model. For Ra and Pb, however, they assumed linear, instantaneous,
23   reversible sorption by clay minerals in the matrix because there were no data available for
24   sorption of these elements by dolomite.

26   The DOE and the state of New Mexico formally recognized deficiencies in the early sorption
27   studies. In 1988, the DOE and the state of New Mexico modified the Consultation and
28   Cooperation agreement to require New Mexico concurrence on any K_ds recommended for use
29   in the final performance assessment. Papenguth and Behl (1996b) planned the current
30   program (see below) in part to satisfy that agreement.

32   Soon after the agreement was reached, the DOE started a mechanistic sorption study,
33   primarily at Stanford University (Lappin et al. 1989; Siegel et al. 1990; Park et al.
34   1992, 1995). The objective of this study is to develop a surface-complexation model for the
35   sorption of UO_2^{2+} by corrensite, the dominant clay mineral in the Culebra. It is infeasible,
36   however, to use this model in performance assessment calculations for three reasons:

38   •   laboratory data for clay-rich rock under expected Culebra conditions are insufficient at
39   this time to include K_ds for clay minerals in performance assessment calculations;

41   •   the Stanford results pertain only to sorption of U(VI) and its oxidation-state analogs
42   Pu(VI) and Np(VI), none of which will significantly affect the long-term performance
43   of the WIPP; and

- even if sorption of U(VI), Pu(VI), or Np(VI) did affect the long-term performance of the WIPP significantly, it would not be possible to incorporate a surface-complexation model in the Culebra flow and transport codes SECOFL2D and SECOTP2D.

At about the same time that the Stanford mechanistic sorption study began, the DOE convened an expert panel consisting of SNL staff to estimate ranges and probability distributions of K_ds for use in performance assessment. This panel estimated ranges and distributions of actinide K_ds for the Culebra as a whole and for the clay-rich fracture surfaces (Trauth et al. 1992). These values were used for the 1991 and 1992 calculations.

MASS.15.3 Colloidal Actinide Transport and Retardation in the Culebra

The purpose of this model is to represent the effects of colloidal actinide transport in the Culebra. This model is also discussed in Section 6.4.6.2.2 and Attachments 15-2, 15-8, and 15-9.

A particle is referred to as being in the colloidal state when the particle size lies roughly in the range between 1 and 1,000 nanometers. These particles are generally much larger than simple ions, and as a result, the transport behavior of colloids in groundwater systems can be quite different from that of dissolved species. In a groundwater system, colloids are essentially a third phase consisting of a mobile solid that can associate with or contain actinides and potentially increase transport rates slightly relative to the average groundwater velocity.

In the WIPP disposal system, for instance, colloids are often too large to pass through the small pore throats of diffusive porosity. Such colloids will be restricted to the advective portion of the flow system. Colloids may also be less reactive than dissolved actinides with the host rock. Therefore, even though a colloid is small enough to penetrate the diffusive porosity, the retardation coefficient associated with the colloid will in some cases be smaller than the retardation coefficient of the actinide associated with the colloid.

Colloid-facilitated actinide transport has not been included in past performance assessment calculations because of a lack of adequate information to model this phenomenon and demonstrate its impact on compliance (see, for example, SNL, 1992-1993, Vol. 1, 4-12, line 29). Transport of actinides by colloidal particles has been recognized only relatively recently as a phenomenon of potential importance to the performance of nuclear waste repositories (Jacquier 1991; Avogadro and de Marsily 1984). In fact, the study of colloid-facilitated contaminant transport is a relatively new topic to the geosciences in general. Nyhan et al. (1985) was one of the first investigations to demonstrate the potential importance of colloid-facilitated radionuclide transport. Since then, a number of researchers have investigated colloids as a potential transport mechanism (for example, McCarthy and Zachara 1989; Corapcioglu and Jiang 1993; Grindrod 1993; Ibaraki and Sudicky 1995). Grindrod (1993) and Ibaraki and Sudicky (1995) addressed the topic of colloid-facilitated transport through fractured porous media. Consequently, their work is most applicable to the colloid transport problem in the Culebra.

1   Among the most sophisticated and rigorous numerical models developed are those by van der
2   Lee et al. (1993, 1994) and Bennett et al. (1993). Many of the colloid transport numerical
3   models described in the literature focus on simulating solute transport through fractured media
4   with double porosity flow characteristics, and they have been generalized to include unique
5   features of colloid transport (for example, Hwang et al. 1989; Grindrod and Worth 1990;
6   Light et al. 1990; Smith and Delgueldre 1993; Harmand and Sardin 1994). Some numerical
7   models, such as the population balance model by Travis and Nuttall (1985), assume
8   equilibrium colloid concentrations. That is, the loss of colloidal particles by attachment to the
9   medium wall is compensated by the generation of new colloidal particles by various
10 mechanisms such as condensation and entrainment. The modeling approach developed by
11 Travis and Nuttall (1985) is similar to the double-porosity transport model.
12
13 MASS.15.3.1 Experimental Results
14
15 As discussed in Section 6.4.6.2.2, the four types of colloids and colloidal sized particles
16 modeled to be introduced to the Culebra are microbes, mineral fragments, humic substances,
17 and actinide intrinsic colloids. To investigate the impact of these four colloid types on
18 radionuclide transport in the Culebra, an experimental program was developed and
19 implemented at SNL with significant contributions from Lawrence Livermore National
20 Laboratory (LLNL), Battelle National Laboratory, Los Alamos National Laboratory (LANL),
21 and Florida State University. The intent of this experimental program was to develop
22 parameter ranges and distributions for the conceptual models discussed above. With the
23 exception of the Pu(IV) polymer, the experimental results indicated that colloid-facilitated
24 actinide transport is not a viable mechanism for actinide transport in the Culebra.
25 Furthermore, the potential amount of Pu(IV) polymer that could be introduced to the Culebra
26 was found to be insignificant with respect to the EPA normalized release limit. Consequently,
27 colloid-facilitated actinide transport was not simulated in the performance assessment.
28
29 The experimental results and implications on performance assessment modeling are
30 summarized as follows:
31
32 •   Mineral fragments and microbes are attenuated so effectively it was deemed
33   unnecessary to include them in the transport calculations (see Attachments 15-8 and
34   15-9).
35
36 •   The total potential amount of Pu(IV) polymer introduced to the Culebra was found to
37   be insignificant with respect to the EPA normalized release limit (Attachment 15-8).
38   Therefore, the contribution of Pu(IV) polymer to the integrated discharge was
39   disregarded in the performance assessment.
40
41 •   Under neutral to slightly basic brine conditions, the presence of humic substances in
42   the brine did not influence the sorption behavior of dissolved actinides. Results
43   indicate that at these geochemical conditions, humic substances were not effective
44   complexants in the presence of dolomite (Attachment 15-8). Therefore, actinides

1   associated with humic substances are assumed to disassociate upon entering the
2   Culebra.
3
4   MASS.15.3.2 Indigenous Colloidal Transport
5
6   In an intrusion scenario at the WIPP, as dissolved actinide elements are introduced to the
7   Culebra, it is possible that those dissolved actinides could sorb onto a separate population of
8   indigenous mineral fragments, microbes, and humic substances. The physical and chemical
9   behavior of these newly formed actinide-bearing colloidal particles will be nearly identical to
10 the behavior of colloids introduced from the repository. Microbes and mineral fragments will
11 be rapidly filtered out of the advective flow domain; hence, disregarding the interaction
12 between dissolved actinides and these types of colloids is considered to be a conservative
13 approach. Experimental results indicate that humic substances do not interact with dissolved
14 actinides under the expected Culebra geochemical conditions. Consequently, the quantity of
15 newly formed actinide-bearing humics will be insignificant.
16
17 MASS.15.3.3 Alternative Approaches Considered
18
19 As discussed above, results of experimental studies show that colloidal actinides are strongly
20 attenuated or present in negligible concentrations, making it unnecessary to include them in
21 performance assessment simulations. The following section describes the three alternative
22 transport conceptual models considered prior to the completion of these experimental results.
23
24 After the introduction of colloidal actinides and dissolved actinides into the Culebra,
25 realistically a new equilibrium condition will be established, with the stipulation that the total
26 concentration of actinide must be preserved. As in the repository, quantifying an equilibrium
27 assemblage is not practicable.
28
29 Three approaches were considered to quantify colloid-facilitated actinide transport at the
30 WIPP. First, the transport of one or more types of actinide-bearing colloidal particles in the
31 Culebra could be assumed to be instantaneous. In other words, as actinides associated with
32 that type of colloidal particle migrate to the Culebra from the repository, or are generated
33 within the Culebra, the mass of actinides associated with those colloidal particles becomes
34 part of the integrated release of actinides at the accessible environment boundary. This
35 approach can be useful if the concentrations of actinides associated with one or more types of
36 colloidal particles are very low. Treating colloid-facilitated actinide transport as
37 instantaneous, however, is a significant shortcoming, because of the potentially large expected
38 retardation effects of colloidal particles.
39
40 Second, SECOTP2D and supporting codes could be used to simulate the effects of one or
41 more of the colloid retardation phenomena (Ramsey 1996). The double porosity advection and
42 diffusion equation solved by SECOTP2D can simulate colloid sorption in the matrix and to
43 the fracture walls. The code can also model colloid filtration using the decay term of the
44 governing equation. For colloids considered too large to diffuse into the matrix, matrix

1 diffusion can be disabled by setting the matrix tortuosity to zero. This approach was used for
2 some calculations completed in 1994. Specifically, microbes, because of their relatively large
3 size, were excluded from matrix diffusion and limited to advective flow in fractures. Humic
4 substances were allowed to diffuse into intercrystalline pores, but at a reduced rate relative to
5 dissolved actinide species.
6
7 This approach requires a number of simplifying assumptions under the presumption they are
8 conservative with respect to the integrated release of radionuclides. The first assumption is
9 that the dissolved concentration will be greatest at the source point and therefore, the
10 concentration of radionuclides associated with colloids will be greatest at the source as well.
11 Second, a radionuclide associated with a colloid is assumed to remain fixed to that colloid
12 throughout the simulation. Given these assumptions, the colloidal actinide concentration is no
13 longer a function of the dissolved actinide concentration, and it is not necessary to solve the
14 dissolved species transport problem and the colloid transport problem simultaneously. As a
15 result, the standard advection diffusion transport equation can be used to predict colloid
16 transport and compute integrated colloid releases. Given the initial concentration of
17 radionuclides sorbed to each specific type of colloid, the integrated colloid release can be
18 converted to an integrated radionuclide release by postprocessing the colloid transport results.
19 Radionuclide decay can also be accounted for in postprocessing.
20
21 The third assumption is that colloid-facilitated actinide transport could be quantified by a
22 rigorous numerical modeling code developed for the WIPP. Such a rigorous transport model
23 would address all physical and chemical processes that could affect the movement and fate of
24 the four colloidal particle types, including colloid generation; interactions with solutes, the
25 dispersant, and rock; advection; dispersion; diffusion; filtration; gravitational settling;
26 attachment and detachment; adsorption and desorption; coagulation; flocculation; and
27 peptization. Ideally, permeability reduction caused by pore clogging by colloids, which would
28 affect solute transport as well, would also be considered. Currently available models do not
29 include all of these processes (see Attachments 15-2, 15-8, and 15-9).
30
31 The most practical approach to evaluating the transport of colloidal actinides is the second
32 option presented above, using the SECOTP2D code. Where possible, the DOE considered
33 reducing the number of phenomena treated in the transport code and address them in the
34 source term. For example, the effect of ionic strength on colloid stability would have been
35 included in the colloid source term. Retardation of colloidal particles was to be quantified
36 using a retardation factor, and filtration was to be quantified through the decay term.
37
38 *MASS.15.4 Subsidence Caused by Potash Mining in the Culebra*
39
40 This model incorporates the effects of potash mining in the McNutt on disposal system
41 performance (see Appendix SCR, Sections SCR.3.2.2 and SCR.3.3.2). 40 CFR Part 194
42 provides a conceptual model and parts of a mathematical model for these effects. The DOE
43 has implemented the EPA conceptual model to be consistent with EPA criteria and guidance.
44 It is described in Section 6.4.6.2.3 of this application. Additional information on the

implementation of the mining subsidence model is available in Attachments 15-4 and 15-5, and Bertram (1995).

The principal parameter in this model is the range assigned to a factor by which hydraulic conductivity in the Culebra is increased (Attachment 15-4). As allowed in supplementary information to 40 CFR Part 194, it is the only parameter changed to account for the effects of mining.

Mining in the McNutt has been considered in the performance of the WIPP since the original siting activities. Siting criteria for both the site abandoned in 1975 and the current site included setbacks from active mines. (See, for example, Section MASS.2.) The 1980 FEIS for the WIPP (DOE 1980) considered the possibility of an indirect dose arising from the effects of solution mining for potash or halite; it concluded that direct access of waste by solution mining for potash was not likely because of the methods that would be used to control the flow of solvent through the formation. The DOE is not aware of solution mining for potash or other minerals in the Salado within the Delaware Basin at this time.

Mining has been included in scenario development for the WIPP since the earliest work on this topic (for example, Hunter 1989; Marietta et al. 1989; Guzowski 1990; Tierney 1991; and WIPP Performance Assessment Division 1991). These early scenario developments considered both solution and room-and-pillar mining. The focus was generally on effects of mining outside the disposal system. The two primary effects of mining considered were changes in the hydraulic conductivity of the Culebra or other units and changes in recharge as a result of surface subsidence. These mining effects were not formally incorporated into quantitative assessment of repository performance in preliminary performance assessments.

The inclusion of mining in performance assessment satisfies the criteria of 40 CFR Part 194 to consider the effects of this activity on the disposal system.

MASS. 16 Intrusion Borehole

The inclusion of intrusion boreholes in performance assessment adds to the number of release pathways for radionuclides from the disposal system. Direct releases to the surface may occur during drilling as particulate material from cuttings, cavings, and spall are carried to the surface. Also, dissolved actinides may be carried to the surface in brine during drilling. Once abandoned, the borehole presents a possible long-term pathway for fluid flow, such as might occur between a hypothetical Castile brine reservoir, the repository, and overlying units. This topic is also addressed in Chapter 6.0 (Section 6.4.7) and Appendix SCR (Sections SCR.3.2.1 and SCR.3.3.1).

MASS.16.1 Cuttings, Cavings, and Spall Releases during Drilling

The purpose of these models is to estimate the quantity of actinides released directly to the surface during drilling through the repository by three mechanisms: the drillbit boring

1   through the waste (cuttings), the drilling fluid eroding the walls of the borehole (cavings), and
2   gas movement forcing particulate matter into the circulating drilling fluid (spallings). See
3   Section 6.4.7.1 and references to other appendices cited in that section for additional
4   information. Stochastic uncertainty with respect to parameters relevant to these release
5   mechanisms is addressed in Section 6.4.12.
6
7   The conceptual model for cuttings, cavings, and spallings is discussed in three parts because
8   of the differing process by which the three types of material are produced.
9
10 Cuttings are materials removed to the surface through drilling mud by the direct mechanical
11 action of the drill bit. The volume of waste removed to the surface is a function of the
12 compacted repository height, the porosity of waste at the time of intrusion, and the drill bit
13 area. The radioactivity of waste removed to the surface is probabilistically determined based
14 on the distribution of waste radioactivity expected in the WIPP.
15
16 Cavings are materials introduced into the drilling mud by the erosive action of circulating
17 drilling fluid on the waste in the walls of the borehole annulus. Erosion is driven solely by the
18 shearing action of the drilling fluid (or mud) as it moves up the borehole annulus. Shearing
19 may be caused by either laminar or turbulent flow. Repository pressure effects on cavings,
20 which are negligible, are covered by the spall process.
21
22 Spallings are the particulate material introduced into drilling mud by the movement of gas
23 from the waste into the borehole annulus. After the drill bit enters the repository, pressure
24 gradients generated by the flow of gas toward the borehole fracture the waste material,
25 permitting the escaping gas to flow within fractures rather than through a porous matrix.
26 Consequently, the intrinsic permeability of the matrix does not restrict gas flow, and the gas
27 pressure at the borehole entrance to the repository can be assumed to be the initial gas
28 pressure in the repository. The gas flow velocity up the borehole is governed by the
29 isothermal flow of gas in a long tube of a given cross-sectional area, tube roughness, and gas
30 pressure at the borehole entrance. The mass-flow rate of gas in the fractured waste at any
31 radial cross-section is equal to the mass-flow rate up the borehole. Radial gas flow within the
32 fractures in the waste matrix erode and widen the fractures. Erosion is assumed to occur if the
33 fracture gas velocity exceeds a threshold velocity related to the terminal velocity of a waste
34 particle at the fracture surface and to the cohesive strength afforded by moisture in the matrix.
35
36 The cuttings model has as a principal parameter the diameter of the drill bit, which according
37 to current practice is constant. This model interacts with the conditions in the repository as
38 calculated by BRAGFLO because the porosity and height of the repository are necessary to
39 calculate the volume of waste removed.
40
41 The principal parameters in the cavings model are the properties of the drilling mud, drilling
42 rates, and the shear resistance of the waste. See Appendix PAR (Parameter 33) for details on
43 the sampled parameter used in the cavings model, effective shear resistance to erosion.
44

1   The principal parameters in the spallings model are the gas pressure in the repository when it
2   is penetrated and properties of the waste such as particle diameters and erosive properties.
3   Appendix PAR (Parameter 32) provides information on the waste particle diameter, which is a
4   sampled parameter in the spallings model. Because the release associated with spalling is
5   sensitive to gas pressure in the repository, it is strongly coupled to the BRAGFLO-calculated
6   conditions in the repository at the time of penetration. In particular, the spall release may be
7   sensitive to whether the repository has been penetrated previously by another borehole.
8
9   Several factors contribute to model uncertainty, principally the undefined nature and
10   complexity of the waste, both in its initial state and during its alteration by chemical and
11   biological processes. Even the most basic information is lacking, such as chemical form,
12   grain size (if the material is granular), partially biodegraded decomposed form, density,
13   cohesion, etc. In the absence of such information, property values typical of surrogate
14   materials are selected to represent the worst case response to the process being investigated
15   (see Appendix PAR, Table PAR-11; Chapter 9.0, Section 9.3.4.4; and Appendix WCA,
16   Section WCA.5.2). In this sense, the model is highly conservative.
17
18   Another uncertainty arises from the drilling scenario assumptions for application of the model.
19   There is no consensus about how the driller will act as the drill approaches the waste horizon,
20   that is, whether he will be able anticipate the presence of the gas-filled repository, much less
21   control the drilling process once penetration occurs. In consequence, the conceptual model
22   assumes the worst possible limiting situation, in which the borehole is driven almost
23   instantaneously through the waste by a driller without any knowledge of the existence of the
24   repository, and the driller is unable to control the subsequent gas release.
25
26   The scale-up from a model qualified on laboratory samples to the full-scale configuration of a
27   drill penetrating the waste gives rise to another uncertainty, the possibility of improper
28   scaling. However, the adverse effect of improper scaling on the amount of waste released is
29   considered to be negligible because of the conservatism of the material and drilling scenario
30   assumptions.
31
32   MASS.16.1.1 Historical Context of Cuttings, Cavings, and Spallings Models
33
34   Releases of cuttings and cavings are straightforward and have been considered in performance
35   analyses since the beginning of direct release evaluation. The analytical equations governing
36   erosion (cavings) based on laminar and turbulent flow (Berglund 1992, Section 2.2) have been
37   implemented in the code CUTTINGS_S. Using appropriately selected input based on
38   assumed physical properties of the waste and other drilling parameters, this code calculates
39   the final caved diameter of the borehole that passes through the waste. Although certain
40   features of the analysis, such as whether the flow of the drilling fluid should be modeled as
41   laminar or turbulent and what drilling parameters might be valid near the WIPP repository,
42   have been debated, the basic model has been generally accepted. The amount of material
43   predicted to be released by cavings is small, and therefore this contribution to surface release
44   has never been considered to be critical.
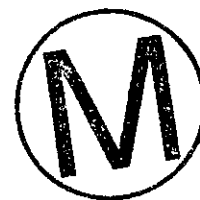
1   The conceptual model of the release of waste by spalling has been changed several times
2   during its development. Early spall conceptual model development focused on transient
3   unrestrained outgasing leading to the spall (dynamic fracture) of porous cohesive granular
4   media (Berglund 1992, Section 3.3). An experimental program related to model development
5   focused on almost instantaneous depressurization and was limited to a one-dimensional linear
6   sample configuration. The pore pressures required to cause spall or dynamic fracture could be
7   closely approximated using the tensile strength of the porous soil medium (Berglund and
8   Lenke 1995), but the model was complex and could not be directly related to an intrusion
9   event. In addition, although the experimental observations showed fracturing under
10   instantaneous release of gas pressure, sample-preparation factors were largely responsible for
11   the locations of the fractures. The fracture patterns also depended on the one-dimensional
12   nature of the experiments, and the model did not explain how the fractured material was
13   removed.
14
15   Subsequently, the dynamic fracture spall model was replaced with a more general three-part
16   model based on the premise that the waste could be removed by any one of three mechanisms:
17   blowout, stuck pipe, and gas-flow assisted erosion (as the result of gas-induced spall). Which
18   mechanism will dominate depends on the permeability and pressure drop at the borehole.
19   Well blowout, an uncontrolled gas release from the well, was considered the dominant
20   mechanism. The two remaining mechanisms, stuck pipe and gas-flow assisted erosion, were
21   not thought to be important because they would occur at waste permeabilities of less than 10^{-16}
22   square meters, much lower than is expected for the waste (1.7×10^{-13} square meters).
23   Consequently, conceptual-model development has focused on the blowout mechanism for
24   removing waste.
25
26   Once the DOE concluded that blowout was the principal cause of direct release of waste by
27   spalling, the nature of the gas flow and the entrainment properties of the waste became the
28   focus of subsequent model development. The first model, used in analyses in 1994, was
29   simplistic. Release was defined in this model by how much gas flowed out into the borehole
30   and an assumed amount of solids entrained in it over a prescribed time period. The time limit
31   for release assumed in the calculations was 5 minutes, the time estimated for the driller to
32   close the blowout preventers and start weighting up the drilling mud. Entrainment was a
33   sampled percentage ranging from 0 to 10 percent. Defending the time limit for release was
34   particularly difficult because opinions about how long it would take before the driller
35   controlled the well varied widely. In addition, the model was not self-limiting, in the sense
36   that release would continue for as long as the unchecked gas flow was assumed to continue,
37   and quantification of the entrainment percentage was of concern.
38
39   To respond to these concerns, model development for release continued. A more-detailed
40   model was developed based on the observation that a critical entrainment or lofting (terminal)
41   velocity represents a threshold erosion condition. This value of the gas velocity defines
42   whether solid particulate matter is separated from the bulk waste. Once separated, the
43   material is assumed to be entrained in the gas and carried up the borehole to the ground
44   surface (Berglund and Lenke 1995, Section 6.1, 33 – 39). Because gas velocities below this

1   threshold can remove no solids, the removal process is self-limiting: gas velocity decreases as
2   a function of distance from the borehole, eventually dropping below the entrainment velocity
3   threshold and terminating the process.
4
5   The first version of the steady-state model incorporating the terminal velocity release process
6   assumed that gas would flow uniformly through the waste and out the borehole. It was based
7   on the fact that the velocity of the gas decreases with distance from the borehole, because of
8   the symmetry of the gas flow field. The flow velocity is greatest at the borehole boundary and
9   decreases with distance away from it. Therefore, at some point sufficiently remote from the
10   borehole, the gas velocity just equals the critical entrainment (terminal) velocity. All material
11   closer to the borehole was assumed to be eroded and lofted up the borehole, but the gas
12   velocity in all material farther from the borehole was too low to cause erosion. This
13   hypothesis permitted a calculation of how much material would be released in connection
14   with an assumed gas-pressure drop in the waste disposal region.
15
16   An experimental program was designed to confirm the model using a test apparatus to
17   simulate gas flow through the waste and up the borehole (Lenke and Berglund 1995). The
18   model-confirmation process was to first experimentally determine the entrainment velocity
19   characteristics of the material, and then apply these data to the model to predict the amount of
20   release expected for various boundary pressures. Boundary pressures were then
21   experimentally applied to the samples in the experimental blowout device, and the amounts of
22   eroded material were determined assuming uniform Darcy flow. The confirmation criterion
23   was that if the measured amount of lofted material was less than the predicted amount of
24   erosion then the model was considered confirmed. Confirmation was never possible,
25   however, because the material release tests revealed that the assumption of uniform gas flow
26   through the waste was not reflected by the response of the material. Instead of formation and
27   expansion of a cavity left behind by eroded material, post-test observations showed that the
28   gas instead created flow channels that increased in thickness as erosion proceeded. Releases
29   were greater than expected because gas velocity in the channels was greater than it would
30   have been had gas flowed through the bulk of the material (Lenke and Berglund 1995, 14).
31   Channel flow was consistent with the heterogeneity of the waste.
32
33   The experimental observation of flow-channels formation by erosion forced another iteration
34   in blowout-model development to make the model consistent with material response. The
35   new model is used in performance assessment and is documented in Appendix CUTTINGS
36   (Section 4).
37
38   Including a channel-flow mechanism in the model requires either precise definition of the
39   number, geometric configuration, and location of all the channels before they form, which is
40   not technically feasible, or scaling the model results in some manner to reflect the channeling
41   process. The scaling method was adopted, adjusting the predicted releases to agree with
42   experimental release observations. Although the uniform-flow model was independent of
43   experiments, in the sense that release predictions did not require direct data from the tests, a
44   coupling between experimental results and the model was necessary for scaling. This was

1   accomplished by introducing certain experimentally determined scaling constants into the
2   model (see Appendix CUTTINGS). The model is applied to different gases and solid
3   materials by prescribing well-defined material properties, such as particle size and density,
4   viscosity, and cementation tensile strength. The scaling factors are the only parameters of the
5   model not directly related to geometry or material properties, but they are necessary to
6   represent the way channels for gas flow are likely to develop.
7
8   *MASS.16.2 Direct Brine Releases during Drilling*
9
10   This model provides a series of calculations to estimate the quantity of brine released directly
11   to the surface during drilling. Direct brine releases may occur when a driller penetrates the
12   WIPP and unknowingly brings contaminated brine to the surface during drilling. (These
13   releases are not accounted for in the cuttings, cavings and spallings calculations, which model
14   only the solids removed during drilling.) Attachment 16-2 describes the direct brine release
15   model used for this performance assessment. The conceptual model is also discussed in
16   Section 6.4.7.1.1.
17
18   Uncertainty in the BRAGFLO direct-brine-release calculations is captured in the 10,000-year
19   BRAGFLO calculations from which the initial and boundary conditions are derived. The
20   model parameters that have the most influence on the direct brine releases are repository
21   pressure and brine saturation at time of intrusion. Brine saturation is influenced by many
22   factors, including Salado and marker bed permeability and gas-generation rates (for
23   undisturbed calculations). For E1 and E2 intrusions, Castile brine-reservoir pressure and
24   volume and abandoned borehole permeabilities influence conditions for the second and
25   subsequent intrusions. Dip in the repository (hence the location of intrusions), two-phase flow
26   parameters (residual brine and gas saturation), time of intrusion, and duration of flow have
27   lesser impacts on brine releases.
28
29   MASS.16.2.1 Historical Context of the Direct Brine Release Model
30
31   The direct brine release model is a relatively new development in WIPP performance
32   assessments, and this performance assessment is the first one to incorporate this mechanism of
33   release. Prior to using the current model in this performance assessment, several iterations of
34   models were performed. At first, a simplistic cylindrical (radial) BRAGFLO model was used
35   to represent the excavated volume of one intruded panel, but this was inadequate to capture
36   the effects of heterogeneities within the site. This model was replaced with the current
37   repository-scale mesh representing the configuration of the WIPP excavation, accounting for
38   drifts, passageways, closures, pillars and rooms, and formation dip in the waste region. The
39   current mesh reflects the configuration used by the DOE in this application, with flow
40   unaffected by backfill within the panels. In addition, the vertical wellbore flow model is
41   coupled to the BRAGFLO mesh, and the effects of solids removal caused by cavings and spall
42   are examined (CUTTINGS_S code). Boundary conditions can account for two intrusions in a
43   single panel, one of which connects to a brine reservoir.
44

1   The assumptions used in the models are based on current drilling practices in the Delaware
2   Basin (see Appendix DEL). The wellbore model description assumes a typical WIPP-area oil
3   or gas well completion, including bit size, casing size and depths, drilling mud, etc. The
4   duration of flow is based on how a present-day driller might react to the pressures and flows
5   predicted by the model when encountering high pressure (see Appendix DEL). The
6   assumptions in the BRAGFLO direct-brine-release model (that is, about permeability, two-
7   phase flow properties, crushed panel height, porosity) match those used in the 10,000-year
8   BRAGFLO and CUTTINGS_S models.
9
10   The WIPP two-phase flow code BRAGFLO is used to simulate the direct brine releases
11   during a drilling intrusion. This code is also used to calculate the 10,000-year flow of brine
12   and gas through the WIPP and surrounding rock. However, a different conceptual model has
13   been constructed to represent the excavated rooms, drift passageways, and the salt pillars
14   between them. This refined mesh, or repository scale model, more accurately captures the
15   flow patterns associated with the short-duration direct releases. The suite of software used to
16   calculate direct brine releases is discussed in Appendix CODELINK. The output from the
17   repository-scale direct release model is the volume of brine (cubic meters) released to the
18   surface. The activity of radioisotopes in the brine released is determined using the actinide
19   source term model.
20

MASS.16.3 Long-Term Properties of the Abandoned Intrusion Borehole

23   The purpose of the model for the long-term properties of the intrusion borehole is to provide
24   in BRAGFLO the physical properties relevant to fluid flow through a plugged and abandoned
25   borehole that intersects the repository. The model includes several possible plugging and
26   configuration patterns based on current practice in the Delaware Basin (Attachment 16-1).
27   Because plugging practice is closely controlled by state regulations, only the New Mexico
28   portion of the Delaware Basin is considered. Section 6.4.7.2 of this application describes the
29   properties assigned to the boreholes and the types of plug configurations considered in
30   performance assessment.
31
32   The conceptual model for long-term flow up a plugged and abandoned borehole addresses the
33   principal parameters in the intrusion borehole model for long-term flow: permeability,
34   porosity, compressibility, and two-phase properties. Because these properties may change
35   with time as the borehole plugs degrade, some types of boreholes have several defined stages
36   for the evolution of borehole properties. No retardation of actinides or other transport-
37   limiting effects in the borehole are assumed.
38
39   Permeability, the most important borehole property, changes according to the stage of
40   borehole degradation. The values assigned to other parameters are held constant for all stages
41   and are set consistent with a borehole fill referred to as silty sand, consisting of the material
42   that would naturally slough off the walls of the borehole or the remains of degraded plugs.
43   The porosity of the plugged and abandoned borehole is set at a low value within the porosities
44   expected of materials that will be in the borehole; the low value was chosen because smaller

1   void volume in the borehole reduces storage in the borehole and slightly increases the total
2   flux of fluids that may pass through it.
3
4   Predictions of the time-dependent permeability of plugged boreholes are based on three
5   configurations for borehole plugs and two concepts of how the plug materials will be altered
6   by fluids. The concepts include steel corrosion and concrete degradation. From the outside
7   inward, the conceptual model for borehole plugs envisions concentric circles of ordinary
8   portland cement as grout attaching the casing to the rock, low carbon steel (the casing), and a
9   central disc of ordinary portland cement (the concrete plug). The bulk of the data used to
10 predict the service lives of borehole plugs comes from the open literature on corrosion of low
11 carbon steel and ordinary portland cement and from tabulated thermodynamic data bases.
12
13 Predictions of plug performance derived from the conceptual models are sensitive to both
14 chemical and physical parameters. Key areas of uncertainty include the following:
15
16   • opened or closed nature of the physical and chemical systems,
17
18   • degree to which performance data from generic materials apply to WIPP-specific
19   materials and conditions,
20
21   • conditions at the precise locations where WIPP plugs are emplaced, and
22
23   • physical dimensions of the plugs.
24
25 The conceptual models for predicting the time-dependent permeability of plugged boreholes
26 recognize two types of systems: open and closed. Open systems are ones in which chemical
27 components can be added or subtracted freely, whereas closed systems are ones in which the
28 identity and amount of chemical components available for reaction are constant. In physical
29 models, a closed system maintains a constant volume, while in open systems volume is
30 unconstrained. The principal area of uncertainty in the conceptual models is the definition of
31 the boundary between open and closed space. This boundary is significant because real
32 systems are somewhere between totally open or closed, and open and closed systems result in
33 very different expected performance lives for plugged boreholes.
34
35 In chemical systems, a very small addition or release of reacting components is insignificant,
36 but a substantial change can have large effects: in open systems reactions proceed until the
37 supply of reactants is exhausted. In open systems, equilibrium considerations may have little
38 or no significance; hence treatment by equilibrium thermodynamics may be unenlightening.
39 Similarly, in physical systems, a small amount of system expansion will have little effect on
40 internal stresses, but unlimited expansion may cause the system to fail in tension.
41

1   MASS.16.3.1 <u>Corrosion</u>

2

3   There are many low-carbon-steel alloys, and not all corrode at the same rate in a given

4   environment. However, because of the aggressive corrosion rate selected for the model, steel

5   composition is not thought to introduce significant uncertainty about the rate. Corrosion of the

6   casing steel has been modeled thermodynamically for plugged boreholes. Hydrogen is a

7   common byproduct of corrosion. An equilibrium hydrogen pressure has been calculated for a

8   number of potential reactions, using metallic iron to represent steel and pure water to

9   represent brines. Attainment of equilibrium hydrogen pressure is taken to indicate cessation

10   of corrosion. To reach equilibrium, the system must contain the hydrogen that is generated.

11   The hydrostatic pressure of the brine column has been assumed to confine hydrogen when the

12   pressure exceeds the equilibrium hydrogen pressure calculated for the corrosion reaction of

13   interest.

14

15   Reactions most representative of corrosion of steel casing produce iron hydroxide corrosion

16   products. Equilibrium hydrogen pressures for these reactions are exceeded by hydrostatic

17   pressures at depths greater than about 1,100 feet (335 meters). Corrosion of casing above this

18   depth is treated as open; the casing corrodes until the supply of metallic iron is exhausted and

19   the casing disintegrates. Without axial support supplied by the casing, the concrete plug also

20   fails. In contrast, corrosion is assumed to take place in a closed system at depths greater than

21   1,100 feet (335 meters). Hydrogen is not free to nucleate as a gas and leave the system.

22   Although local perforations in the casing are expected, the casing does not disintegrate. It

23   supports the concrete plugs, and permeability changes in the plugs are attributed to alteration

24   of cement phases by the brine that flows through them.

25

26   The greatest uncertainty associated with composition is likely to arise from the

27   thermodynamic calculations used in the model. Pure phases (Fe for steel and H_2O for brine)

28   have been assumed so that hand calculations may be more readily performed. Various

29   reactions and environments have been modeled without directly considering complexities in

30   the chemical system (other than volatiles). Qualitatively, the added complexities are likely to

31   have no substantial consequence on the ability of the brines to dissolve a pathway through the

32   casing. However, system complexities might decrease the equilibrium hydrogen pressures

33   calculated for the corrosion reactions or lead to unexpected reaction products.

34

35   Data supporting low-carbon-steel corrosion models come primarily from the literature. The

36   empirical data support the assumption that general corrosion is the dominant mechanism for

37   corrosion under oxic conditions and that pitting will occur under low oxygen (and high pH) or

38   elevated carbon dioxide and hydrogen disulfide conditions. Corrosion rates are a function of

39   the conditions under which corrosion occurs. Published data include rates as rapid as

40   3 millimeters per year, which is the value assumed in the model. Such rapid rates are not

41   inconsistent with reports in the Delaware Basin of casing failures occurring from corrosion

42   within months to years (Attachment 16-3, B-17). Data from corrosion of steel enshrouded in

43   concrete come from the literature on marine construction and the data base on reinforcing

44   steels. These data support the assumption that steel encased in concrete cannot be assumed to
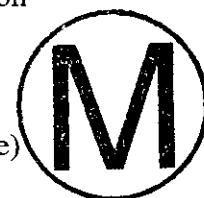
1   corrode more slowly than exposed steel. This subject area is discussed in detail in Attachment
2   16-3 (Section 3.2 and Appendix B).
3
4   MASS.16.3.2 Portland Cement Concrete
5
6   The cementitious materials used in hydrocarbon exploration are variable. The degree to
7   which oil-field materials might perform differently from the cement mixtures investigated and
8   reported in the literature is unknown. There is no standard mix formulation that specifies
9   plugging cements precisely; the use of generic data is reasonable, because the vagaries of
10   cement composition are implicitly included. The published empirical studies of concrete
11   degradation include a large body of data for reacting solutions ranging from pure water to
12   marine brines. Waters with higher chloride and magnesium contents cause greater reaction.
13   This level of detail has not been factored into the model directly; rather, alteration by brines
14   has been the favored source when extracting information on degradation.
15
16   Chemical alteration of cement phases by brine produces new solids with greater molar
17   volumes than the unaltered, hardened cement phase. In a closed physical system, the
18   alteration will lead to decreased internal porosity and consequent decrease in permeability. In
19   an open physical system, alteration will lead to increased internal pore pressures that will
20   eventually exceed the tensile strength of the concrete plug. The result is often seen on
21   concrete sidewalks or other unreinforced concrete structures: without something to restrain
22   expansion, the concrete cracks, increasing its porosity and permeability.
23
24   Current plugging practices create configurations that favor each model. Plugs installed to
25   respond to the New Mexico Oil Conservation Division regulation R-111-P approach
26   2,000 feet (610 meters) in length (State of New Mexico 1988). These plugs are judged to be
27   long enough that they are self-confining. As a result, alteration of R-111-P plugs produces a
28   situation in which performance is indistinguishable from the undisturbed rock. In contrast,
29   plugs emplaced in response to regulations of the U.S. Bureau of Land Management have a
30   mean length near 40 meters. This length is judged to be too short to provide self-confinement;
31   alteration of the concrete results in fracturing and increased porosity and permeability in the
32   plug. The plug length that changes the physical system from open to closed is undetermined.
33   For both chemical and physical model elements, a closed system enhances performance.
34
35   Simulation of concrete plug degradation follows a model proposed by Berner (1990), in which
36   the matrix degrades after dissolution and removal of soluble materials such as alkali salts.
37   The model is grounded in empirical observations that concrete alteration sequentially removes
38   excess alkalis, portlandite, and tobermorite or calcium-silicate-hydrate (CSH). Decreased
39   strength attends removal of portlandite.
40
41   A critical amount of flow must occur before this degradation threshold is crossed. A volume
42   equivalent to 100 pore volumes has been taken as the critical flow volume, based on values
43   for common compositions of ordinary portland cement concrete (Berner 1990). Also
44   following Berner, the model tracks the amount of flow as pore volumes, reasoning that flow

1   occurs only through pores and that alteration is therefore limited to the solids that surround the
2   pores. The model does not explicitly account for the strength of the concrete but instead
3   makes the conservative assumption that physical failure occurs suddenly at the onset of
4   chemical attack on CSH, that is, at approximately 100 pore volumes. As a result, initial
5   porosity of the hardened concrete is a key parameter for timing plug degradation.

6

7   The initial permeability of hardened cement is directly related to the connected porosity that
8   permits flow to occur. Initial permeability of ordinary portland cement is a strong function of
9   the water:cement ratio of the mix. Higher water contents produce higher porosity and
10   permeability. To simplify the analysis, initial plug permeability has been taken as a constant
11   at 5×10^{-17} square meters. This value lies in the upper range of permeabilities reported for
12   ordinary portland cement and is verified by field measurements made during a single field test
13   of borehole plugging conducted for the DOE (Attachment 16-3, C-4).

14

15   The initial permeability of the concrete plug is an important parameter because water must
16   penetrate and flow through the structure before it can alter the hardened plug. The lower the
17   permeability, the longer it takes for 100 pore volumes to pass through the plug. Somewhat
18   paradoxically, the lower the porosity, the smaller the volume of water needed before attack of
19   the CSH begins, because the model decouples the relationship between porosity and
20   permeability by holding permeability constant. In the real world, cement formulations with
21   low water:cement ratios generally produce fewer alkalis and have both lower porosities and
22   lower permeabilities. Less water must pass through the concrete body before onset of CSH
23   degradation, but the lower permeabilities lead to a longer life. The simplified model is
24   conservative: it holds the permeability constant at the upper end of the established range
25   while allowing porosity to vary over the full range commonly encountered in ordinary
26   portland cement. This accommodation reflects better knowledge of permeabilities than
27   porosities in as-emplaced borehole plugs. The range in porosity modeled (5 to 40 percent) can
28   create an order-of-magnitude spread in predicted performance life.

29

30   Data supporting the concrete degradation model come primarily from two sources: the
31   international repository literature and journals on concrete construction (for example, dams or
32   bridges). The international literature on repositories contains both models and empirical
33   studies confirming that alteration of concrete will result in decreased porosities and
34   permeabilities in closed systems. Experience for dams confirms this conclusion and confirms
35   the diffusion-driven concrete alteration rates used in the model. The general concrete
36   literature confirms the values of initial permeability and porosity of hardened concrete used in
37   the model.

38

39   Observations made on cores recovered from potash mines near the WIPP confirm that
40   alteration of concrete plugs is not extensive after decades of service. Qualitative data have
41   been produced by recovery, microscopic inspection, and leach testing of concrete cores
42   recovered from nearby potash mines. These data establish that plugs placed in boreholes will
43   have low initial permeabilities and that plugs placed in the Salado will form tight interfaces at
44   the borehole-rock interface and will not degrade substantially by contact with formation brines

1   in the amounts and compositions that might reasonably be expected. Attachment 16-3
2   (Section 3.3 and Appendices C and D) discusses concrete alteration of plugs and creep closure
3   of boreholes in more detail.
4
5   MASS.16.3.3 Borehole Configurations
6
7   The conceptual models for borehole plugs examine three basic possibilities: a continuous
8   plug through the evaporite sequence, a plug below the brine reservoir horizon coupled with a
9   plug between the repository and the Rustler, and three or more plugs with at least one
10 intermediate plug between the brine reservoir and the repository and another between the
11 repository and the Rustler. These possibilities represent simplifications of the plugging
12 schemes documented in the 1996 survey (see Chapter 6.0, Sections 6.4.7.2.1 through
13 6.4.7.2.3, and Attachments 16-1 and 16-3, Section 2.1).
14
15 As stated, the basis for these assumptions is a detailed survey of plugging practices in the
16 Delaware Basin. The survey examined the lengths, locations, and intervals plugged, as well
17 as the materials used for construction. The locations of plugs are determined partly by
18 stratigraphic changes and partly by operational considerations during exploration and
19 recovery. Variations in plug length and location affect pressure regimes and flow rates
20 through plugs. The 120-foot (40-meter) length of the plugs is the approximate mean value of
21 approximately 188 plugs in the survey. Minimum lengths prescribed by regulations are
22 50 feet (15 meters) above plus 50 feet (15 meters) below casing transitions or recovery points.
23 Additional plug lengths sometimes occur for unspecified reasons. When all else is equal,
24 performance life is proportional to plug length. For conservatism, the model does not
25 consider the longer plugs. In the conceptual model, all plugs are taken to be 120 feet (40
26 meters) long. See Attachment 16-3 (Section 5.0) for a more detailed discussion of plug
27 performance.
28
29 The borehole permeability model was assembled beginning in February 1996. Initially, the
30 model considered only the plug configuration stipulated by Oil Conservation Division
31 regulations, but it was subsequently expanded to consider all regulations and practices
32 documented in the New Mexico portion of the Delaware Basin, without specific consideration
33 of their applicability to the WIPP in the future. The model was developed to be
34 straightforward and easy to understand. Use of hand calculations was favored over the use of
35 complex computer codes. As a result, no detailed evaluation of potentially applicable codes
36 was undertaken, and no screening of codes was performed.
37
38 The text of the attached report (Attachment 16-3) describing the model and its predictions
39 contains about 40 references with data that support the model. In general, these references
40 support the plug configurations, steel corrosion mechanisms and rates, and concrete alteration
41 processes that underpin the model.
42

1 **MASS.17 Climate Change**
2
3 The purpose of this model is to allow quantitative consideration of the extent to which
4 uncertainty about future climate may contribute to uncertainty in estimates of cumulative
5 radionuclide releases from the disposal system. Consideration is limited to conditions that
6 could result from reasonably possible natural climatic changes. The model is not intended to
7 provide a quantitative prediction of future climate, nor is it intended to address uncertainty in
8 system properties other than estimated cumulative radionuclide releases that may be affected
9 by climate change. This model is also discussed in Chapter 6.0 (Section 6.4.9).
10
11 As discussed in Appendix CLI, paleoclimatic data from the literature form the basis for
12 reconstructing the climatic variability in southeastern New Mexico since late Pleistocene time,
13 spanning the transition from full glacial conditions in North America (ice sheets as far south
14 as the Northern Great Plains) to the present interglacial period. The wettest and coolest
15 climate at the WIPP corresponded to periods of continental glaciation. During Holocene time
16 (the past 10,000 years), the climate has been predominantly dry, like that of the present, with
17 several wetter episodes.
18
19 Future climate at the WIPP may differ in the next 10,000 years from that of the present, but it
20 should be bounded by the extremes of the late Pleistocene glaciation. For the purposes of
21 performance assessment, the DOE assumes that uncertainty about future climate is adequately
22 captured by considering two possible patterns: one in which the Holocene pattern of
23 predominantly dry conditions alternating with wetter conditions continues; and one in which
24 the climate becomes continuously wetter.
25
26 Effects of climatic change on the WIPP are limited in the performance assessment model to
27 effects on groundwater flow in the Culebra. Flow (that is, specific discharge in the
28 SECOFL2D model) is increased from its present calibrated value by a sampled factor that
29 ranges from 1.0 to 2.25 to simulate effects of wetter climates. Possible decreases in flow
30 during drier climates are not considered. Justification for limiting the effects of climate
31 change to flow in the Culebra is based on regional three-dimensional modeling that estimates
32 the extent to which changes in recharge will alter the altitude of the water table and in turn
33 affect flow in the Culebra and other units. Maximum recharge rates considered in the analysis
34 result in a simulated water-table altitude at or near the ground surface throughout the region.
35 Other effects of climatic change, including changes in temperature, wind, evapotranspiration,
36 and vegetation, are not modeled explicitly but are qualitatively included in this analysis
37 through the consideration of the effects of varying recharge.
38
39 The climate change model is implemented through the use of a single parameter, the Climate
40 Index. This parameter is a dimensionless factor by which the specific discharge in each grid
41 block of the SECOFL2D domain is multiplied. It is a sampled parameter in the performance
42 assessment, with a bimodal distribution ranging from 1.00 to 1.25 and from 1.50 to 2.25. See
43 Corbet (1995) and Attachment 17-1 for a discussion of this distribution.
44

1   The climate change model used for performance assessment is predicated on the assumption
2   that climate will change during the next 10,000 years. The extent of this change is uncertain,
3   but it should be bounded by the changes that occurred in the past during the peaks of
4   Pleistocene glaciation. Other conceptual models for climate change are not consistent with
5   present scientific understanding of the Earth's climate or with the EPA's guidance to consider
6   natural processes of climatic change (EPA 1996, 5227-5228). For example, climate could be
7   assumed to remain constant for 10,000 years, but this would be inconsistent with scientific
8   understanding of climate. Alternatively, climate could be assumed to change to conditions
9   unlike any known from the Pleistocene; however, no natural processes are known that could
10 result in such change within 10,000 years.

11
12 As discussed in Corbet (1995) and Attachment 17-1, the implementation of climate change in
13 the performance assessment incorporates uncertainty about future climates within the range
14 known from the Pleistocene. Alternative approaches to treating climate change in the
15 performance assessment (that is, varying boundary conditions rather than specific discharge)
16 are discussed in the following section. Past analyses performed using a different approach as
17 part of the 1991 and 1992 preliminary performance assessments suggest that disposal system
18 performance is not sensitive to climate change (Swift et al. 1994, 12).

19
20 *MASS.17.1 Historical Context of the Climate Change Model*

21
22 Past changes in climate at the WIPP have been recognized since the earliest site
23 characterization work. As described in Appendix GCR (3-102), Brokaw et al. (1972) and
24 Bachman (1974) interpreted the sedimentary record of the Gatuña, the Mescalero caliche, and
25 the overlying surficial sediments (see Chapter 2.0, Sections 2.1.3.8, 2.1.3.9, and 2.1.3.10) as
26 , indicating alternating wetter and drier climates during the Pleistocene. Bachman continued
27 extensive geologic work in the WIPP region throughout site characterization and further
28 documented the sedimentary evidence for Pleistocene climatic change (Bachman 1976, 1980,
29 1981, 1985, 1987). One borehole, WIPP-15, was drilled in 1978 in San Simon Sink southeast
30 of the WIPP to examine the causes of subsidence in the sink and to obtain paleoclimatic data
31 (SNL and University of New Mexico, 1981). Core from the borehole indicates about 547 feet
32 (167 meters) of total subsidence in the Quaternary. Aquatic fauna and flora from the upper 98
33 feet (30 meters) of core indicate a wet climate followed by an arid period before the present.

34
35 In addition to site-specific geologic evidence, past climatic changes have been inferred by
36 other workers throughout the southwest based on various data. Bachman (1989) prepared an
37 annotated bibliography of relevant information published as of 1984. Swift (see Appendix
38 CLI) prepared a synthesis of Pleistocene climate at the WIPP based on detailed examination
39 of available literature. Swift's analysis forms the basis for the DOE's present understanding
40 of climatic change.

41
42 Early interest in the possible effects of climatic change on disposal system performance
43 focused on the possibility that wetter climates might increase rates of salt dissolution. As
44 discussed in Chapter 2.0 (Section 2.1.6.2), and Appendix SCR (Section SCR.1.1.5.1), average

dissolution rates over the past several hundred thousand years include both wet and dry climates and are too low to affect disposal system performance during the next 200,000 years. Questions have also been raised about whether dissolution or precipitation of fracture fillings in the Culebra could occur during climatic changes and alter the rate of radionuclide transport in groundwater. As discussed in Appendix SCR (Section SCR.1.1.5.2), isotopic data from Siegel et al. (1991, 5-53 to 5-57), Chapman (1986), and Lambert (1987) indicate that mineralogical changes from interactions with groundwater have been minimal during late Pleistocene time in the units above the Salado. Future mineralogical changes that might occur during climate changes are therefore also expected to be minimal.

Based on their interpretation of uranium isotope activity ratios and other isotopic data from WIPP area groundwater, Lambert and Carter (1987) and Lambert (1991) proposed that climatic change in the past could have had a significant effect on groundwater flow direction. In their interpretation, wetter conditions during the late Pleistocene recharged the Rustler in the vicinity of Nash Draw, with flow occurring to the southeast. Drier conditions of the Holocene (including the present) resulted in no recharge and a gradual shift in flow directions to those observed at present.

Current understanding of regional groundwater flow is consistent with Lambert and Carter's general observation that flow directions may change with changing climate, but the specifics of their proposal are not supported by regional three-dimensional modeling. Flow in the Rustler during the wet period of the late Pleistocene was probably driven by a higher water table than that of the present and probably followed the local topography from east to west at the WIPP, rather than northwest to southeast. Drier conditions of the Holocene resulted in less, but perhaps not zero, recharge, and the altitude of the water table fell. Flow directions in the Culebra shifted to their present north-to-south direction, reflecting regional topography of the Delaware Basin.

Early assessments of system performance (for example, DOE 1980) did not consider the possibility that climatic change could affect the transport of radionuclides through its effects on groundwater flow. The 1991 preliminary performance assessment for the WIPP contained the first quantitative analysis of the possible effects of climatic change on radionuclide transport through the Culebra (WIPP Performance Assessment Division 1991, 6-35 to 6-43). The effects were approximated by varying heads along a portion of the northern boundary of a two-dimensional flow model for the Culebra. Heads were varied using a function that resulted in three peaks during the next 10,000 years, separated by periods in which heads were lowered to their present values. The maximum head elevations were prescribed by a sampled parameter that, at its largest value, allowed heads to reach the land surface and resulted in the maximum potentiometric gradient across the domain.

The 1992 preliminary performance assessment for the WIPP used an approach similar to that of the 1991 analyses (WIPP Performance Assessment Department 1993, 6-11 to 6-19). Sensitivity analyses performed for both the 1991 and 1992 preliminary performance assessments indicated that cumulative radionuclide releases were not sensitive to the variation

1   in heads at the northern boundary, conditional on the other assumptions adopted in the
2   preliminary performance assessments (Swift et al. 1994, 9 – 12).
3
4   Variations in boundary heads were abandoned for this performance assessment because the
5   regional three-dimensional modeling provided the basis for an approach that was better linked
6   to the near-surface processes of infiltration and recharge and that offered more control over
7   groundwater flow within the controlled area. The degree to which variations in boundary
8   heads affected flow over the repository in previous analyses was in part determined by the
9   location of the boundaries and their distance from the site. Setting boundary conditions closer
10 to the repository could have had a greater effect on flow over the site. Furthermore, restricting
11 changes in boundary heads to a single location restricted the possibility for changes in flow
12 direction.
13
14 In addition to work performed to address the treatment of climatic change in this application,
15 additional work was performed using the regional three-dimensional groundwater model to
16 examine the validity of approximating three-dimensional flow in the Rustler with a two-
17 dimensional model of the Culebra. This work indicates that within the controlled area
18 essentially all flow out of the Culebra is lateral. This result, documented by Corbet (1995),
19 provides the basis for applying a scaling factor derived from a three-dimensional model to a
20 two-dimensional model.
21

MASS.18 Castile Brine Reservoir

23
24 The conceptual model for the brine reservoir is included in the performance assessment to
25 estimate the extent to which uncertainty about the existence of a brine reservoir under the
26 waste disposal region may contribute to uncertainty in the estimate of cumulative radionuclide
27 releases from the disposal system. The conceptual model is not intended to provide a realistic
28 approximation of an actual brine reservoir under the waste disposal region: data are
29 insufficient to determine whether such a brine reservoir exists.
30
31 The Castile is treated as an impermeable unit in performance assessment and plays no role in
32 the analysis except to separate the Salado from the brine reservoir, that is important in human-
33 intrusion scenarios. Properties of the brine reservoir, including its permeability, porosity,
34 volume, and initial pressure, are chosen to be consistent with available data from borehole
35 penetrations of brine reservoirs in the region.
36
37 Basic geologic information about the Castile is given in Chapter 2.0 (Section 2.1.3.3). The
38 hydrology of the known brine reservoirs is discussed in Section 2.2.1.2.2. The treatment of
39 the brine reservoir in the performance assessment is discussed in Chapter 6.0 (Section 6.4.8),
40 which also points to supplementary information included in this application.
41
42 The principal parameters used in the brine reservoir model, described in Section 6.4.8, include
43 permeability, porosity, pore compressibility, initial pressure, and two-phase flow properties.
44 These parameters are implemented in the BRAGFLO model and affect the amount and rate of

1 brine flow up an intrusion borehole. Brine flow up a borehole is also affected by conditions in
2 other regions of the BRAGFLO model, including most directly the permeability of borehole-
3 fill material and fluid pressure in the borehole. The volume of the brine reservoir is treated as
4 an uncertain quantity in the performance assessment.
5
6 Attachment 18-4 discusses the estimate of the probability of intercepting a pressurized brine
7 reservoir used in BRAGFLO to develop the brine reservoir volumes. The probabilities
8 described in this memorandum are used to determine the cumulative distribution function for
9 the volume of a Castile brine reservoir. According to the method used, there is a 6/32
10 probability of a 32,000-cubic-meter brine reservoir (the probability of 0 and 1 reservoirs
11 combined), a 10/32 probability of a 64,000-cubic-meter brine reservoir, a 10/32 probability of
12 a 96-cubic-meter brine reservoir, a 5/32 probability of a 128,000-cubic-meter brine reservoir,
13 and a 1/32 probability of a 164,000-cubic-meter brine reservoir. See Chapter 6.0 (Section
14 6.4.12.6) for additional discussion of the probability of intercepting a brine reservoir.
15
16 *MASS.18.1 Historical Context of the Castile Brine Reservoir Model*
17
18 The FEIS (DOE 1980) acknowledged the possible importance of Castile brine, based largely
19 on the encounter at ERDA-6. However, it concluded that brine probably was not present
20 beneath the WIPP site, based on geologic structure and available well data (including the
21 absence of brine in WIPP-12, prior to deepening). Scenario development for the FEIS
22 considered brine occurrences, but consequences of a brine reservoir were not modeled
23 explicitly. The presence of brine beneath the repository was considered to be extremely
24 unlikely. No natural pathways connecting any brine reservoir with the repository were
25 thought to be present. Boreholes penetrating the repository and any brine reservoir were
26 assumed to be cased, and any flow from a reservoir would, therefore, have no impact
27 (borehole-casing degradation was not considered).
28
29 Spiegler (1982) concluded that brine reservoirs, originally at hydrostatic pressure, formed
30 several million years ago, prior to regional-scale erosion and decrease of overburden. He
31 assumed an original connection of the reservoir to the water table and concluded that
32 reservoirs formed (and were presumably isolated) several million years ago.
33
34 Spiegler and Updegraff (1983) concluded that the original brines were sea water, but that
35 release of water from gypsum dehydration could not be ruled out. Popielak et al. (1983)
36 agreed that Castile brines were relict or ancient sea water. They estimated a brine-residence
37 time of about one million years, believing that isolation preceded the latest stage of basin
38 tilting.
39
40 Popielak et al. (1983) and Faith et al. (1983), on the basis of analyses of brines from the
41 WIPP-12 and ERDA-6 occurrences, concluded that these two reservoirs are isolated
42 occurrences.
43

1   Lambert and Carter (1984) hypothesized that there may have been a Pleistocene connection of
2   the reservoirs to the Capitan Limestone, that is, that the brines were originally fresh water.
3   Using several assumptions, they calculated minimum residence times for WIPP-12 and
4   ERDA-6 brines ranging from 360,000 to 880,000 years on the basis of ^{234}U/^{238}U activity
5   ratios.
6
7   By the time of the Site and Preliminary Design Validation, Borns et al. (1983) concluded that
8
9   •   reservoirs formed mainly because of gravity tectonics (in response to density inversion
10   of thick halites and anhydrites),
11
12   •   the WIPP-12 structure (1 percent strain) took a minimum of 10,000 years to form, and
13
14   •   gravity tectonics were probably continuing, although at a reduced rate, because of
15   decreased overburden over the past few million years.
16
17   The conceptual understanding of the origin of reservoirs did not change between the early
18   1980s and the time of the DSEIS (DOE 1989) and FSEIS (DOE 1990). Brine reservoirs were
19   (and still are) believed to be isolated occurrences. Based on a Time Domain ElectroMagnetic
20   (TDEM) survey over the repository area, Earth Technology Corporation (1988) estimated that
21   a conductive horizon, which could be interpreted to represent Castile brine reservoirs,
22   underlies portions of the waste-emplacement panels (four out of nine soundings directly over
23   the panels). A recent interpretation of this data set is in Attachment 18-5.
24
25   For purposes of numerical modeling, hypothetical brine reservoirs were assumed to be radially
26   symmetrical, with an inner highly-fractured zone of high transmissivity, and an outer (less-
27   fractured) zone of moderate transmissivity. The outer zone is surrounded by an infinitely
28   extending anhydrite matrix, representative of intact (unfractured) Castile. The brine-reservoir
29   model produced double-porosity fluid-flow responses. This treatment implicitly assumes that
30   any borehole intersecting an area underlain by a brine reservoir will produce large amounts of
31   brine; the possibility that boreholes could penetrate the highly fractured reservoir, but miss
32   highly conductive fractures, was not considered.
33
34   Assuming that the reservoirs are radial, and based on an areal view of wells penetrating the
35   Castile (some of which did and some of which did not encounter a brine reservoir), Reeves et
36   al. (1991) determined that brine reservoirs could be expected to have radii varying from
37   approximately 2,625 to 10,499 feet (800 to 3,200 meters). Deterministic calculations in the
38   DSEIS and FSEIS assumed that any borehole penetrating the WIPP repository would
39   penetrate a Castile brine reservoir, and that this reservoir could be represented by the
40   estimated characteristics of the WIPP-12 brine reservoir.
41
42   There was no fundamental change in the conceptual understanding of brine reservoirs in the
43   December 1992 performance assessment. Performance assessment calculations included gas
44   pressurization of the repository, which was not considered in DSEIS calculations. This

1   pressurization helped delay brine depressurization of the Castile reservoirs. It was estimated
2   that brine underlay 25 to 57 percent of the waste-emplacement panels, with a median of
3   40 percent. This estimate was based on a contouring of the existing TDEM data, and was
4   implemented as a probability of a given borehole intersecting brine. Any borehole penetrating
5   a reservoir was assumed to produce brine. A broad range of significant reservoir properties
6   (for example, initial pressure, storativity) were sampled probabilistically, without assuming
7   that any reservoir present would be represented by WIPP-12 properties. The WIPP-12
8   characteristics did, however, fall within the sampled range.
9
10   Section 6.4.8 describes the DOE's current model of a fractured Castile brine reservoir, as
11   implemented by performance assessment. The main conceptual change is the idea that,
12   because of the high angle of vertical fracturing in Castile brine reservoirs, many boreholes
13   may penetrate a brine occurrence without penetrating a conductive fracture. Thus, even though
14   the recent interpretation (Attachment 18-5) of the TDEM data suggest that 10 to 55 percent of
15   the waste-panel area may be underlain by one or more brine reservoirs, the probability of a
16   borehole in the panel area encountering brine may be lower. The geostatistical study
17   performed by Powers et al. (Attachment 18-6) indicated an 8 percent probability of a borehole
18   in the panel area encountering Castile brine. This probability is assigned to determine
19   whether deep boreholes are of the E1 or E2 type in the 1996 performance assessment.
20

REFERENCES

Section MASS.2 References:

Channell, J.K. 1982. *Calculated Radiation Doses form Radionuclides Brought to the Surface if Future Drilling Intercepts the WIPP Repository and Pressurized Brine.* EEG-11. The Environmental Evaluation Group, Albuquerque, NM .

DOE (U.S. Department of Energy). 1980. *Final Environmental Impact Statement, Waste Isolation Pilot Plant.* DOE/EIS-0026, U.S. Department of Energy, Washington, DC. WPO 38835, WPO 38838 – 38839.

DOE (U.S. Department of Energy). 1990. *Final Safety Analysis Report.* WP 02-9, Rev. 0, May 1990. Westinghouse Electric Corporation, Waste Isolation Division, Carlsbad, NM.

Tyler, L.D., Matalucci, R.V., Molecke, M.A., Manson, DE, Nowak, E.J., and Stormont, J.C. 1988. *Summary Report for the WIPP Technology Development Program for Radioactive Waste.* SAND88-0844, Sandia National Laboratories, Albuquerque, NM. WPO 24040.

Westinghouse Electric Corporation (WEC). 1996. *Backfill Engineering Analysis Report, Waste Isolation Pilot Plant.* Westinghouse Electric Corporation, Waste Isolation Division, Carlsbad, NM. WPO 37909.

WIPP Performance Assessment Department. 1993. *Preliminary Performance Assessment for the Waste Isolation Pilot Plant, December 1992, Volume 4: Uncertainty and Sensitivity Analyses for 40 CFR 191, Subpart B.* SAND92-0700/4, Sandia National Laboratories, Albuquerque, NM. WPO 20958.

Woolfolk, S.W., 1982. *Radiological Consequences of Brine Release by Human Intrusion Into the WIPP.* TME-3151, U.S. Department of Energy, Waste Isolation Pilot Plant, Albuquerque, NM.

Zimmerman, D.A. and Gallegos, D.P. 1993. A Comparison of Geostatistically-Based Inverse Techniques for Use in Performance Assessment Analyses at the WIPP Site: Results from Test Case No. 1. *High Level Radioactive Waste Management, Proceedings from the Fourth Annual International Conference, Las Vegas, Nevada, April 26-30, 1993.* SAND92-2127C, Volume 2, p. 1426 – 1436. American Nuclear Society, La Grange Park, IL, and American Society of Civil Engineers, New York, NY. WPO 27840.

Section MASS.3 References:

Amyx, J.W., Bass, D.M. Jr., and Whiting, R.L. 1960. *Petroleum Reservoir Engineering, Physical Properties.* ISBN 07-001600-3, McGraw-Hill Book Company, New York, NY. (derived from equation 2-33) pp. 78.

Bear, J. 1972. *Dynamics of Fluid in Porous Media.* ISBN 0-486-65675-6, Dover Publications, New York, NY.

Beauheim, R.L., Saulnier, Jr., G.J. and Avis, J.D. 1991. *Interpretation of Brine-Permeability Tests of the Salado Formation at the Waste Isolation Pilot Plant: First Interim Report.* SAND90-0083, Sandia National Laboratories, Albuquerque, NM. WPO 26003.

Beauheim, R.L., Roberts, R.M., Dale, T.F., Fort, M.D., and Stensrud, W.A. 1993. *Hydraulic Testing of Salado Formation Evaporites at the Waste Isolation Pilot Plant Site: Second Interpretive Report.* SAND92-0533, Sandia National Laboratories, Albuquerque, NM. WPO 23378.

Brush, L.H. 1990. *Test Plan for Laboratory and Modeling Studies of Repository and Radionuclide Chemistry for the Waste Isolation Pilot Plant.* SAND90-0266, Sandia National Laboratories, Albuquerque, NM. WPO 26015.

Christian-Frear, T.L., and Webb, S.W. 1996. *The Effect of Explicit Representation of the Stratigraphy on Brine and Gas Flow at the Waste Isolation Pilot Plant.* SAND94-3173, Sandia National Laboratories, Albuquerque, NM.

Collins, R.E. 1961. *Flow of Fluids Through Porous Materials.* Reinhold, New York, NY.

Friend, D.G., and Huber, M.L. 1994. Thermophysical Property Standard Reference Data from NIST, *International Journal of Thermophysics.* Vol. 15, no. 6, 1279 – 1288.

NIST (National Institute of Standards and Technology). 1992. *Thermophysical Properties of Hydrogen Mixtures Database (SUPERTRAPP): Version 1.0 User's Guide.* U.S. Department of Commerce, National Institute of Standards and Technology Standard Reference Data Program, Gaithersburg, MD.

Wang, Y. 1995. Maximum gas generation rate and maximum quantity of gas generated. Memorandum to P. Chen dated December 21, 1995. SWCF-A W.B.S 1.1.09.1.1 (WPO 36288). Sandia National Laboratories, Albuquerque, NM.

WIPP Performance Assessment Division. 1991. *Preliminary Comparison with 40 CFR Part 191, Subpart B for the Waste Isolation Pilot Plant, December 1991 - Volume 3: Reference Data.* SAND91-0893/3. Eds. R.P. Rechard, A.C. Peterson, J.D. Schreiber, H.J. Iuzzolino, M.S. Tierney, and J.S. Sandha. Sandia National Laboratories, Albuquerque, NM.

Section MASS.4 References:

Sandia WIPP Project. 1992. *Preliminary Performance Assessment for the Waste Isolation Pilot Plant, December 1992. Volume 3: Model Parameters.* SAND92-0700/3, Sandia National Laboratories, Albuquerque, NM. WPO 23529.

WIPP Performance Assessment Department. 1992a. *Long-Term Gas and Brine Movement at the Waste Isolation Pilot Plant: Preliminary Sensitivity Analyses for Post-Closure 40 CFR 268 (RCRA), May 1992.* SAND92-1933, Sandia National Laboratories, Albuquerque, NM. WPO 23513.

WIPP Performance Assessment Department. 1992b. *Preliminary Performance Assessment for the Waste Isolation Pilot Plan, December 1992- Volume 5: Uncertainty and Sensitivity Analyses of Gas and Brine Migration for Undisturbed Performance.* SAND92-0700/5, Sandia National Laboratories, Albuquerque, NM. WPO 20929.

WIPP Performance Assessment Division. 1991. *Preliminary Comparison with 40 CFR Part 191, Subpart B for the Waste Isolation Pilot Plant, December 1991 - Volume 2: Probability and Consequence Modeling.* SAND91-0893/2, Sandia National Laboratories, Albuquerque, NM. WPO 26415.

Section MASS.5 References:

Rechard, R.P., Beyeler, W., McCurley, R.D., Rudeen, D.K., Bean, J.E., and Schreiber, J.D. 1990. *Parameter Sensitivity Studies of Selected Components of the Waste Isolation Pilot Plant Repository/Shaft System.* SAND89-2030, Sandia National Laboratories, Albuquerque, NM. Chapter 5, Summary and Conclusions, pp. 153 - 160. WPO 25946.

WIPP Performance Assessment Department. 1993. *Preliminary Performance Assessment for the Waste Isolation Pilot Plant, December 1992, Volume 4: Uncertainty and Sensitivity Analyses for 40 CFR 191, Subpart B.* SAND92-0700/4, Sandia National Laboratories, Albuquerque, NM. Section 4.1, Model Geometry, 4-1, 4-3. WPO 23599.

Section MASS.7 References:

Deal, D.E., and Case, J.B. 1987. *Brine Sampling and Evaluation Program, Phase I Report.* DOE-WIPP 87-008, Westinghouse Electric Corporation, Carlsbad, NM.

Deal, D.E., and Roggenthen, W.M. 1989. "The Brine Sampling and Evaluation Program (BSEP) at WIPP: Results of Four Years of Brine Seepage Data," *Waste Management '89, Waste Processing, Transportation, Storage and Disposal, Technical Programs and Public Education, Tucson, AZ, February 26-March 2, 1989.* Ed. R.G. Post. University of Arizona, Tucson, AZ. Vol. 1, 405 – 406.

Deal, D.E., Case, J.B., Deshler, R.M., Drez, P.E., Myers, J., and Tyburski, J.R. 1987. *Brine Sampling and Evaluation Program Phase II Report.* DOE-WIPP-87-010, Westinghouse Electric Corporation, Carlsbad, NM.

Deal, D.E., Abitz, R.J., Belski, D.S., Case, J.B., Crawley, M.E., Deshler, R.M., Drez, P.E., Givens, C.A., King, R.B., Lauctes, B.A., Myers, J., Niou, S., Pietz, J.M., Roggenthen, W.M., Tyburski, J.R., and Wallace, M.G. 1989. *Brine Sampling and Evaluation Program, 1988 Report.* DOE-WIPP-89-015, Westinghouse Electric Corporation, Carlsbad, NM.

Deal, D.E., Abitz, R.J., Belski, D.S., Clark, J.B., Crawley, M.R., and Martin, M.L. 1991a. *Brine Sampling and Evaluation Program, 1989 Report.* DOE-WIPP-91-009. Prepared for U.S. Department of Energy by IT Corporation and Westinghouse Electric Corporation. Westinghouse Electric Corporation, Waste Isolation Division, Carlsbad, NM.

Deal, D.E., Abitz, R.J., Myers, J., Case, J.B., Martin, M.L., Roggenthen, W.M., and Belski, D.S. 1991b. *Brine Sampling and Evaluation Program, 1990 Report.* DOE-WIPP-91-036. Prepared for U.S. Department of Energy by IT Corporation and Westinghouse Electric Corporation. Westinghouse Electric Corporation, Waste Isolation Division, Carlsbad, NM.

Deal, D.E., Abitz, R.J., Myers, J., Martin, M.L., Milligan, D.J., Sobocinski, R.W., Lipponer, P.P.J., and Belski, D.S. 1993. *Brine Sampling and Evaluation Program, 1991 Report.* DOE-WIPP-93-026. Prepared for U.S. Department of Energy by IT Corporation and Westinghouse Electric Corporation. Westinghouse Electric Corporation, Waste Isolation Division, Carlsbad, NM.

McTigue, D.F. 1993. *Permeability and Hydraulic Diffusivity of Waste Isolation Pilot Plant Repository Salt Inferred from Small-Scale Brine Inflow Experiments.* SAND92-1911, Sandia National Laboratories, Albuquerque, NM.

Vaughn, P., Lord, M., and MacKinnon, R. 1995a. "DR-6: Brine Puddling in the Repository due to Heterogeneities." Summary Memo of Record to D.R. Anderson, December 21, 1995, SWCF-A:1.1.6.3. Sandia National Laboratories, Albuquerque, NM. WPO 30795.

Vaughn, P., Lord, M., and MacKinnon, R. 1995b. "DR-7: Permeability Varying with Porosity in Closure Regions." Summary Memo of Record to D.R. Anderson, December 21, 1995, SWCF-A:1.1.6.3. Sandia National Laboratories, Albuquerque, NM. WPO 30796.

Vaughn, P., Lord, M., and MacKinnon, R. 1995c. "DR3: Dynamic Closure of the North End and Hallways." Summary Memorandum of Record to D. R. Anderson, September 28, 1995. SWCF-A:1.1.6.3. Sandia National Laboratories, Albuquerque, NM. WPO 30798.

Vaughn, P., Lord, M., Garner, J., and MacKinnon, R. 1995d. "GG-1: Radiolysis of Brine." Summary Memo of Record to D.R. Anderson, October 10, 1995, SWCF-A:1.1.6.3. Sandia National Laboratories, Albuquerque, NM. Contained in WPO 30791.

Vaughn, P., Lord, M., and MacKinnon, R. 1995e. "DR-2: Capillary Action (Wicking) within the Waste Materials." Summary Memo of Record to D.R. Anderson, December 21, 1995, SWCF-A:1.1.6.3. Sandia National Laboratories, Albuquerque, NM. WPO 30793.

Webb, S. 1995. "DR-1:3D Room Flow Model with Dip." Planning Memo of Record to D.R. Anderson, May 30, 1995. SWCF-A:1.1.6.3. Sandia National Laboratories, Albuquerque, NM. WPO 22494.

Section MASS.8 References:

Brush, L.H. 1990. *Test Plan for Laboratory and Modeling Studies of Repository and Radionuclide Chemistry for the Waste Isolation Pilot Plant.* SAND90-0266, Sandia National Laboratories, Albuquerque, NM. WPO 26015.

Brush, L.H., and Anderson, D.R. 1989a. "Potential Effects of Chemical Reactions on WIPP Gas and Water Budgets," *Systems Analysis, Long-Term Radionuclide Transport, and Dose Assessments, Waste Isolation Pilot Plant (WIPP), Southeastern New Mexico; March 1989.* Eds. A.R. Lappin, R.L. Hunter, D.P. Gabber, and P.B. Davies. SAND89-0462, Sandia National Laboratories, Albuquerque, NM. A-3 through A-30. In Appendix A of WPO 24125.

Brush, L.H., and Anderson, D.R. 1989b. "First Meeting of the WIPP PA Source Term Group," *Systems Analysis, Long-Term Radionuclide Transport, and Dose Assessments, Waste Isolation Pilot Plant (WIPP), Southeastern New Mexico; March 1989.* Eds. A.R. Lappin, R.L. Hunter, D.P. Gabber, and P.B. Davies. SAND89-0462, Sandia National Laboratories, Albuquerque, NM. A-31 through A-50. In Appendix A of WPO 24125.

Brush, L.H., and Anderson, D.R. 1989c. "Second Meeting of the WIPP PA Source-Term Group," *Systems Analysis, Long-Term Radionuclide Transport, and Dose Assessments, Waste Isolation Pilot Plant (WIPP), Southeastern New Mexico; March 1989.* Eds. A.R. Lappin, R.L. Hunter, D.P. Gabber, and P.B. Davies. SAND89-0462, Sandia National Laboratories, Albuquerque, NM. A-51 through A-59. In Appendix A of WPO 24125.

Brush, L.H., Grbic-Galic, D., Reed, D.T., Tong, X., Vreeland, R.H., and Westerman, R.E. 1991a. "Preliminary Results of Laboratory Studies of Repository Chemistry for the Waste Isolation Pilot Plant," *Scientific Basis for Nuclear Waste Management XIV, Materials Research Society Symposium Proceedings, Boston, MA, November 26-29, 1990.* Eds. T. Abrajano, Jr., and L.H. Johnson. SAND90-1031C, Materials Research Society, Pittsburgh, PA. Vol. 212, 893-900. WPO 25093.

Brush, L.H., Molecke, M.A., Lappin, A.R., Westerman, R.E., Tong, X., Black, J.N.P., Grbic-Galic, D., Vreeland, R.E., and Reed, D.T. 1991b. "Laboratory and Bin-Scale Tests of Gas Generation for the Waste Isolation Pilot Plant," *Waste-Generated Gas at the Waste Isolation Pilot Plant: Papers Presented at the Nuclear Energy Agency Workshop on Gas Generation and Release from Radioactive Repositories.* Eds. P.B. Davies, L.H. Brush, M.A. Molecke,

F.T. Mendenhall, and S.W. Webb. SAND91-2378, Sandia National Laboratories, Albuquerque, NM. 2-1 through 2-14. In Chapter 2 of WPO 25381.

Brush, L.H., Molecke, M.A., Westerman, R.E., Francis, A.J., Gillow, J.B., Vreeland, R.H. and Reed, D.T. 1993. "Laboratory Studies of Gas Generation for the Waste Isolation Pilot Plant," *Scientific Basis for Nuclear Waste Management XVI, Materials Research Society Symposium Proceedings, Boston, MA, November 30-December 4, 1992.* Eds. C.G. Interrante and R.T. Pabalan. SAND92-2160C, Materials Research Society, Pittsburgh, PA. Vol. 294, 335-340. WPO 29332.

Brush, L.H., Garner, J.W., and Storz, L.J. 1994. "Development of a Gas-Generation Model for the Waste Isolation Pilot Plant," *Scientific Basis for Nuclear Waste Management XVII, Materials Research Society Symposium Proceedings, Boston, MA, November 29-December 3, 1993.* Eds. A. Barkatt and R.A. Van Konynenburg. SAND93-1145C, Materials Research Society, Pittsburgh, PA. Vol. 333, 241-246. WPO 26689.

Butcher, B.M., and Mendenhall, F.T. 1993. *A Summary of the Models Used for the Mechanical Response of Disposal Rooms in the Waste Isolation Pilot Plant with Regard to Compliance with 40 CFR Part 191, Subpart B.* SAND92-0427, Sandia National Laboratories, Albuquerque, NM. WPO 23356.

Francis, A.J., and Gillow, J.B. 1994. *Effects of Microbial Processes on Gas Generation Under Expected Waste Isolation Pilot Plant Repository Conditions, Progress Report Through 1992.* SAND93-7036, Sandia National Laboratories, Albuquerque, NM. WPO 10673.

Lappin, A.R., Hunter, R.L., Gabber, D.P., and Davies, P.B., eds. 1989. *Systems Analysis, Long-Term Radionuclide Transport, and Dose Assessments, Waste Isolation Pilot Plant (WIPP), Southeastern New Mexico; March 1989.* SAND89-0462, Sandia National Laboratories, Albuquerque, NM. WPO 24125.

Molecke, M.A. 1978. *Waste Isolation Pilot Plant Transuranic Wastes Experimental Characterization Program: Executive Summary.* SAND78-1356, Sandia National Laboratories, Albuquerque, NM. WPO 23671.

Molecke, M.A. 1979. *Gas Generation from Transuranic Waste Degradation: Data Summary and Interpretation.* SAND79-1245, Sandia National Laboratories, Albuquerque, NM. WPO 26715.

Reed, D.T., Okajima, S., Brush, L.H., and Molecke, M.A. 1993. "Radiolytically-Induced Gas Production in Plutonium-Spiked WIPP Brine," *Scientific Basis for Nuclear Waste Management XVI, Materials Research Society Symposium Proceedings, Boston, MA, November 30-December 4, 1992.* Eds. C.G. Interrante and R.T. Pabalan. SAND92-7283C, Materials Research Society, Pittsburgh, PA. Vol. 294, 431-438. WPO 28639.

Sandia National Laboratories. 1979. *Summary of Research and Development Activities in Support of Waste Acceptance Criteria for WIPP.* Comp. T.O. Hunter. SAND79-1305, Sandia National Laboratories, Albuquerque, NM. WPO 26734.

Telander, M.R., and Westerman, R.E. 1993. *Hydrogen Generation by Metal Corrosion in Simulated Waste Isolation Pilot Plant Environments, Progress Report for the Period November 1989 Through December 1992.* SAND92-7347, Sandia National Laboratories, Albuquerque, NM. WPO 23456.

Trauth, K.M., Hora, S.C., Rechard, R.P., and Anderson, D.R. 1992. *The Use of Expert Judgment to Quantify Uncertainty in Solubility and Sorption Parameters for Waste Isolation Pilot Plant Performance Assessment.* SAND92-0479, Sandia National Laboratories, Albuquerque, NM. WPO 23526.

WIPP Performance Assessment Division. 1991. *Preliminary Comparison with 40 CFR Part 191, Subpart B for the Waste Isolation Pilot Plant, December 1991. Volume 3: Reference Data.* SAND91-0893/3. Eds. R.P. Rechard, A.C. Peterson, J.D. Schreiber, H.J. Iuzzolino, M.S. Tierney and J.S. Sandha. Sandia National Laboratories, Albuquerque, NM. WPO 26419.

Section MASS.12 References:

Bertram-Howery, S.G., Marietta, M.G., Rechard, R.P., Swift, P.N., Anderson, D.R., Baker, B.L., Bean, Jr., J.E., Beyeler, W., Brinster, K.F., Guzowski, R.V., Helton, J.C., McCurley, R.D., Rudeen, D.K., Schreiber, J.D., and Vaughn, P. 1990. *Preliminary Comparison with 40 CFR Part 191, Subpart B for the Waste Isolation Pilot Plant, December 1990.* SAND90-2347, Sandia National Laboratories, Albuquerque, NM.

Callahan, G.D. 1994. *SPECTROM-32: A Finite Element Thermomechanical Stress Analysis Program Version 4.06*, RSI-0531, RE/SPEC Inc., Rapid City, SD. WPO 36814.

DOE (U.S. Department of Energy). 1995. *Conceptual Design for Operational Phase Panel Closure Systems.* DOE-WIPP-95-2057, U.S. Department of Energy, Carlsbad Area Office, Carlsbad, NM.

Nowak, E.J., Tillerson, J.R., and Torres, R.M. 1990. *Initial Reference Seal System Design: Waste Isolation Pilot Plant.* SAND90-0355, Sandia National Laboratories, Albuquerque, NM.

Pruess, K. 1991. *TOUGH2: A General-Purpose Numerical Simulator for Multiphase Fluid and Heat Flow.* LBL-29400, Earth Science Division, Lawrence Berkeley Laboratories, Berkeley, CA.

Reeves, M., Ward, D.S., Johns, N.D., and Cranwell, R.M. 1986. *Theory and Implementation for SWIFT II, The Sandia Waste-Isolation Flow and Transport Model for Fractured Media, Release 484.* SAND83-1159, NUREG/CR-3328, Sandia National Laboratories, Albuquerque, NM.

Sandia WIPP Project. 1992. *Preliminary Performance Assessment for the Waste Isolation Pilot Plant, December 1992. Volume 3: Model Parameters.* SAND92-0700/3, Sandia National Laboratories, Albuquerque, NM.

Stormont, J.D. 1988. *Preliminary Seal Design Evaluation for the Waste Isolation Pilot Plant.* SAND87-3083, Sandia National Laboratories, Albuquerque, NM.

WIPP Performance Assessment Division. 1991. *Preliminary Comparison with 40 CFR Part 191, Subpart B for the Waste Isolation Pilot Plant, December 1991—Volume 1: Methodology and Results.* SAND91-0893/1, Sandia National Laboratories, Albuquerque, NM.

Section MASS.13 References:

Christian-Frear, T.L., and Webb, S.W. 1996, *The Effect of Explicit Representation of the Stratigraphy on Brine and Gas Flow at the Waste Isolation Pilot Plant.* SAND94-3173, Sandia National Laboratories, Albuquerque, NM. WPO 37240.

Davies, P.B. 1991. *Evaluation of the Role of Threshold Pressure in Controlling Flow of Waste-Generated Gas into Bedded Salt at the Waste Isolation Pilot Plant.* SAND90-3246, Sandia National Laboratories, Albuquerque, NM. WPO 26169

Davies, P.B., Webb, S.W., and Gorham, E.D. 1993. "Feedback on 'PA Modeling Using BRAGFLO -- 1992' memo by J. Schreiber, July 14, 1992," pp. A-23 through A-37 in Sandia WIPP Project, 1992. *Preliminary Performance Assessment for the Waste Isolation Pilot Plant, December 1993. Volume 3, Model Parameters.* SAND92-0700/3, Sandia National Laboratories, Albuquerque, NM.

Freeze, G.A., Larson, K.W., and Davies, P.B. 1995. *Coupled Multiphase Flow and Closure Analysis of Repository Response to Waste-Generated Gas at the Waste Isolation Pilot Plant (WIPP).* SAND93-1986, Sandia National Laboratories, Albuquerque, NM. WPO 29557.

Gorham, E., Beauheim, R., Davies, P., Howarth, S., and Webb, S. 1992. "Recommendation to PA on Salado Formation Intrinsic Permeability and Pore Pressure for 40 Subpart B Calculations, June 15, 1992," pages A-49 through A-65 in Sandia WIPP Project, 1992. *Preliminary Performance Assessment for the Waste Isolation Pilot Plant, December 1993. Volume 3, Model Parameters.* SAND92-0700/3, Sandia National Laboratories, Albuquerque, NM.

Lappin, A.R., Hunter, R.L., Gabber, D.P., and Davies, P.B., eds. 1989. *Systems Analysis, Long-Term Radionuclide Transport, and Dose Assessments, Waste Isolation Pilot Plant (WIPP), Southeastern New Mexico; March 1989*. SAND89-0462, Sandia National Laboratories, Albuquerque, NM. WPO 24125.

Mendenhall, F.T., and Gerstle, W. 1993. WIPP Anhydrite Fracture Modeling. Memorandum to Distribution, December 6, 1993. SWCF-A: W.B.S. 1.1.7.1 (WPO #39830). Sandia National Laboratories, Albuquerque, NM. WPO 39830.

Sandia WIPP Project. 1992. *Preliminary Performance Assessment for the Waste Isolation Pilot Plant, December 1992. Volume 3: Model Parameters*. SAND92-0700/3, Sandia National Laboratories, Albuquerque, NM. WPO 23529.

Vaughn, P., Lord, M., and MacKinnon, R. 1995. S-6: Dynamic Alteration of the DRZ/Transition Zone: Summary Memo of Record to D.R. Anderson, September 28, 1995. SWCF-A (WPO #30798). Sandia National Laboratories, Albuquerque, NM.

WIPP Performance Assessment Department. 1992. *Preliminary Performance Assessment for the Waste Isolation Pilot Plant, December 1992. Volume 2: Technical Basis*. SAND92-0700/2, Sandia National Laboratories, Albuquerque, NM. WPO 23528.

WIPP Performance Assessment Department. 1993. *Preliminary Performance Assessment for the Waste Isolation Pilot Plant, December 1992, Volume 4: Uncertainty and Sensitivity Analyses for 40 CFR 191, Subpart B*. SAND92-0700/4, Sandia National Laboratories, Albuquerque, NM. WPO 23528.

Section MASS.14 References:

Barr, G.E., Miller, W. B., and Gonzalez, D.D. 1983. *Interim Report on the Modeling of the Regional Hydraulics of the Rustler Formation*. SAND83-0391, Sandia National Laboratories, Albuquerque, NM. WPO 27557.

Bear, J., and Verruijt, A. 1987. *Modeling Groundwater Flow and Pollution*. Dordrecht; Boston, MA: D. Reidel Publishing; Norwell, MA: Sold and distributed in the U.S. and Canada by Kluwer Academic Publishers.

Beauheim, R.L. 1986. *Hydraulic-Test Interpretations for Well DOE-2 at the Waste Isolation Pilot Plant (WIPP) Site*. SAND86-1364, Sandia National Laboratories, Albuquerque, NM. WPO 27656.

Chapman, J.B. 1986. *Stable Isotopes in Southeastern New Mexico Groundwater: Implications for Dating Recharge in the WIPP Area*. EEG-35, DOE/AL/10752-35, Environmental Evaluation Group, Santa Fe, NM.

Chapman, J.B. 1988. *Chemical and Radiochemical Characteristics of Groundwater in the Culebra Dolomite, Southeastern New Mexico.* EEG-39, Environmental Evaluation Group, Santa Fe, NM.

Corbet, T.F. 1994. "Evolution of Patterns of Regional Groundwater Flow in Southeastern New Mexico: Response to Post-Pleistocene Changes in Climate," *Abstracts with Programs, 1994 Annual Meeting, The Geological Society of America, October 24-27, 1994.* SAND94-1856A, Seattle, WA. Vol. 26, no. 7, 414. WPO 23733.

Corbet, T.F., and Wallace, M.G. 1993. "Post-Pleistocene Patterns of Shallow Groundwater Flow in the Delaware Basin, Southeastern New Mexico and West Texas," *Carlsbad Region, New Mexico and West Texas, New Mexico Geological Society Forty-fourth Annual Field Conference, Carlsbad, NM, October 6-9, 1993.* Eds. D.W. Love, J.W. Hawley, B.S. Kues, J.W. Adams, G.W. Austin, and J.M. Barker. SAND93-1318J, New Mexico Geological Society, Socorro, NM. 321-325. WPO 28644.

Corbet, T.F., and Knupp, P.M. 1996. *The Role of Regional Groundwater Flow in the Hydrogeology of the Culebra Member of the Rustler Formation at the Waste Isolation Pilot Plant (WIPP), Southeastern New Mexico.* SAND96-2133, Sandia National Laboratories, Albuquerque, NM.

Dagan, G. 1989. *Flow and Transport in Porous Formations.* Springer-Verlag, New York, NY.

Davies, P.B. 1989. *Variable-Density Ground-Water Flow and Paleohydrology in the Waste Isolation Pilot Plant (WIPP) Region, Southeastern New Mexico.* Open-File Report 88-490, U.S. Geological Survey, Albuquerque, NM. WPO 38854.

de Marsily, G. 1986. *Quantitative Hydrogeology: Groundwater Hydrology for Engineers.* Academic Press, Orlando, FL.

DOE (U.S. Department of Energy). 1989. *Draft Supplement, Environmental Impact Statement, Waste Isolation Pilot Plant.* DOE/EIS-0026-DS, Department of Energy, Washington, DC. Vols. 1 – 2.

Knupp, P. 1996. "A Moving Mesh Algorithm for 3-D Regional Groundwater Flow with Water Table and Seepage Face," *Advances in Water Resources.* Vol. 19, no. 2, 83-95.

Lambert, S.J. 1987. *Feasibility Study: Applicability of Geochronologic Methods Involving Radiocarbon and Other Nuclides to the Groundwater Hydrology of the Rustler Formation, Southeastern New Mexico.* SAND86-1054, Sandia National Laboratories, Albuquerque, NM. WPO 24475.
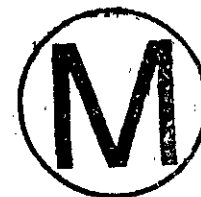
Lambert, S.J., and Carter, J.A. 1987. *Uranium-Isotope Systematics in Groundwaters of the Rustler Formation, Northern Delaware Basin, Southeastern New Mexico. I: Principles and Preliminary Results.* SAND87-0388, Sandia National Laboratories, Albuquerque, NM. WPO 24453.

Lambert, S.J., and Harvey, D.M. 1987. *Stable-Isotope Geochemistry of Groundwaters in the Delaware Basin of Southeastern New Mexico.* SAND87-0138, Sandia National Laboratories, Albuquerque, NM. WPO 24150.

Lappin, A.R., Hunter, R.L., Gabber, D.P., and Davies, P.B., eds. 1989. *Systems Analysis, Long-Term Radionuclide Transport, and Dose Assessments, Waste Isolation Pilot Plant (WIPP), Southeastern New Mexico; March 1989.* SAND89-0462, Sandia National Laboratories, Albuquerque, NM. WPO 24125.

McDonald, M.G., and Harbaugh, A.W. 1988. *A Modular Three-Dimensional Finite-Difference Ground-Water Flow Model.* Open-File Report 83-875, U.S. Geological Survey, Denver, CO.

Siegel, M.D., Lambert, S.J., and Robinson, K.L., eds. 1991. *Hydrogeochemical Studies of the Rustler Formation and Related Rocks in the Waste Isolation Pilot Plant Area, Southeastern New Mexico.* SAND88-0196, Sandia National Laboratories, Albuquerque, NM. WPO 25624.

Section MASS.15 References:

Avogadro, A., and de Marsily, G. 1984. "The Role of Colloids in Nuclear Waste Disposal," *Scientific Basis for Nuclear Waste Management VII, Materials Research Society Symposia Proceedings, Boston, MA, November 14-17, 1983.* Ed. G.L. McVay. North-Holland, New York, NY. Vol. 26, 495-505.

Beauheim, R.L. 1987a. *Analysis of Pumping Tests of the Culebra Dolomite Conducted at the H-3 Hydropad at the Waste Isolation Pilot Plant (WIPP) Site.* SAND86-2311, Sandia National Laboratories, Albuquerque, NM. WPO 28468.

Beauheim, R.L. 1987b. *Interpretations of Single-Well Hydraulic Tests Conducted At and Near the Waste Isolation Pilot Plant (WIPP) Site, 1983-1987.* Sandia National Laboratories, Albuquerque, NM. WPO 27679.

Bennett, D.G., Liew, S.K., Nanu, L., Read, D., and Thomas, J.B. 1993. "Modelling Colloidal Transport of Radionuclides Through Porous Media," *High Level Radioactive Waste Management, Proceedings of the Fourth Annual International Meeting, Las Vegas, NV, April 26-30, 1993.* American Nuclear Society, La Grange Park, IL; American Society of Civil Engineers, New York, NY. Vol. 4, 638-645.

Bertram, S.G. 1995. "NS-11: Subsidence Associated with Mining Inside or Outside of the Controlled Area." Summary Memo of Record to D.R. Anderson, December 8, 1995. SWCF-1:1.1.6.3. Sandia National Laboratories, Albuquerque, NM. WPO 30761.

Corapcioglu, M.Y., and Jiang, S. 1993. "Colloid-Facilitated Groundwater Contaminant Transport," *Water Resources Research*. Vol. 29, no. 7, 2216 – 2226.

DOE (U.S. Department of Energy). 1980. *Final Environmental Impact Statement, Waste Isolation Pilot Plant*. DOE/EIS-0026, U.S. Department of Energy, Washington, DC. Vols. 1 - 2. WPO 38835, WPO 38839.

DOE (U.S. Department of Energy). 1990. *Final Supplement Environmental Impact Statement, Waste Isolation Pilot Plant*. DOE/EIS-0026-FS, U.S. Department of Energy Office of Environmental Restoration and Waste Management, Washington, DC. Vols. 1 – 13.

Dosch, R.G. 1979. "Radionuclide Migration Studies Associated with the WIPP Site in Southeastern New Mexico," *Scientific Basis for Nuclear Waste Management, Proceedings of the Symposium on Science Underlying Radioactive Waste Management, Boston, MA, November 28-December 1, 1978*. Ed. G.J. McCarthy. SAND78-1178J, Plenum Press, New York, NY. Vol. 1, 395-398. WPO 29589.

Dosch, R.G. 1980. *Assessment of Potential Radionuclide Transport in Site-Specific Geologic Formations*. SAND79-2468, Sandia National Laboratories, Albuquerque, NM. WPO 28085.

Dosch, R.G. 1981. *Solubility and Sorption Characteristics of Uranium (VI) Associated with Rock Samples and Brines/Groundwaters from WIPP and NTS*. SAND80-1595, Sandia National Laboratories, Albuquerque, NM. WPO 30252.

Dosch, R.G., and Lynch, A.W. 1978. *Interaction of Radionuclides with Geomedia Associated with the Waste Isolation Pilot Plant (WIPP) Site in New Mexico*. SAND78-0297, Sandia National Laboratories, Albuquerque, NM. WPO 28145.

Grindrod, P. 1993. "The Impact of Colloids on the Migration and Dispersal of Radionuclides Within Fractured Rock," *Journal of Contaminant Hydrology*. Vol. 13, no. 1 – 4, 167-181.

Grindrod, P., and Worth, D.J. 1990. *Radionuclide and Colloid Migration in Fractured Rock: Model Calculations*. SKI Technical Report 91:11, Swedish Nuclear Power Inspectorate, Stockholm, Sweden.

Guzowski, R.V. 1990. *Preliminary Identification of Scenarios for the Waste Isolation Pilot Plant, Southeastern New Mexico*. SAND90-7090, Sandia National Laboratories, Albuquerque, NM. WPO 25771.

Harmand, B., and Sardin, M. 1994. "Modelling the Coupled Transport of Colloids and Radionuclides in a Fractured Natural Medium," *Chemistry and Migration Behaviour of Actinides and Fission Products in the Geosphere, Proceedings of the Fourth International Conference, Charleston, SC, December 12-17, 1993.* R. Oldenbourg Verlag, Munich. Vol. 66/67, 691-699.

Haug, A., Kelley, V.A., LaVenue, A.M., and Pickens, J.F. 1987. *Modeling of Ground-Water Flow in the Culebra Dolomite at the Waste Isolation Pilot Plant (WIPP) Site: Interim Report.* SAND86-7167, Sandia National Laboratories, Albuquerque, NM. WPO 28486.

Holt, R.M., and Powers, D.W. 1984. *Geotechnical Activities in the Waste Handling Shaft.* WTSD-TME-038, U.S. Department of Energy, Carlsbad, NM.

Holt, R.M., and Powers, D.W. 1986. *Geotechnical Activities in the Exhaust Shaft.* DOE-WIPP 86-008, U.S. Department of Energy, Carlsbad, NM.

Holt, R.M., and Powers, D.W. 1988. *Facies Variability and Post-Depositional Alteration Within the Rustler Formation in the Vicinity of the Waste Isolation Pilot Plant, Southeastern New Mexico.* DOE-WIPP 88-004, U.S. Department of Energy, Carlsbad, NM.

Holt, R.M., and Powers, D.W. 1990. *Geologic Mapping of the Air Intake Shaft at the Waste Isolation Pilot Plant.* DOE-WIPP 90-051, U.S. Department of Energy, Carlsbad, NM.

Hunter, R.L. 1989. *Events and Processes for Constructing Scenarios for the Release of Transuranic Waste from the Waste Isolation Pilot Plant, Southeastern New Mexico.* SAND89-2546, Sandia National Laboratories, Albuquerque, NM. WPO 27731.

Hwang, Y., Pigford, T.H., Lee, W.W.-L., and Chambre, P.L. 1989. "Analytic Solution of Pseudocolloid Migration in Fractured Rock," *Transactions of the American Nuclear Society.* Vol. 60, 107-109.

Ibaraki, M., and Sudicky, E.A. 1995. "Colloid-Facilitated Contaminant Transport in Discretely Fractured Porous Media. 1. Numerical Formulation and Sensitivity Analysis," *Water Resources Research.* Vol. 31, no. 12, 2945 – 2960.

Jacquier, P. 1991. "Geochemical Modelling: What Phenomena are Missing?" *Radiochimica Acta.* Vol. 52/53, pt. 1, 495-499.

Jones, T.L., Kelley, V.A., Pickens, J.F., Upton, D.T., Beauheim, R.L., and Davies, P.B. 1992. *Integration of Interpretation Results of Tracer Tests Performed in the Culebra Dolomite at the Waste Isolation Pilot Plant Site.* SAND92-1579, Sandia National Laboratories, Albuquerque, NM. WPO 23504.

Lappin, A.R., Hunter, R.L., Gabber, D.P., and Davies, P.B., eds. 1989. *Systems Analysis, Long-Term Radionuclide Transport, and Dose Assessments, Waste Isolation Pilot Plant (WIPP), Southeastern New Mexico; March 1989.* SAND89-0462, Sandia National Laboratories, Albuquerque, NM. WPO 24125.

LaVenue, A.M., and RamaRao, B.S. 1992. *A Modeling Approach to Address Spatial Variability Within the Culebra Dolomite Transmissivity Field.* SAND92-7306, Sandia National Laboratories, Albuquerque, NM. WPO 23889.

LaVenue, A.M., Cauffman, T.L., and Pickens, J.F. 1990. *Ground-Water Flow Modeling of the Culebra Dolomite: Volume 1 - Model Calibration.* SAND89-7068/1, Sandia National Laboratories, Albuquerque, NM.

Light, W.B., Lee, W.W.-L., Chambre, P.L., and Pigford, T.H. 1990. "Radioactive Colloid Advection in a Sorbing Porous Medium: Analytical Solution," *Transactions of the American Nuclear Society.* Vol. 61, 81-83.

Lynch, A.W., and Dosch, R.G. 1980. *Sorption Coefficients for Radionuclides on Samples from the Water-Bearing Magenta and Culebra Members of the Rustler Formation.* SAND80-1064, Sandia National Laboratories, Albuquerque, NM. WPO 28223.

Lynch, A.W., Dosch, R.G., and Hills, C.R. 1981. *Migration of Cesium-137 Through a Solid Core of Magenta Dolomite Taken from the Rustler Formation in Southeastern New Mexico.* SAND80-1259, Sandia National Laboratories, Albuquerque, NM. WPO 24234.

Marietta, M.G., Bertram-Howery, S.G., Anderson, D.R. (Rip), Brinster, K.F., Guzowski, R.V., Iuzzolino, H., and Rechard, R.P. 1989. *Performance Assessment Methodology Demonstration: Methodology Development for Evaluating Compliance with EPA 40 CFR 191, Subpart B, for the Waste Isolation Pilot Plant.* SAND89-2027, Sandia National Laboratories, Albuquerque, NM. WPO 25952.

McCarthy, J.F., and Zachara, J.M. 1989. "Subsurface Transport of Contaminants," *Environmental Science and Technolology.* Vol. 23, no. 5, 496 – 502.

Mercer, J.W., and Orr, B.R. 1979. *Interim Data Report on the Geohydrology of the Proposed Waste Isolation Pilot Plant Site, Southeast New Mexico.* Water-Resources Investigations 79-98, U.S. Geological Survey, Albuquerque, NM.

Nyhan, J.W., Drennon, B.J., Abeele, W.V., Wheeler, M.L., Purtymun, W.D., Trujillo, G., Herrera, W.J., and Booth, J.W. 1985. "Distribution of Plutonium and Americium Beneath a 33-yr-old Liquid Waste Disposal Site," *Journal of Environmental Quality.* Vol. 14, no. 4, 501 – 509.
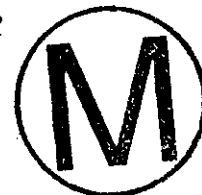
Paine, R.T., and Dosch, R.G. 1992. "Summary of Previously Unpublished Experimental Measurements of Plutonium and Americium Sorption onto Culebra Substrates from Brine B Containing Organic Ligands," *An Evaluation of Radionuclide Batch Sorption Data on Culebra Dolomite for Aqueous Compositions Relevant to the Human Intrusion Scenario for the Waste Isolation Pilot Plant.* C.F. Novak. SAND91-1299, Sandia National Laboratories, Albuquerque, NM. D-1 through D-8. In Appendix D of WPO 26181.

Papenguth, H.W., and Behl, Y.K. 1996a. "Test Plan for Evaluation of Colloid-Facilitated Actinide Transport at the Waste Isolation Pilot Plant." SNL Test Plan TP 96-01, Sandia National Laboratories, Albuquerque, NM. WPO 31337.

Papenguth, H.W., and Behl, Y.K. 1996b. "Test Plan for Evaluation of Dissolved Actinide Retardation at the Waste Isolation Pilot Plant." TP 96-02, Sandia National Laboratories, Albuquerque, NM. WPO 31336.

Park, S.-W., Leckie, J.O., and Siegel, M.D. 1992. *Surface Complexation Modeling of Uranyl Adsorption on Corrensite from the WIPP Site.* Technical Report No. 315, Stanford University Department of Civil Engineering, Palo Alto, CA.

Park, S.-W., Leckie, J.O., and Siegel, M.D. 1995. *Surface Complexation Modeling of Uranyl Adsorption on Corrensite from the Waste Isolation Pilot Plant Site.* SAND90-7084, Sandia National Laboratories, Albuquerque, NM. WPO 29367.

Ramsey, J. 1996. "Culebra Dissolved Actinide Parameter Request." Unpublished memorandum to E. J. Nowak, March 18, 1996. Sandia National Laboratories, Albuquerque, NM. WPO 35269.

Serne, R.J., Rai, D., Mason, M.J., and Molecke, M.A. 1977. *Batch K_d Measurements of Nuclides to Estimate Migration Potentials at the Proposed Waste Isolation Pilot Plant in New Mexico.* PNL-2448, Battelle Pacific Northwest Laboratory, Richland, WA.

Sewards, T. 1991. *Characterization of Fracture Surfaces in Dolomite Rock, Culebra Dolomite Member, Rustler Formation.* SAND90-7019, Sandia National Laboratories, Albuquerque, NM. WPO 23872.

Sewards, T., Williams, M.L., and Keil, K. 1991. "Mineralogy of the Culebra Dolomite," *Hydrogeochemical Studies of the Rustler Formation and Related Rocks in the Waste Isolation Pilot Plant Area, Southeastern New Mexico.* SAND88-0196. Eds. M.D. Siegel, S.J. Lambert, and K.L. Robinson. Sandia National Laboratories, Albuquerque, NM. 3-1 to 3-43. Chapter 3 of WPO 25624.

Sewards, T., Brearly, A., Glenn, R., MacKinnon, I.D.R., and Siegel, M.D. 1992. *Nature and Genesis of Clay Minerals of the Rustler Formation in the Vicinity of the Waste Isolation Pilot*

Plant in Southeastern New Mexico. SAND90-2569, Sandia National Laboratories, Albuquerque, NM. WPO 26157.

Siegel, M.D., Leckie, J.O., Park, S.-W., Phillips, S.L., and Sewards, T. 1990. *Studies of Radionuclide Sorption by Clays in the Culebra Dolomite at the Waste Isolation Pilot Plant Site, Southeastern New Mexico.* SAND89-2387, Sandia National Laboratories, Albuquerque, NM. WPO 17722.

Smith, P.A., and Degueldre, C. 1993. "Colloid-Facilitated Transport of Radionuclides Through Fractured Media," *Journal of Contaminant Hydrology.* Vol. 13, no. 1 – 4, 143 – 166.

SNL (Sandia National Laboratories). 1992 – 1993. *Preliminary Performance Assessment for the Waste Isolation Pilot Plant, December 1992.* SAND92-0700, Vols. 1-5, Sandia National Laboratories, Albuquerque, NM. Vol. 1 – WPO 20762, Vol. 2 – WPO 20805, Vol. 3 – WPO 23529, Vol. 4 – WPO 20958, Vol. 5 – WPO 20929.

Tien, P.-L., Nimick, F.B., Muller, A.B., Davis, P.A., Guzowski, R.V., Duda, L.E., and Hunter, R.L. 1983. *Repository Site Data and Information in Bedded Salt: Palo Duro Basin, Texas.* SAND82-2223, Sandia National Laboratories, Albuquerque, NM. WPO 28328.

Tierney, M.S. 1991. *Combining Scenarios in a Calculation of the Overall Probability Distribution of Cumulative Releases of Radioactivity From the Waste Isolation Pilot Plant, Southeastern New Mexico.* SAND90-0838, Sandia National Laboratories, Albuquerque, NM. WPO 26030.

Trauth, K.M., Hora, S.C., Rechard, R.P., and Anderson, D.R. 1992. *The Use of Expert Judgment to Quantify Uncertainty in Solubility and Sorption Parameters for Waste Isolation Pilot Plant Performance Assessment.* SAND92-0479, Sandia National Laboratories, Albuquerque, NM. WPO 23526.

Travis, B.J., and Nuttall, H.E. 1985. "A Transport Code for Radiocolloid Migration: With an Assessment of an Actual Low-Level Waste Site," *Scientific Basis for Nuclear Waste Management VIII, Materials Research Society Symposia Proceedings, Boston, MA, November 26-29, 1984.* Eds. C.M. Jantzen, J.A. Stone, and R.C. Ewing. Materials Research Society, Pittsburgh, PA. Vol. 44, 969-976.

van der Lee, J., de Marsily, G., and Ledoux, E. 1993. "Are Colloids Important for Transport Rate Assessment of Radionuclides? A Microscopic Modeling Approach," *High Level Radioactive Waste Management, Proceedings of the 4th Annual International Conference, Las Vegas, NV, April 26-30, 1993.* American Society of Civil Engineers, New York, NY. 646-652.

van der Lee, J., Ledoux, E., and de Marsily, G. 1994. "Microscopic Description of Colloid Transport in Fractured or Porous Media," *Transport and Reactive Processes in Aquifers: Proceedings of the IAHR/AIRH Symposium, Zurich, Switzerland, April 11-15, 1994.* Eds. Th. Dracos and F. Stauffer. A.A. Balkema, Brookfield, VT. 349-355.

WIPP Performance Assessment Division. 1991. *Preliminary Comparison with 40 CFR Part 191, Subpart B for the Waste Isolation Pilot Plant, December 1991—Volume 1: Methodology and Results.* SAND91-0893/1, Sandia National Laboratories, Albuquerque, NM.

Section MASS.16 References:

Berglund, J.W. 1992. *Mechanisms Governing the Direct Removal of Wastes from the Waste Isolation Pilot Plant Repository Caused by Exploratory Drilling.* SAND92-7295, Sandia National Laboratories, Albuquerque, NM. WPO 23946.

Berglund, J.W., and Lenke, L.R. 1995. "One Dimensional Experiments of Gas Induced Spall." NMERI Contractor Report NMERI 1995/3. New Mexico Engineering Research Institute, University of New Mexico, Albuquerque, NM. WPO 27589.

Berner, U. 1990. "A Thermodynamic Description of the Evolution of Pore Water Chemistry and Uranium Speciation During the Degradation of Cement," Technical Report 90-12, Paul Scherrer, Villigen, Switzerland.

Lenke, L.R., and Berglund, J.W. 1995. "Blowout Experiments in an Axisymmetric Geometry," New Mexico Engineering Research Contractor's Report, Contract AL-7022, November, 1995. WPO 29181.

State of New Mexico, Oil Conservation Division, Energy, Minerals, and Natural Resources Department. 1988. Application of the Oil Conservation Division Upon Its Own Motion to Revise Order R-111, As Amended, Pertaining to the Potash Areas of Eddy and Lea Counties, New Mexico. Case 9316, Revision to Order R-111-P, April 21, 1988. Santa Fe, NM.

Section MASS.17 References:

Bachman, G.O. 1974. *Geologic Processes and Cenozoic History Related to Salt Dissolution in Southeastern New Mexico.* Open-File Report 74-194, United States Geological Survey, Sandia National Laboratories.

Bachman, G.O. 1976. "Cenozoic Deposits of Southeastern New Mexico and an Outline of the History of Evaporite Dissolution," *Journal of Research, United States Geological Survey.* Vol. 4, no. 2, 135 – 149.

Bachman, G.O. 1980. *Regional Geology and Cenozoic History of Pecos Region, Southeastern New Mexico.* Open-File Report 80-1099, United States Geological Survey, Denver CO.

Bachman, G.O. 1981. *Geology of Nash Draw, Eddy County, New Mexico.* Open-File Report 81-31. United States Geological Survey, Denver, CO.

Bachman, G.O. 1985. *Assessment of Near-Surface Dissolution At and Near the Waste Isolation Pilot Plant (WIPP), Southeastern New Mexico.* SAND84-7178, Sandia National Laboratories, Albuquerque, NM. WPO 24609.

Bachman, G.O. 1987. *Karst in Evaporites in Southeastern New Mexico.* SAND86-7078, Sandia National Laboratories, Albuquerque, NM. WPO 24006.

Bachman, G.O. 1989. *Annotated Bibliography of Paleoclimate Studies Relevant to the Waste Isolation Pilot Plant, Southeastern New Mexico.* SAND89-7087, Sandia National Laboratories, Albuquerque, NM. WPO 24426.

Brokaw, A.L., Jones, C.L., Cooley, M.E., and Hays, W.H. 1972. *Geology and Hydrology of the Carlsbad Potash Area, Eddy and Lea Counties, New Mexico.* USGS-4339-1, United States Geological Survey, Denver, CO.

Chapman, J.B. 1986. *Stable Isotopes in the Southeastern New Mexico Groundwater: Implications for Dating Recharge in the WIPP Area.* EEG-35, Environmental Evaluation Group, Santa Fe, NM.

Corbet, T. 1995. "NS-9: Justification of SECO2D Approximation for PA Transport Calculations." Summary Memo of Record to D.R. Anderson, September 21, 1995. SWCF-A:1.1.6.3. Sandia National Laboratories, Albuquerque, NM. Contained in WPO 30802.

DOE (U.S. Department of Energy). 1980. *Final Environmental Impact Statement, Waste Isolation Pilot Plant.* DOE/EIS-0026, U.S. Department of Energy, Washington, DC. WPO 38835, WPO 38838 – 38839.

EPA (U.S. Environmental Protection Agency). 1996. "40 CFR Part 194. Criteria for the Certification and Re-Certification of the Waste Isolation Pilot Plant's Compliance with the 40 CFR Part 191 Disposal Regulations; Final Rule," *Federal Register.* Vol. 61, no. 28, 5224 – 5245.

Lambert, S.J. 1987. "Stable-Isotope Studies of Groundwaters in Southeastern New Mexico," *The Rustler Formation at the WIPP Site.* Ed. L. Chaturvedi. EEG-34; SAND85-1978C, Environmental Evaluation Group, Santa Fe, NM. WPO 28418.
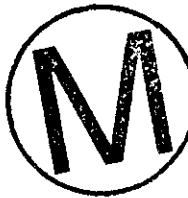
Lambert, S.J. 1991. Chapter 4: "Isotopic Constraints on the Rustler and Dewey Lake Groundwater Systems," *Hydrogeochemical Studies of the Rustler Formation and Related Rocks in the Waste Isolation Pilot Plant Area, Southeastern New Mexico.* Eds. M.D. Siegel, S.J. Lambert, and K.L. Robinson. SAND88-0196, Sandia National Laboratories, Albuquerque, NM. 5-1 through 5-79.

Lambert, S.J., and Carter, J.A. 1987. *Uranium-Isotope Systematics in Groundwaters of the Rustler Formation, Northern Delaware Basin, Southeastern New Mexico. I. Principles and Preliminary Results.* SAND87-0388, Sandia National Laboratories, Albuquerque, NM.

Siegel, M.D., Lambert, S.J., and Robinson, K.L., eds. 1991. *Hydrochemical Studies of the Rustler Formation and Related Rocks in the Waste Isolation Pilot Plant Area, Southeastern New Mexico.* SAND88-7096, Sandia National Laboratories, Albuquerque, NM. WPO 25624.

SNL (Sandia National Laboratories) and University of New Mexico. 1981. *Basic Data Report for Drillhole WIPP 15 (Waste Isolation Pilot Plant - WIPP).* SAND79-027, Sandia National Laboratories, Albuquerque, NM. WPO 26960.

Swift, P.N., Baker, B.L., Economy, K., Garner, J.W., Helton, J.C., and Rudeen, D.K. 1994. *Incorporating Long-Term Climate Change in Performance Assessment for the Waste Isolation Pilot Plant.* SAND93-2266, Sandia National Laboratories, Albuquerque, NM. WPO 27827.

WIPP Performance Assessment Division. 1991. *Preliminary Comparison with 40 CFR Part 191, Subpart B for the Waste Isolation Pilot Plant, December 1991. Volume 2: Probability and Consequence Modeling.* SAND91-0893/2, Sandia National Laboratories, Albuquerque, NM. WPO 26415.

WIPP Performance Assessment Department. 1993. *Preliminary Performance Assessment for the Waste Isolation Pilot Plant, December 1992. Volume 4: Uncertainty and Sensitivity Analyses for 40 CFR 191, Subpart B.* SAND92-0700/4, Sandia National Laboratories, Albuquerque, NM. WPO 20958.

Section MASS.18 References:

Borns, D. J., Barrows, L.J., Powers, D.W., and Snyder, R.P. 1983. *Deformation of Evaporites Near the Waste Isolation Pilot Plant (WIPP) Site.* SAND82-1069, Sandia National Laboratories, Albuquerque, NM. WPO 27532.

DOE (U.S. Department of Energy). 1980. *Final Environmental Impact Statement, Waste Isolation Pilot Plant.* DOE/EIS-0026, U.S. Department of Energy, Washington, DC. Vols. 1-2. WPO 38835, WPO 38838 – 38839.

DOE (U.S. Department of Energy). 1989. *Draft Supplement, Environmental Impact Statement, Waste Isolation Pilot Plant.* DOE/EIS-0026-DS, Department of Energy, Washington, DC. Vols. 1 – 2.

DOE (U.S. Department of Energy). 1990. *Final Supplement Environmental Impact Statement, Waste Isolation Pilot Plant.* DOE/EIS-0026-FS, U.S. Department of Energy Office of Environmental Restoration and Waste Management, Washington, DC. Vols. 1 – 13.

Earth Technology Corporation. 1988. *Final Report for Time-Domain Electromagnetic (TDEM) Survey at the WIPP Site.* SAND87-7144, Sandia National Laboratories, Albuquerque, NM.

Faith, S., Spiegler, P., and Rehfeldt, K.R. 1983. *The Geochemistry of Two Pressurized Brines from the Castile Formation in the Vicinity of the Waste Isolation Pilot Plant (WIPP) Site.* EEG-21, Environmental Evaluation Group, Santa Fe, NM.

Lambert, S.J., and Carter, J.A. 1984. *Uranium-Isotope Disequilibrium in Brine Reservoirs of the Castile Formation, Northern Delaware Basin, Southeastern New Mexico. I. Principles and Methods.* SAND83-0144, Sandia National Laboratories, Albuquerque, NM. WPO 28341.

Popielak, R.S., Beauheim, R.L., Black, S.R., Coons, W.E., Ellingson, C.T., and Olsen, R.L. 1983. *Brine Reservoirs in the Castile Formation, Waste Isolation Pilot Plant Project, Southeastern New Mexico.* TME-3153, U.S. Department of Energy, Waste Isolation Pilot Plant, Carlsbad, NM.

Reeves, M., Freeze, G., Kelley, V.A., Pickens, J., Upton, D.T., and Davies, P.B. 1991. *Regional Double-Porosity Solute Transport in the Culebra Dolomite Under Brine-Reservoir-Breach Release Conditions: An Analysis of Parameter Sensitivity and Importance.* SAND89-7069, Sandia National Laboratories, Albuquerque, NM. WPO 24048.

Spiegler, P. 1982. *Hydrologic Analyses of Two Brine Encounters in the Vicinity of the Waste Isolation Pilot Plant (WIPP) Site.* EEG-17, Environmental Evaluation Group, Santa Fe, NM.

Spiegler, P., and Updegraff, D. 1983. *Origin of the Brines Near WIPP from the Drill Holes ERDA-6 and WIPP-12, Based on Stable-Isotope Concentrations of Hydrogen and Oxygen.* EEG-18, Environmental Evaluation Group, Santa Fe, NM.

BIBLIOGRAPHY

Section MASS.4 Bibliography:

Christian-Frear, T.L., and Webb, S.W. 1996. *Effect of Explicit Representation of Detailed Stratigraphy on Brine and Gas Flow at the Waste Isolation Pilot Plant.* SAND94-3173, Sandia National Laboratories, Albuquerque, NM. WPO 37240.

Webb, S.W., and Larson, K.W. 1996. *The Effect of Stratigraphic Dip on Brine and Gas Migration at the Waste Isolation Pilot Plant.* SAND94-0932, Sandia National Laboratories, Albuquerque, NM. WPO 31271.

Section MASS.5 Bibliography:

Marietta, M.G., Bertram-Howery, S.G., Anderson, D.R. (Rip), Brinster, K.F., Guzowski, R.V., Iuzzolino, H., and Rechard, R.P. 1989. *Performance Assessment Methodology Demonstration: Methodology Development for Evaluating Compliance with EPA 40 CFR 191, Subpart B, for the Waste Isolation Pilot Plant.* SAND89-2027, Sandia National Laboratories, Albuquerque, NM. pp. III-4 through III-16, and pp. IV-2 through IV-49. WPO 25952.

Section MASS.7 Bibliography:

Butcher, B.M., Thompson, T.W., VanBuskirk, R.G., and Patti, N.C. 1991. *Mechanical Compaction of Waste Isolation Pilot Plant Simulated Waste.* SAND90-1206, Sandia National Laboratories, Albuquerque, NM.

Section MASS.8 Bibliography:

DOE (U.S. Department of Energy) Office of Environmental Restoration and Waste Management. 1993. *Independent Technical Review of the Bin and Alcove Test Programs at the Waste Isolation Pilot Plant.* DOE/EM-0130T, U.S. Department of Energy, Office of Environmental Restoration and Waste Management, Washington, DC.

Lappin, A.R., Gotway, C.A., Molecke, M.A., Hunter, R.L., and Lorusso, E.N. 1991. *Rationale for Revised Bin-Scale Gas-Generation Tests with Contact-Handled Transuranic Wastes at the Waste Isolation Pilot Plant.* SAND90-2481, Sandia National Laboratories, Albuquerque, NM. WPO 23963.

Molecke, M.A. 1990. "Test Plan: WIPP Bin-Scale CH TRU Waste Tests." Sandia National Laboratories, Albuquerque, NM. WPO 27063.

Molecke, M.A. 1990. "Test Plan: WIPP In Situ Alcove CH TRU Waste Tests." Sandia National Laboratories, Albuquerque, NM. WPO 40317.

Molecke, M.A., and Lappin, A.R. 1990. *Test Plan Addendum #1: Waste Isolation Pilot Plant Bin-Scale CH TRU Waste Tests.* SAND90-2082, Sandia National Laboratories, Albuquerque, NM. WPO 23959

Sandia WIPP Project. 1992. *Preliminary Performance Assessment for the Waste Isolation Pilot Plant, December 1992. Volume 3: Model Parameters.* SAND92-0700/3, Sandia National Laboratories, Albuquerque, NM. WPO 23529.

Section MASS.13 Bibliography:

Bear, J. 1988. *Dynamics of Fluids in Porous Media.* Reprinted. Dover Publications, Inc., New York, NY.

Bear, J., Tsang, C.F., and de Marsily, G., eds. 1993. *Flow and Contaminant Transport in Fractured Rock.* Academic Press, Inc., San Diego, CA.

Beauheim, R.L., Saulnier, Jr., G.J., and Avis, J.D., 1991, *Interpretation of Brine-Permeability Tests of the Salado Formation at the Waste Isolation Pilot Plant: First Interim Report.* SAND90-0083, Sandia National Laboratories, Albuquerque, NM. WPO 37240

Beauheim, R.L., Roberts, R.M., Dale, T.F., Fort, M.D., and Stensrud, W. 1993. *Hydraulic Testing of Salado Formation Evaporites at the Waste Isolation Pilot Plant: Second Interpretive Report.* SAND92-0533, Sandia National Laboratories, Albuquerque, NM. WPO 23378.

Domski, P.S., Upton, D.T., and Beauheim, R.L. 1996. *Hydraulic Testing Around Room Q: Evaluation of the Effects of Mining on the Hydraulic Properties of Salado Evaporites.* SAND96-0435, Sandia National Laboratories, Albuquerque, NM. WPO 37380.

Kazemi, H., Merrill, L.S., Porterfield, K.L., and Zeman, P.R. 1976. "Numerical Simulation of Water-Oil Flow in Naturally Fractured Reservoirs," *SPEJ, Society of Petroleum Engineers Journal.* Vol. 16, no. 6, 317 – 326.

Section MASS.14 Bibliography:

WIPP Performance Assessment Department. 1992. *Preliminary Performance Assessment for the Waste Isolation Pilot Plant, December 1992. Volume 2: Technical Basis.* SAND92-0700/2, Sandia National Laboratories, Albuquerque, NM. WPO 23528.

WIPP Performance Assessment Department. 1993. *Preliminary Performance Assessment for the Waste Isolation Pilot Plant, December 1992. Volume 4: Uncertainty and Sensitivity Analyses for 40 CFR 191, Subpart B.* SAND92-0700/4, Sandia National Laboratories, Albuquerque, NM. WPO 23599.
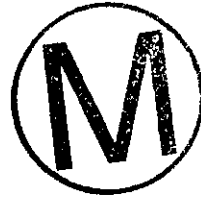
Section MASS.15 Bibliography:

Guzowski, R.V. 1990. *Preliminary Identification of Scenarios that May Affect the Escape and Transport of Radionuclides From the Waste Isolation Pilot Plant, Southeastern New Mexico.* SAND89-7149, Sandia National Laboratories, Albuquerque, NM. WPO 24067.

LaVenue, A.M., Haug, A., and Kelley, V.A. 1988. *Numerical Simulation of Ground-Water Flow in the Culebra Dolomite at the Waste Isolation Pilot Plant (WIPP) Site. Second Interim Report.* SAND88-7002, Sandia National Laboratories, Albuquerque, NM. WPO 28558.

Molecke, M.A. 1983. *A Comparison of Brines Relevant to Nuclear Waste Experimentation.* SAND83-0516, Sandia National Laboratories, Albuquerque, NM. WPO 24500.

Popielak, R.S., Beauheim, R.L., Black, S.R., Coons, W.E., Ellingson, C.T., and Olsen, R.L. 1983. *Brine Reservoirs in the Castile Formation, Waste Isolation Pilot Plant Project, Southeastern New Mexico.* TME 3153, U.S. Department of Energy, Waste Isolation Pilot Plant, Carlsbad, NM.

Roache, P.J. 1993. *The SECO Suite of Codes for Site Performance Assessment.* SAND93-7007, Sandia National Laboratories, Albuquerque, NM. WPO 29007.

Siegel, M.D., Robinson, K.L., and Myers, J. 1991. "Solute Relationships in Groundwaters from the Culebra Dolomite and Related Rocks in the Waste Isolation Pilot Plant Area, Southeastern New Mexico," *Hydrogeochemical Studies of the Rustler Formation and Related Rocks in the Waste Isolation Pilot Plant Area, Southeastern New Mexico.* SAND88-0196. Eds. M.D. Siegel, S.J. Lambert, and K.L. Robinson. Sandia National Laboratories, Albuquerque, NM. 6-1 to 6-35. Chapter 2 of WPO 25624.

Section MASS.17 Bibliography:

Bachman, G.O. 1983. *Regional Geology of Ochoan Evaporites, Northern Part of Delaware Basin.* New Mexico Bureau of Mines and Mineral Resources Open File 184, New Mexico Bureau of Mines and Mineral Resources, Socorro, NM.

Corbet, T.F., and Wallace, M.G. 1993. "Post-Pleistocene Patterns of Shallow Groundwater Flow in the Delaware Basin, Southeastern New Mexico and West Texas," *Carlsbad Region, New Mexico and West Texas, New Mexico Geological Society Forty-Fourth Annual Field Conference, Carlsbad, NM, October 6-9, 1993.* Eds. D.W. Love, J.W. Hawley. 321-325.

Swift, P.N. 1993. "Long-Term Climate Variability at the Waste Isolation Pilot Plant, Southeastern New Mexico, USA," *Environmental Management* v. 17, 83-87. (Also published in 1992 with the same title as SAND91-7055, and reproduced in this application as Appendix CLI). WPO 27093.

ATTACHMENTS

Model Geometries (Section MASS.4)

Attachment 4-1
SWCF WPO 30840. FEP Screening Analysis: S1: Verification of 2D-Radial Flaring Using 3D Geometry

Repository Fluid Flow (Section MASS.7)

Attachment 7-1
SWCF WPO 40418   Thompson, T.W. and F.D. Hansen. 1996. "Long Term Performance of Panel Closures." Unpublished memorandum to M.G. Marietta, August 2, 1996. Albuquerque, NM: Sandia National Laboratories.

Gas Generation (Section MASS.8)

Attachment 8-1
SWCF WPO 36290   Brush, L.H., Wang, Y., and Garner, J.W. 1995. "Rationale for Discontinuing the Development of the Reaction-Path Gas-Generation Model." Unpublished memorandum to distribution, November 30, 1995. Albuquerque, NM: Sandia National Laboratories.

Attachment 8-2
SWCF WPO 31943   Wang, Y. and Brush, L. 1996. "Estimates of Gas-Generation Parameters for The Long-Term WIPP Performance Assessment." Unpublished memorandum to Martin S. Tierney, January 26, 1996. Albuquerque, NM: Sandia National Laboratories.

Attachment 8-3
SWCF WPO 36289   Wang, Y. and Brush, L. 1995. "Input Parameter Value Adjustments for the Average-Stoichiometry Model." Unpublished memorandum to D.R. Anderson, September 20, 1995. Albuquerque, NM: Sandia National Laboratories.

Salado (Section MASS.13)

See also Attachment 4-1

Attachment 13-1
SWCF WPO 30790   Lord, M., Vaughn, P., and MacKinnon, R. 1995. "S-7: GAS EXSOLUTION - Summary Memo of Record." Unpublished memorandum to D. R. Anderson, December 21, 1995. Albuquerque, NM: Sandia National Laboratories.

Attachment 13-2

SWCF WPO 39166   Larson, K. 1996. "Memorandum of Record for meeting held 1/22/96 to discuss symmetry of intact rock properties, possible gas-pressure induced fracture properties, and fluid flow properties around the WIPP." Unpublished memorandum of record to Distribution, June 5, 1996. Albuquerque, NM: Sandia National Laboratories.

Culebra (Section MASS.15)

Attachment 15-1

SWCF WPO 38801   Brush, L.H. 1996. "Ranges and Probability Distributions of K_ds for Dissolved Pu, Am, U, Th, and Np in the Culebra for the PA Calculations to Support the WIPP CCA." Unpublished memorandum to M.S. Tierney, June 10, 1996. Albuquerque, NM: Sandia National Laboratories.

Attachment 15-2

SWCF WPO 36385   Ramsey, J. 1996. "Numerical Implementation of the Colloid Transport Conceptual Model." Unpublished memorandum to Distribution, April 8, 1996. Albuquerque, NM: Sandia National Laboratories.

Attachment 15-3

SWCF WPO 37533   Brush, L.H. 1996. "Revised Free-Solution Tracer Diffusion Coefficients (D_{sol}s) for Dissolved Pu, Am, U, Th, Np, Cm, and Ra in Boreholes and the Culebra for Use in the PA Calculations to Support the WIPP CCA." Unpublished memorandum to M.S. Tierney, May 11, 1996. Albuquerque, NM: Sandia National Laboratories.

Attachment 15-4

SWCF WPO 37455   Larson, K.W. 1996. "Mining Transmissivity Multiplier - Area to be Mined." Unpublished memorandum to M. Wallace, April 25, 1996. Albuquerque, NM: Sandia National Laboratories.

Attachment 15-5

SWCF WPO 38571   Howard, B.A. 1996. "Future Mining Events in the Performance Assessment." Unpublished letter to M. Marietta, April 3, 1996. Carlsbad, NM: Westinghouse Electric Corporation.

Attachment 15-6

SWCF WPO 37450   Meigs, L. and McCord, J. 1996. "Physical Transport in the Culebra Dolomite." Unpublished memorandum to File, July 11, 1996. Albuquerque, NM: Sandia National Laboratories.

1   Attachment 15-7
2   SWCF WPO 30802   Corbet, T. 1995. "FEP NS-9, Two-dimensional assumption for
3   Culebra Calculations." Unpublished summary memorandum of record,
4   September 21, 1995. Albuquerque, NM: Sandia National Laboratories.
5
6   Attachment 15-8
7   SWCF WPO 38797   Stockman, C.T. 1996. "Treatment of colloids in Culebra transport."
8   Unpublished memorandum to J.C. Helton, June 19, 1996.
9   Albuquerque, NM: Sandia National Laboratories.
10
11 Attachment 15-9
12 SWCF WPO 38250   Perkins, W.G. 1996. "Calculations of Filtration for Microbial and
13   Mineral Fragment Colloids." Unpublished memorandum to J.L.
14   Ramsey, June 4, 1996. Albuquerque, NM: Sandia National
15   Laboratories.
16 Attachment 15-10
17 SWCF WPO 40484   McCord, J. 1996. "Cross-Correlations for WIPP PA: Culebra
18   Physical Transport Parameters." Unpublished memorandum to K.
19   Larson, September 2, 1996. Albuquerque, NM: Sandia National
20   Laboratories.
21
22 *Intrusion Borehole (Section MASS.16)*
23
24 Attachment 16-1
25 SWCF WPO 38579   Howard, B.A. 1996. "Borehole Plugging in the Delaware Basin."
26   Unpublished letter to M. Marietta, April 4, 1996. Carlsbad, NM:
27   Westinghouse Electric Corporation.
28
29 Attachment 16-2
30 SWCF WPO 39090   Stoelzel, D.M. and O'Brien, D.G. 1996. "Conceptual Model
31   Description for BRAGFLO Direct Brine Release Calculations to
32   Support the Compliance Certification Application." Unpublished
33   report, July 9, 1996. Albuquerque, NM: Sandia National Laboratories.
34
35 Attachment 16-3
36 SWCF WPO 39624   Thompson, T.W., Coons, W.E., Krumhansl, J.L., and Hansen, F.D.
37   1996. "Inadvertent Intrusion Borehole Permeability." Unpublished
38   report, July 8, 1996. Albuquerque, NM: Sandia National Laboratories.
39   Filed as an attachment to WPO 39624, 39622, 39626.
40
41

Climate Change (Section MASS.17)

Attachment 17-1 (two items)

SWCF WPO 36425   Corbet, T.F. 1996. "Non-Salado Record Package: Culebra Transmissivity Zone: Climate Index." Unpublished memorandum to NWM Records Center, April 24, 1996. Albuquerque, NM: Sandia National Laboratories.

SWCF WPO 37465   Corbet, T. and Swift, P. 1996. "Distribution for the Non-Salado Parameter for SECOFL2D: Climate Index." Unpublished memorandum to M. Tierney, April 12, 1996. Albuquerque, NM: Sandia National Laboratories.

Castile Brine Reservoir (Section MASS.18)

Attachment 18-1

SWCF WPO 37148   Freeze, G. and Larson, K. 1996. "Initial Pressure in the Castile Brine Reservoir." Unpublished memorandum to M. Tierney, March 20, 1996. Albuquerque, NM: Sandia National Laboratories.

Attachment 18-2

SWCF WPO 37973   Freeze, G. and Larson, K. 1996. "Castile Brine Reservoir Pressure Record Package." Unpublished memorandum to SWCF-A Records Center, May 20, 1996. Albuquerque, NM: Sandia National Laboratories.

Attachment 18-3

SWCF WPO 37971   Larson, K. and Freeze, G. 1996. "Castile Brine Reservoir Volume Revision." Unpublished memorandum to SWCF-A, May 27, 1996. Albuquerque, NM: Sandia National Laboratories.

Attachment 18-4

SWCF WPO 37147   Helton, J. 1996. "Addition of Discrete Parameter." Unpublished memorandum to M. Tierney, March 21, 1996. Albuquerque, NM: Sandia National Laboratories.

Attachment 18-5

SWCF WPO 39121   Borns, D.J. 1996. "Proportion of the waste panel area, WIPP site, that is underlain by brine reservoirs in the Castile Formation as Inferred from Transient Electromagnetic Method (TEM or TDEM) Surveys." Unpublished memorandum to M. Chu, February 20, 1996. Albuquerque, NM: Sandia National Laboratories.

1   Attachment 18-6
2   SWCF WPO 40199   Powers, D.W., Sigda, J.M., and Holt, R.M. 1996. "Probability of
3   Intercepting a Pressurized Brine Reservoir Under the WIPP."
4   Unpublished report, July 10, 1996. Albuquerque, NM: Sandia
5   National Laboratories.
6